LUKAS, ARI D., M.A. Geophysical Investigation at 31MA684 Floodplain
and 31MA774 Hilltop, Macon County, North Carolina. (2017)
Directed by Dr. Roy Stine. 106pp.

On October 8th and 9th and December 11th, 2014 a geophysical survey was conducted on two areas adjacent to McCoy Bridge in Macon County, North Carolina. The purpose of the survey was to identify a potential Cherokee Indian habitation site that may have existed in this location. This project was unique in that the geophysical survey maps were created prior to mechanical stripping and compared to feature locations created by archaeologists after the topsoil had been removed. Researchers were then able to accurately determine the ability of ground penetrating radar (GPR) and magnetic gradiometer to detect subsurface features within the cultural landscape that once existed at sites 31MA684, floodplain, and 31MA774, hilltop. The geophysical survey used a 400 megahertz (MHz) GPR antenna and a Bartington fluxgate gradiometer; all data were collected at 50 cm transects. The geophysical survey successfully identified approximately 50 percent of the larger features. However, of the 402 features found by archaeologists, most (288) were small post holes. Coupled with the relative dielectric permittivity (RDP) of the site, identification of these features proved extremely difficult with the GPR. Additionally, the field in which the survey was conducted had years of documented plowing that created deep furrows, resulting in multiple GPR coupling errors. The negligible difference between the feature matrix and surrounding soil combined with the lack of burning also contributed to the inability of either the GPR or gradiometer to detect features. Possible solutions for a higher recovery rate would be to

decrease the transect spacing and using a higher frequency antenna in conjunction with the 400 MHz antenna.

GEOPHYSICAL INVESTIGATION AT 31MA684 FLOODPLAIN AND 31MA774 HILLTOP, MACON COUNTY, NORTH CAROLINA

by

Ari D. Lukas

A Thesis Submitted to
the Faculty of The Graduate School at
The University of North Carolina at Greensboro
in Partial Fulfillment
of the Requirements for the Degree
Master of Arts

Greensboro
2017

Approved by

____

Committee Chair

APPROVAL PAGE

This thesis written by Ari D. Lukas has been approved by the following committee of the Faculty of The Graduate School at The University of North Carolina at Greensboro.

Committee Chair ______________________________________

Committee Members ______________________________________

____

____
Date of Acceptance by Committee

____
Date of Final Oral Examination

ACKNOWLEDGMENTS

This work would not have been possible without the help and support of those who gave it when it was most needed. Thank you to the Geography Department of the University of North Carolina. The generous funding that was provided made the completion of this thesis possible.

I cannot thank my committee chair Dr. Roy Stine enough. Throughout my academic career he was an indispensable advisor, friend and was always there to push me when I needed it most. I would also like to thank my other committee members, Dr. Dan Royall and Dr. Elizabeth Nelson. Dr. Royall was always there to answer any questions that arose concerning soil and I could always count on Dr. Nelson to give me her advice on how to make my maps and figures look their best. Though not officially on my committee I must thank Dr. Linda Stine. She not only took time out of her day to show me around UNCG way back even before my undergraduate days but was the first to introduce me to GPR and all that could be accomplished with it.

Thank you to TRC, INC., particularly Bruce Idol and Paul Webb, for allowing me to conduct my geophysical research on your site. Additionally, thank you Matt Wilkerson and Damon Jones from DOT and John Mintz from NC State Archeaology.

I wish to also thank my fellow graduate students Jacob Turner, Doug Gallaway, Michael Enoch, Megan Cope and Keith Watkins. Each spent countless hours in the field and in the lab lending a hand, giving advice and providing comic relief when needed.

Lastly, I must thank my friends and family who were always there to give me encouragement and let me vent whenever times became too tough, chiefly my amazing wife Afton Lukas. She was always there to offer encouragement, give me support and keep me stocked with all the caffeine and snacks one could ask for when pulling long nights in the lab. Thank you so much. This would not had been possible without you by my side.

TABLE OF CONTENTS

LIST OF FIGURES

CHAPTER I

INTRODUCTION

Geophysical surveys using multiple geophysical tools allow geographers and cultural landscape archaeologists to discover and map subsurface features in ways not previously possible (Conyers 2004; Kvamme 2003, 2006). Typical archaeological survey practices consist of tedious shovel tests and surface collections which can become very expensive and time consuming. The benefits of conducting a geophysical survey before or in lieu of a full-scale excavation can give researchers a better understanding of where to focus research efforts before any excavation takes place. This has the potential to not only save time and money for both researchers and contractors of a project but also helps to preserve the cultural integrity of a site.

A geophysical survey was conducted prior to mechanical stripping on two areas adjacent to McCoy Bridge in Macon County, NC (Figure 1) to look for any cultural remains that might exist and potentially be destroyed upon widening of the bridge. Field work for this project took place on the 8th and 9th of October and the 11th of December, 2014. The site was located in the Appalachian summit region of western North Carolina (Figure 1). This area of North Carolina exhibits evidence of continued habitation from the Paleoindian to the historic period (Idol et al. 2017; Keel 1976; Rodning 2004; Ward and Davis 1999; Wetmore 2002). The survey consisted of using a ground penetrating radar (GPR) and magnetic gradiometer to collect all geophysical data.

The primary questions being investigated by UNCG and TRC archaelogoist:

1. Will this geophysical survey lead to a better understanding of the Qualla Cherokee landscape at these sites and the surrounding region?
2. What is the relative effectiveness of ground penetrating radar and magnetic gradiometer in identifying the location of cultural features at these sites (31MA684 and 31MA774)?

Additionally, researchers sought to ascertain:

3. What challenges are associated with using geophysical equipment?
4. Can a systematic soil sampling or ground-truthing/excavation at various feature locations help to refine the efficiency of the geophysical equipment?

The second chapter of this thesis will be a literature review which will give a brief description of general geophysical survey methods, focusing on GPR and magnetic gradiometer. Three sites located within the Appalachian Summit region of North Carolina that utilized a GPR and a magnetic gradiometer survey will be discussed in detail within this section as well. The third chapter will provide a brief cultural and physical description of sites 31MA684 (floodplain) and 31MA774 (hilltop) and will review the methods used both in the field and in the laboratory to collect and process all of the data. The fourth chapter will present the field and laboratory results. This will be followed by a discussion comparing the geophysical results with the mapped results of the cultural features found by TRC. The final section will discuss the results and what they mean for the site as a whole and present the conclusion along with future research suggestions.

Figure 1. McCoy Bridge Geophysical Survey Grids with Topography

CHAPTER II

LITERATURE REVIEW

Many archaeologists have come to realize that to fully grasp a site's use and purpose, geophysical methods need to be incorporated into the survey process (Clay 2001a; Kvamme 2003,2006; Leckebusch 2003; Bruseth, Pierson, and Johnson 2007; Hargrave, Britt, and Reynolds 2007; Perttula, Walker, and Schultz 2008; King et al 2011). Conyers (2004:1) describes geophysics pertaining to archaeology as "...a method of data collection that allows field archaeologists to discover and map buried archaeological features in ways not possible using traditional field methods."

Geophysical methods employ a multitude of tools to measure, actively or passively the feature's physical and chemical properties of the subsurface that can then be mapped and measured (Kavamme 2003; Conyers 2012). Kvamme (2003: 435) argues that,

> …by placing focus on such buried features as dwellings, storage facilities, public structures, middens, fortifications, trails, or garden spaces that are not commonly revealed through most contemporary surface inspection methods, a richer view of archaeology, the past, and cultural landscapes can be achieved.

He goes on to argue that the best way to view these features is through geophysical surveying by using such techniques as magnetic gradiometer, resistivity, electromagnetic conductivity and ground penetrating radar (GPR), to name a few. Of these technologies GPR and magnetometers configured as gradiometers are commonly used in the archaeological field to aid in site interpretation prior to excavation (Conyers 2012; Kavamme 2003; Moore 2009; Perttula, Schultz, Walker 2008).

GPR is an active remote sensing method that transmits radio waves in the megahertz (MHz) or gigahertz (GHz) range into the ground from a single send/receive antenna or antenna pair. As the energy is transmitted through various materials and reflected back to the receiving antenna, signal velocity can be calculated and converted into depth of a buried feature/soil matrix. As the antenna is either pushed or pulled along transects in a georeferenced grid a two-dimensional vertical profile of radio waves is produced (Conyers 2004, 2012). For archaeological purposes, transects are usually spaced one half meter or less apart, depending on the frequency of the antenna in use. The signal transmitted from higher frequency antennas (900MHz) attenuates much faster than lower frequency antennas (200MHz); therefore, the target size and depth is always an important factor to take into consideration before conducting a survey (Conyers 2012). When the radar wavelengths encounter features (pits, walls surfaces, house floors), or soil changes that differ in their dielectric constant from the surrounding soil matrix, a portion of the energy is reflected back towards the receiving antenna where the amplitude (seen as a hyperbolic reflection) and time (in nano seconds) is recorded in the vertical profile (Conyers 2013).

Most GPR antennas used for archaeological purposes produce frequencies that fall within the 200 to 900MHz range and can accurately detect features 1-3 meters below the surface; depending on the antenna (Conyers 2012; Wright 2014; Kvamme 2003). Additional factors that must be considered before choosing what type of antenna to use are soil types, soil chemistry, hydrology and natural features such as rocks, tree roots, or animal burrows. The spatial distribution and type of cultural features that may be present must be considered as well. These factors can cause the antenna's signal to attenuate and affect the quality of vertical profiles and depth slice maps that can be produced (Conyers 2012; Kvamme 2003; Leckebusch 2003). When properly used GPRs can predict with relative accuracy where culturally significant features are located and at what depth (Kvamme 2003; Leckebusch 2003). It is the GPR's ability to calculate depth that enables specialized software to create accurate three-dimensional data sets of subsurface features. Once exported to a Geographic Information System (GIS), other spatial information (elevation, slope, historic maps, total station data) can be combined to map and aid in geographical and cultural management (Leckebusch 2003; Turner, Stine, Lukas 2015).

Magnetometers, often referred to as gradiometers, are passive sensors that are sensitive to objects and soils that contain iron and are capable of recording the strength of the earth's magnetic field at a given time and place (Clay 2001a). Under the proper conditions, they are able to measure relatively small local variations in magnetism and distinguish buried objects and features as anomalies. These anomalies must differ in magnetic strength from the earth's magnetic field in order to be 'seen' by a magnetometer. Magnetic variation is recorded in units of nanoTeslas (nT) and is often restricted to +/- 100 nT range, but today's sensors are very sensitive and are capable of precision down to the .01 nT. Gradiometers can typically measure to roughly 2 m in depth, depending on the magnetic strength of the anomaly being observed (Clay 2001a).

There are many factors that contribute to variations in magnetism. Kvamme (2008) states that while there are natural causes for magnetic variations, there are certain anthropogenic processes that are unique to culturally significant sites and can be observed using a magnetometer. Heating or burning of features and objects (such as pits, posts, hearths, cooking pits, bricks, etc.), can cause what is known as thermoremnant magnetism. This is when iron oxide and other ferrous minerals contained in the soil or object is heated over its Curie Point and loses its magnetism. The magnetic domains then become aligned with the local magnetic field at the time of cooling (Aspinall, Gaffney, and Schmidt 2008). Waste heaps are another feature that can be observed with a magnetometer. Fermentation can occur due to microorganisms such as bacteria, yeast, and fungi can cause weakly magnetic minerals (ex. Hematite) to be converted to minerals with increased magnetic susceptibility (maghemite). However, this phenomenon is usually best observed with a magnetic susceptibility meter. Certain bacteria have also been recorded in abundance in decaying wooden posts. These bacteria have been found to create magnetic, micron sized, crystals within their bodies. Small signatures such as these can be recorded with a sensitive magnetometer. Back-filling a ditch or hole can also result in an area of differing magnetic properties due to the topsoil having higher magnetic susceptibility than the surrounding subsoil (Aspinall, Gaffney, and Schmidt 2008).

There are multiple sensors and configurations used for magnetometry. This report focuses on the hand-held fluxgate gradiometer (Clay 2001a; Bruseth, Pierson, and Johnson 2007). A fluxgate gradiometer measures the difference in magnetism (measured in nanotesla (nT)) between two vertically separated heads, usually a meter apart, that simultaneously records the earth's magnetic field and local magnetic variation at the time of collection (Clay 2001a). The uppermost sensor records the earth's magnetic field strength at the time of collection. While the bottom sensor is equally sensitive to the ambient magnetism, it will also record any local influences, potentially identifying subsurface features of geographic and cultural interest. The difference results in positive and/or negative local contrasts (Clay 2001a; Turner, Stine, Lukas 2015). These contrasts appear as either dipole (both positive and negative peaks) or monopolar (either positive or negative peaks) anomalies in magnetic surveys (Hargrave, Britt, Reynolds 2007).

Gradiometers are most often carried by an operator who walks along georeferenced survey transects, collecting data at a given number of samples per meter, also factoring in the operators walking speed (Turner, Stine, Lukas 2015). The data are viewed in specialized software that can produce an image/map with a grayscale; low to no local variation appearing as gray, positive variation appearing as black and negative variation appearing as white. Though the exact depths of features or objects cannot be ascertained, magnetometers can pick up small variations in magnetic fields that would otherwise be undetectable. The distribution of these local variations can often form patterns or shapes that are indicators of buried cultural or natural features (Clay 2001a; Turner, Stine, Lukas 2015).

There are many publications that represent geophysical surveys' ability to map sub-surface cultural features with impressive clarity (Conyers 2012; Kvamme 2008; Sturm and Crown 2015; Whiting, McFarland and Hackenberger 2001). Often, however, geophysical equipment can only give researchers a general idea of the feature of interest. Conyers (2012) discusses areas were projects did not go well or mistakes were made and Jensen (2003) has noted where traditional optical remote sensing has often been oversold as to its abilities. Issues can occur such as the signatures recorded by survey instruments may not have the same dimensions as the sub-surface feature which they represent. Additionally, buried features with weaker signatures can be masked if there are objects with stronger signatures overlying them or in close proximity. Hargrave (2006) Conyers (2012) and Rogers et al. (2012) have noted that buried objects will vary in intensity depending on the soil matrix and level of moisture; which can also mask features.

Though these issues are certainly challenges, they are noted to inform the researcher that to truly understand a site ground-truthing is still a necessary task. A geophysical survey map, while highly effective at narrowing down the location of culturally significant features, should not be assumed to perfectly portray the features they represent (Hargrave 2006), and necessary steps need to be taken to optimize subsurface mapping efforts.

Some of the uncertainty of geophysical surveys can be alleviated by using more than one instrument. Thus, the use of multiple instruments has become common practice and allowed researchers to discover and map subsurface features in ways not previously possible (Conyers 2004; Kvamme 2003, 2006; Stine and Stine 2013). While there are a wide variety of instruments capable of conducting a geophysical survey (e.g. resistivity, conductivity, magnetic susceptibility, aerial photography, multi spectral satellite imagery), GPR and magnetic survey have become the most commonly used together as complementary methods (Patch and Lowry 2013; Stine and Stine 2013; Wright 2014).

Three geophysical projects (Figure 2) that exhibit geographic and cultural similarities that are relevant to this research and have undergone extensive geophysical and archaeological investigations: Kituhwa mound (31SW2), village (31SW1) and surrounding sites, Garden Creek (31HW8), and the Berry Site (31BK22). Each is reviewed below, with several questions in mind: What is the relative effectiveness of GPR and magnetic gradiometer in identifying the location of cultural features at these sites? What information can the geophysical survey provide concerning the location and characteristics of subsurface features, and how useful are these techniques in guiding the data recovery process? Can ground-truthing/excavation at various feature locations help to refine the efficiency of the geophysical equipment? What challenges are associated with using these tools?

The Berry site, known as Joara, was the central town of a Mississippian chiefdom that was located along the upper Catawba River in present day Burke County, North Carolina. This site was one of the largest late prehistoric sites in the upper Catawba valley with an example of a Mississippian mound, and one of the earliest European settlement in the interior of the present-day United States. In the 16th century the Spanish conducted expeditions to colonize parts of what was to be become the southeastern United States. One of these expeditions, led by Spanish Captain Juan Pardo, left present-day Paris Island, South Carolina on December 1566 with orders to pacify the local Indians to claim the land for Spain and to find an overland route to central Mexico. In

January 1567 Captain Pardo reached the town of Joara and constructed Fort San Juan. The Pardo expedition constructed 5 other forts on his expedition across North Carolina and eastern Tennessee, though it was said he believed San Juan to be the most important. However, by May 1568, word had reached Spanish officials that all 6 forts had been attacked by the local Indians and been destroyed (Beck, Moore, Rodning 2006).

In June of 1997 (Hargrove and Beck 2001) a magnetometer survey was conducted on a 0.9 acre section of the Berry site. A Geoscan FM fluxgate gradiometer was used to collect the data with readings taken every 25cm along transect spaced 50cm apart. The area chosen for survey was situated on a field that was used for corn cultivation and as such had been repeatedly plowed. Of interest to note is the authors did not mention any type of distortion or stripping effect caused by plowing scars that was reported by the authors of the next two studies.

Over the course of the survey 5 large positive anomalies were detected with the magnetometer, indicating the presence of large cultural features. The anomalies were tested using an auger; with soil cores every meter along a grid. All the samples had thick lenses of burned debris below the plow zone which confirmed that there were burned structures (Hargrove and Beck 2001). One of the structures, Anomaly 1, was described by Hargrove and Beck (2001:4) "…in form and size it has a striking resemblance to the footprints of late prehistoric Pisgah phases houses of the Appalachian Summit area." Excavations the following spring were able to confirm that these were in-fact burned structures and likely associated with Fort San Juan (Hargrove and Beck 2001). An additional 4 hectare (ha) of the site was surveyed with a gradiometer. These results revealed five burned structures along with a possible palisade (Beck, Moore and Rodning 2006).

The use of a gradiometer at the Berry site enabled researchers to identify and locate with a high degree of accuracy five burned structures. Though auger testing and limited excavation were used to confirm these findings, the structures would not have been found with such ease had it not been for the implemented geophysical equipment. The Berry site demonstrates the value of using a single geophysical tool in conjunction with ground truthing to find significant cultural remains.

The Garden Creek site (Figure 2) was located at the confluence area of Pigeon River and Garden Creek in Haywood County, North Carolina. Over the years there have been multiple periods of excavations here, both professional and amateur, as well as geophysical surveys (Keel 1976; Wright 2014). Garden Creek was one of the Appalachian Summit region's earliest known mound (Wright 2014). This site has also seen multiple periods of regular plowing for agriculture and beginning in 1950s, much of the land containing the mounds was sold for residential development. None the less, two existing mounds were identified and became the focus of excavations and surveys beginning in the early 1960s. Mound 1 revealed several Mississippian Period (Pisgah phase (1000-1450)) earth lodges and homes. Mound 2 showed evidence of occupation from the Middle Woodland Period (Swannanoa (1000-300 B.C.) (Early), Pigeon (300 B.C.- A.D. 200) (Middle), and Connestee (A.D. 200-800) (Late) as defined by Keel (1976)).

The area around Mound 2 was surveyed over the course of 2 field seasons (2011 and 2012) (Wright 2014) The geophysical survey conducted primarily on the non-mound components to identify and map the extent of the Middle Woodland occupation at Garden Creek. The survey during the 2011 season utilized a magnetic gradiometer and the 2012 season included additional gradiometer work, GPR and magnetic susceptibility (Wright 2014).

The 2011 field season was conducted in an area having the least proximity to iron objects associated with the modern subdivision which would present magnetic disturbances in the magnetometer data. A Bartington Grad601-2 dual fluxgate gradiometer was used to survey these areas along transects that were spaced 0.5m apart. These surveys yielded little evidence of archaeological features. One of the hayfields surveyed exhibited very strong magnetic anomalies but these were believed to have been of geological origin or possibly caused by a lightning strike. There were other anomalies consistent with buried archaeological features but due to similar magnetic responses between the features of interest and plowing scars, coupled with high levels of background noise, identification was extremely difficult (Horsley 2014).

One area of the survey however, showed numerous discrete magnetic anomalies. Due to the absence of strong plowing effects seen elsewhere on the site, a better feature definition could be seen. The signatures of these anomalies were consistent with buried pits and hearths (Horsley 2014). These features were confirmed via coring and excavation, helping to enhance the interpretation of magnetic readings from other portions of the site. A curvilinear anomaly was also discovered, representative of a subrectangular ditched enclosure, which was confirmed via excavation to be a 1m deep ditch with significant quantities of Early Woodland/early Middle Woodland ceramics (Wright 2014). Additionally, a possible mound feature appeared to be located over one of the enclosures mentioned above. The discovery of these 2 rectangular features and mound feature warranted a second geophysical survey the following season.

The 2012 Geophysical survey included additional magnetometer surveys, as well as magnetic susceptibility and GPR. The magnetometer survey used the same parameters as the 2011 season to ensure consistency in the results; producing similar data as well (Horsely in Wright 2014: Appendix A). While there appeared to be a combination of modern and prehistoric anomalies in the magnetometer data, background noise (similar to that of previous years) from nearby ferrous material and plow scar stripping caused by agricultural practices partially obscured the magnetic signature of any archaeological feature present.

The GPR survey used Noggin sensors and software system, equipped with a 250 MHz antenna. Due to the GPR being unaffected by the nearby ferrous material, it was employed particularly to investigate the two previously identified geometric enclosures. Horsely (2014) states that the GPR could detect features through the disturbed plow zone and provide a clearer image of the subsurface features. The GPR survey in the area of the enclosures resulted in the identification of basins, pits, trenches, and even large postholes below the plow zone (Wright 2014). Magnetic susceptibility was the final geophysical tool to be implemented in the 2012 season. It was employed in the hopes that a magnetic susceptibility survey could quickly and accurately determine the entire extent of the site by locating where human activity had increased the magnetic qualities of the soil (Horsely 2014). At the conclusion of the 2012 field season, a total of 8 hectares were covered by gradiometer survey, 0.9 hectares by GPR, and 11 hectares by magnetic susceptibility survey.

The work at Garden Creek illustrates the importance of incorporating a variety of geophysical tools into a survey. Unwanted noise and other issues that were encountered in the 2011 survey with the use of a single sensor were overcome by employing complimentary geophysical tools. These allowed known and newly discovered features to be mapped and placed into their proper cultural context.

The work most geographically and culturally relevant to geophysical investigations at 31MA684 and 31MA774 was conducted at Kituhwa mound and village area in Swain County, North Carolina (Figure 2). Kituhwa is the “largest continuous mound and village complex in North Carolina” (Riggs and Shumate 2003:73) with Archaic, Woodland, Mississippian (Pisgah and Qualla) and historic (Qualla and Anglo) components.

The first geophysical survey was conducted at the Kituhwa mound and surrounding area by Berle Clay (2001b) in May of the same year at the request of the Eastern Band of the Cherokee Indians. The survey was conducted using a Geoscan FM36 fluxgate gradiometer, covering a total area of 2.76 ha. The survey primarily centered on a pre-existing mound and nearby surrounding area. The gradiometer data could provide evidence for the existence of at least one burned structure, as well as a possible Cherokee ‘townhouse’, with evidence of other burned structures existing below it (Clay 2001b). A central hearth associated with the townhouse is also identified in the mound vicinity, in addition to a doorway, walls, and a mound construction ramp (Riggs and Shumate 2003). The anomalies seen in the gradiometer data of this area correlate with cultural material found from surface collection and shovel tests, indicating a high likelihood of archaeological features. The stripping effect, observed in the above studies, obscured many of the potential features. Clay (2001b: 8) states, “The act of plowing ‘restructures’ the magnetic materials in the plow zone...,” and goes on to say, “Because the range in nT of these stripes is the same as the range of variation in nT of archaeological features below plow zone, they powerfully obscure the archaeological features.” The gradiometer was able to identify two known residential hearths in an area that the plow zone removed.

Two additional sections were surveyed with the gradiometer in conjunction with plow zone removal by Riggs and Shumate (2003) in the same year. Riggs and Shumate (2003) note that features encountered after plow zone removal vaguely corresponded to the magnetic maps produced of the same area. They believe this is likely due to the lack of magnetic contrast between feature fill and the surrounding soil matrix. Both surveys collected gradiometer data along transects that were spaced 1 meter apart, with 4 readings taken per meter. Clay (2001b) states that greater resolution of archaeological features below the plow zone could be obtained with closer transects and more samples taken per meter.

Palmyra Moore (2009) returned to Kituhwa in 2006 and 2007 to conduct a geophysical survey. Moore (2009) resurveyed the mound and surrounding area with a gradiometer, using closer transects intervals (0.5m instead of 1m) as recommended by

Clay (2001b). In addition, Moore conducted a resistivity survey and a GPR survey, which could identify structural features, middens, as well as image the internal structure of the townhouse and mound in greater detail, all of which was not possible using only the gradiometer at a coarser resolution. Smaller isolated features, such as postholes, proved to be a challenge to identify, however. The only geophysical tool that could distinguish these types of features with any degree of success was the gradiometer. Moore (2009) found that fragments of fire baked clay were a strong 'indicator' of the presence of postholes in the magnetic data. It should be noted that the clay fragments were only seen as 'indicators' and instances occurred where these fragments were present with no associated posthole. Moore (2009) goes on to state in general that burials and pit features were not detected by the geophysical instruments used because they didn't provide enough contrast with the surrounding soil matrix. She believes this was because the organic contents of the graves and pits decomposed to such an extent as to blend into the surrounding soil matrix (Moore 2009).

The original gradiometer survey was able to map several burned structures on the mound that were not able to be detected with the GPR. Several features in the vicinity of the mound were obscured in the original gradiometer survey due to plow zone stripping but were able to be clearly detected due to the addition of the GPR and resistivity survey. Despite being unable to easily discern smaller isolated features such as burial and pits, Moore's work at Kituhwa mound demonstrates the benefits of using multiple geophysical tools.

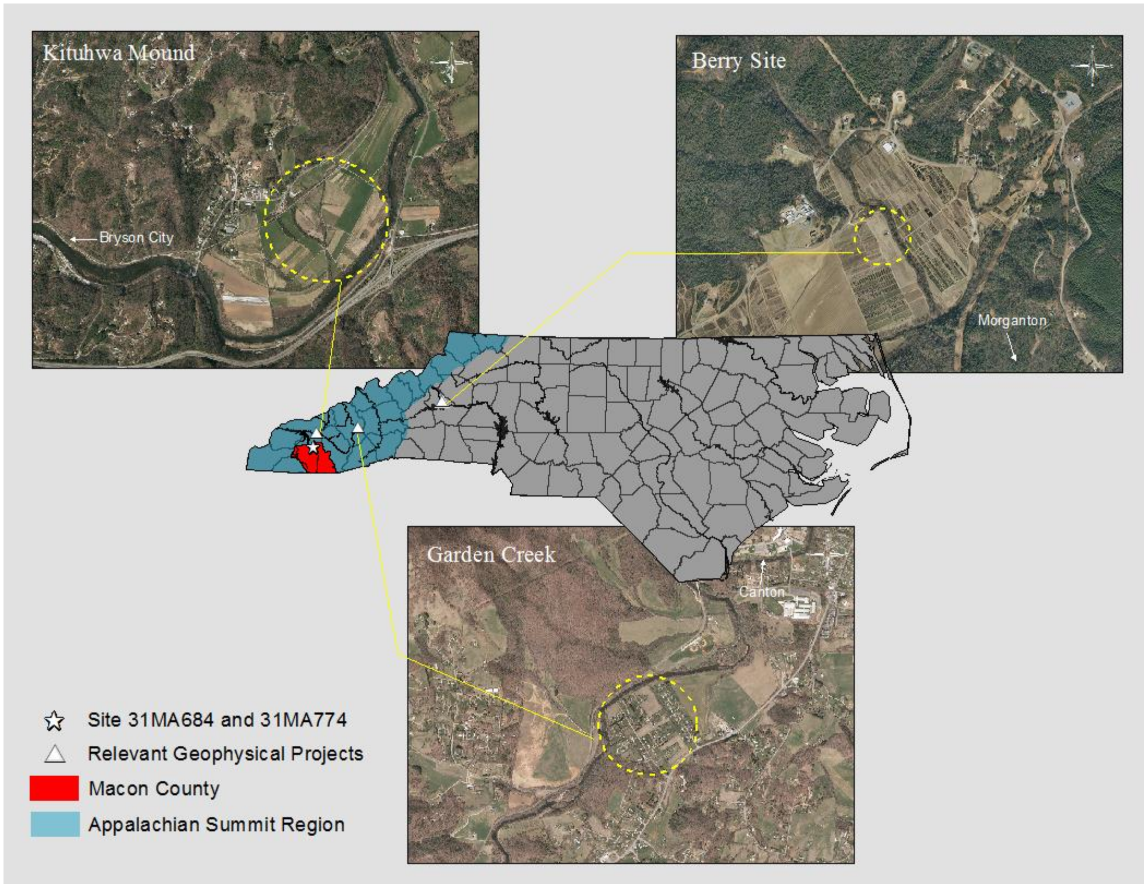

Figure 2. Geophysical Projects Relevant to the Work at 31MA684 and 31MA774

CHAPTER III

METHODS

The project area is located roughly seven miles (11.3km) northwest of the town of Franklin in Macon County, NC (Figure 1). Site 31MA684 is located on the east side of the Little Tennessee River on a floodplain terrace used for agricultural purposes. Site 31MA774 is located directly east of site 31MA684 and east of NC 28 and its intersection with Rose Creek Road, in a fallow field on a hilltop terrace. The elevations range from roughly 1,930 AMSL, on the floodplain, to about 1,990 AMSL, on the hilltop (Figure 1). The floodplain consisted of Rosman fine sandy loam, 0 to 2 percent slopes, frequently flooded. The hilltop area was predominately Braddock clay loam, eroded with 2 to 8 percent slopes with some Braddock clay loam, eroded with 8 to 15 percent slopes (Figure 3) (http://websoilsurvey.sc.egov.usda.gov). Rosman soils are found on flood plains in the Southern Appalachian Mountains and form in recent loamy alluvium derived from igneous, high-grade metamorphic or low-grade metasedimentary geology (https://soilseries.sc.egov.usda.gov). In this location, the soil is characterized by a dark brown surface layer (A horizon) and a strong brown (Bw horizon) subsoil (Idol 2017). Braddock clay loam soils are found on foot slopes of ridges and high terraces in colluvium and alluvium derived mainly from a mixture of crystalline rocks (https://soilseries.sc.egov.usda.gov). It ranges in color from reddish brown surface layer (Ap horizon) and a red clay (Bw) subsoil (Idol 2017).

The project area resides within the Appalachian summit region of North Carolina (Figure 2). This region can be divided into 5 main cultural time periods- Paleoindian (9000-8000 B.C.), Archaic (8000-1000 B.C.), Woodland (1000 B.C.-1000 A.D.), Mississippian (1000-1500), and Protohistoric/Historic (1500-1838 A.D.)-with each period being subdivided into several phases (Idol 2017; Keel 1976; Rodning 2004; Ward and Davis 1999; Wetmore 2002). Site 31MA684 had evidence of continued habitation from the Paleoindian period through the historic period; site 31MA774 primarily exhibited evidence of habitation in the Late Qualla phase (Idol 2017).

Five grids were established to conduct the geophysical survey across both sites. A Topcon GTS 233W total station was used to mark all grid corners in relation to the temporary datums established by TRC Inc. This insured that the coordinates collected by the geophysical team and TRC would accurately match within the Geographical Information System (GIS) used to analyze the data. A Topcon GR-3 Global Positioning System (GPS) was then used in concert with the total station to tie the previously established grids and TRC datums to Universal Transverse Mercator (UTM) Zone 17.

Site 31MA684 (floodplain) was initially surveyed with the magnetic gradiometer followed by the GPR (Figures 4 and 5); 31MA774 (Hilltop) was surveyed in the same manner (Figures 6, 7, 8 and 9). Magnetometer data were collected by a Bartington 601 Dual Gradiometer (Figure 10) and TerraSurveyor2 software was used for all data processing. The Bartington internal software limits survey grid size to either 10X10, 20X20, or 30X30 meters. After field inspection, it was determined that 30x30 meter grids would most effectively cover 31MA684, the floodplain (Grids 1 and 2). After inspection of 31MA774, the hilltop, three survey locations were chosen by TRC and the geophysical team; these included two 10X10 meter locations, grids three and five, and one 20x20 meter location, grid four (Note: Due to the lack of significant geophysical findings in grid 5, it was decided by TRC to not excavate this area and as such will not be discussed any further in this paper).

The Ground Penetrating Radar (GPR) used was a GSSI 3000 with a 400 MHz antenna (Figure 11). The same grids were used in the GPR survey as with the magnetometer, with the GPR area coverage extending slightly further south at 31MA684 towards Rose Creek Road and McCoy Bridge (Figure 5). Each of the grid corners were located by the total station (Figure 1).

Prior to magnetometer data collection, the machine must be calibrated. This is done in as magnetically neutral an area as possible on site; the same location was used each day. The pace of the instrument operator was tested and the instrument was setup for that individual’s pace. The data were collected in a zigzag manner, walking the grid in transects based on true north then south. Two lines were collect per meter, creating transects at 50 centimeter intervals. Eight samples were taken per meter for a total of one hundred sixty per transect. The range was set to 100 nT (nanoTesla) with a threshold of 1nT and a reject range of 50 Hertz (Hz) (Aspinall et al. 2008). The data were downloaded from the Bartington to computers in the Geography GIS laboratory that contained the TerraSurveyor software.

The magnetometer data of each grid were individually processed, then combined into a composite so they could be clipped, despiked and viewed as a whole. Each individual grid was first clipped to approximately 10 nT to improve visibility, then DeStaggered to help compensate for errors generated when operators started too soon or too late. All the individual grids were also DeStriped. This process helps to compensate for effects of different operators, instrument setup and drift. Every effort was made to assure that data were collected as consistently as possible. Overall the data aligned fairly consistently between collection units and the same and/or similar anomalies can be detected between the grids (Clark 1996; Kvamme 2006).

GPR data were gathered similar to that of the magnetometer. However, there were no constraints on grid size and dimensions as seen with the magnetometer. This allowed the geophysical team to run longer transects on the floodplain. Rose Creek Road, which runs perpendicular to the floodplain, contains a metal guard rale that obscured the magnetometer data (Figure 4), so it was hoped that the GPR might be of greater use in that location (Figure 5). A 400 MHz antenna was used collecting data at 50 centimeter transects, with a dielectric constant set to 8 and data were collected in 16-bit format.

All GPR data were downloaded from the Radan SIR3000 unit to computers in the Geography GIS laboratory where the data could be post-processed using Radan 7 software. The first post-processing step was to set the data to time zero, this helps the profile create a true ground surface by removing space generated by the antenna carrier. A background filter was then applied to help normalize the data and remove noise. Finally, the average relative dielectric permittivity (RDP) of the soils was determined for each date using hyperbolic reflections visible in the vertical profiles. This was accomplished by using the ghost fitting tool in the migration pane of RADAN 7. After fitting the curve to match hyperbolic shapes, the profile number and reflector distance from the transect start were recorded in a spreadsheet, along with the velocity estimated by the ghost fitting tool. The RDP of the soils above each reflection was calculated in another column using the formula published by Conyers (2004):

K = (C/V)2

Where:
K = Relative Dielectric Permittivity
C = speed of light in a vacuum, .2998 m/ns
V = velocity of radar energy through soil, m/ns

Following the calculation of RDP for each reflector, the mean RDP of the collection date were used for slice map export. Each slice was examined at a .10 m thickness. Each grid was saved as a .tiff file and then georeferenced for excavation planning and dimensional analysis using ArcMap 10.2.2 (Conyers, 2004; Lowry and Patch, 2010; Patch 2008; Patch 2009; Patch 2010; Radan7 Users' Manual, 2011).

A total of four hundred two features excavated by TRC were located within the remote sensing grids. A total station was used to mark each feature's centroid. A point file was then created and overlaid onto the corresponding remote sensing grids in ArcMap 10.2.2. Transect lines, spaced 50cm apart, were generated on each grid so that features identified by TRC could be quickly located in the specialized geophysical software (RADAN 7.4.15, for GPR, and TerraSurveyor, for magnetic gradiometer) for analysis purposes. When comparing the geophysical signatures with the TRC generated feature location map, each documented feature would fall into one of three categories for analysis purposes:

- Yes (y), the geophysical data indicated the presence of a feature located in the field
- Maybe (m), potential evidence for a feature may be recognizable in the geophysical data, but not enough to positively identify
- No (n), no geophysical evidence exists that would lead researchers to identify the presence of a feature

Once each feature's location was determined in the GPR and magnetometer software the analyst would determine which category (Yes, No or Maybe) the feature would be placed. In RADAN the profile view and 3D cube were inspected to see if any hyperbolic reflections or anomalies existed. If a hyperbolic reflection could be seen or a significant geophysical anomaly was present the analyst would indicate depth and probably cause, such as pit or post, and a 'y', meaning highly confident that the geophysical equipment detected the feature, would be entered under the 'GPR' heading into the attribute table. Features that exhibited weak hyperbolic reflections or were in areas that exhibited 'noise,' such as coupling errors caused by the antenna going over furrows in a plowed field or the point location was very close to other strong geophysical returns, were given an 'm'. TRC mapped features with no geophysical evidence associated with their locations were given an 'n' in the attribute table. The analysis of the magnetometer data was conducted in a manner similar to that of the GPR data.

Each feature's centroid was used to create a point file which was then overlaid on the gradiometer remote sensing grid. A 'y' was input into the attribute table under the 'Mag' heading if monopolar or dipolar signatures were present and were associated with a feature. Magnetic signatures that appeared near the TRC points, within 50 centimeters or less from the marked location, and points that were located on the edge of the remote sensing grids, where a complete analysis could not be completed, were given a 'm' under the 'Mag' heading in the attribute table. If no magnetic variance was seen within the vicinity of the associated point, the feature was given a 'n' under the 'Mag' heading in the attribute table.

Ten sets of samples (2 in a set) of soil were collect in the field for bulk density analysis, which gives an indication of soil compaction (www.nrcs.usda.gov). Each set consisted of a sample taken from within the designated feature's matrix and the soil matrix directly outside the same feature. The soil auger used to take each sample had a width of 0.6 tenths of an inch with a collection sample length of 3 tenths of an inch. English units were converted to centimeter to make calculations easier:

Diameter=1.7
radius=.85
Height=9.1

These numbers were placed into the formula:

$V=\pi r^2 h$

To compute the Volume of the sample

A wet and dry weight was established for all samples used in the bulk density analysis. This was accomplished by first weighing the tin foil tray that the soil was placed in, weighing the tray with the soil, and then baking the soil in a 100 degree Celsius oven for at least two hours to remove all the moisture from the soil. The trays were then weighed after the removal from the oven, subtracting the tin foil tray weight from the wet and dry weights of the soil so that each sample's bulk density could be determined. The Bulk Density equation is:

BD=DW/V

Where:
BD is bulk density
DW is the dry weight of the soil sample and
V is the volume of the soil sample
(www.nrcs.usda.gov)

Figure 3. McCoy Bridge Geophysical Survey Grids with SSURGO Soils Overlay

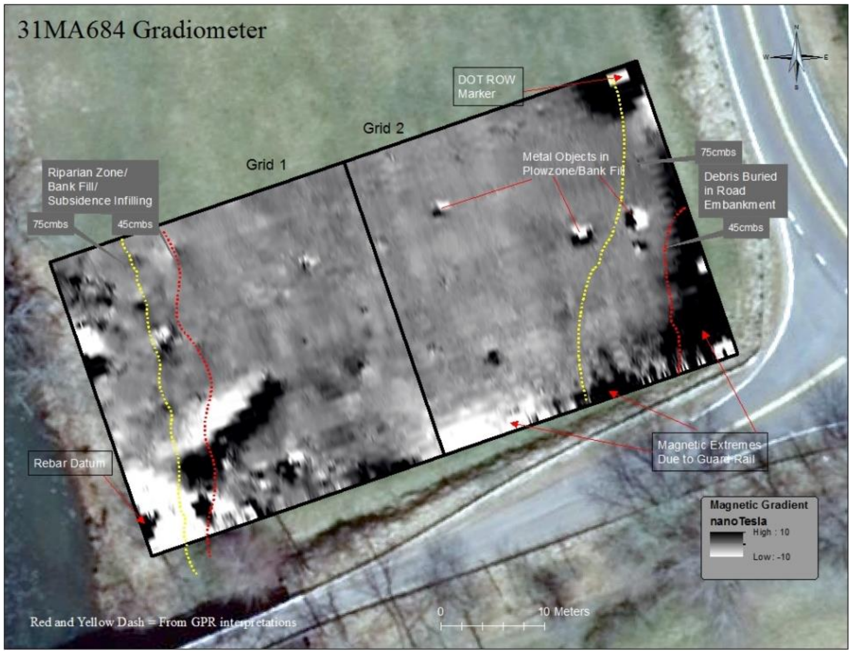

Figure 4. **MA684 Grids 1 and 2 Magnetic Gradiometer Results**

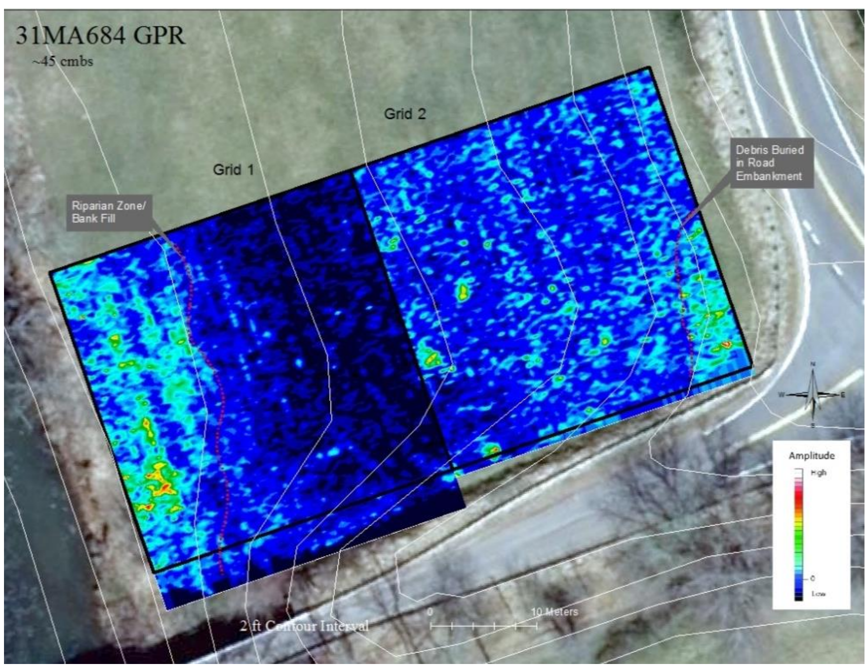

Figure 5. **MA684 Grids 1 and 2 GPR Results, 45 Centimeters Below**

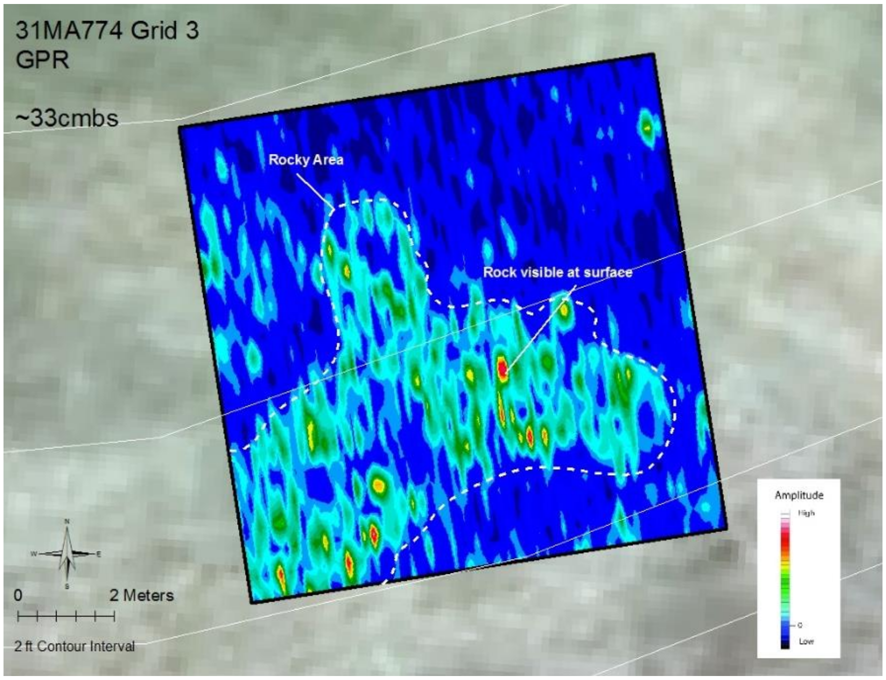

Figure 6. MA774 Grid 3 GPR Results; 33 Centimeters Below the Surface

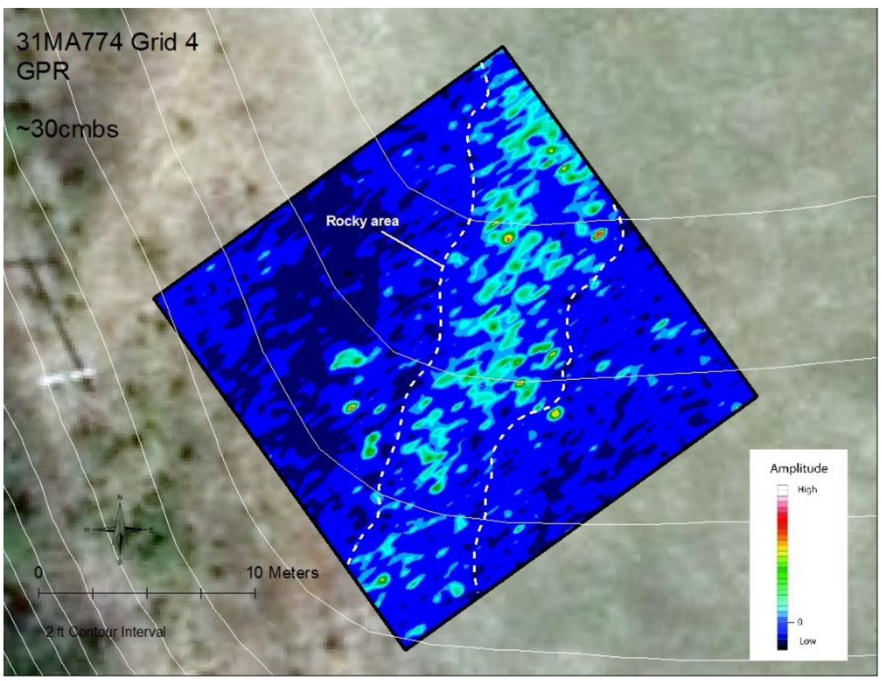

Figure 7. MA774 Grid 4 GPR Results, 30 Centimeters Below the Surface

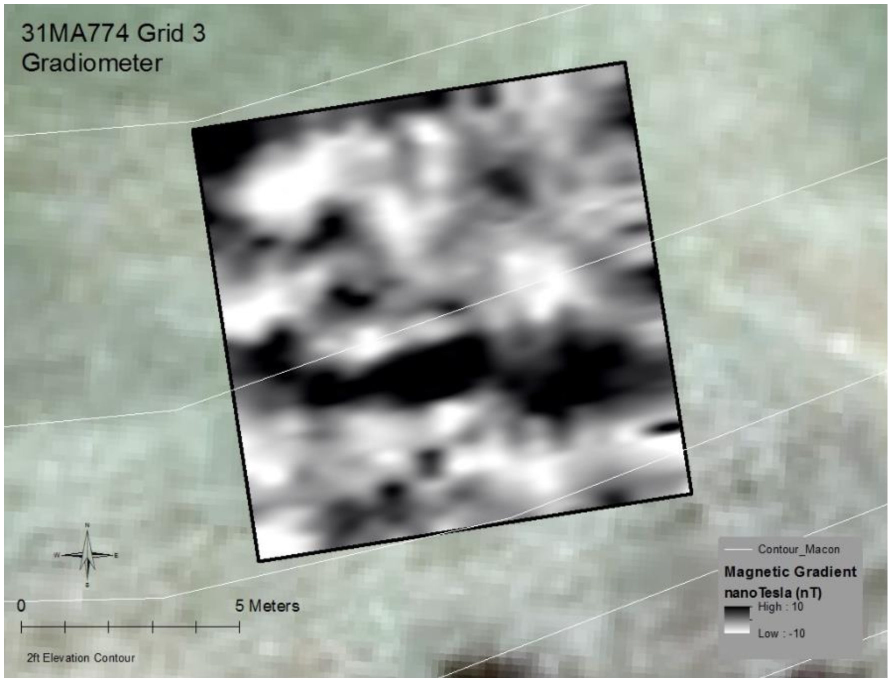

Figure 8. MA774 Grid 3 Gradiometer Results

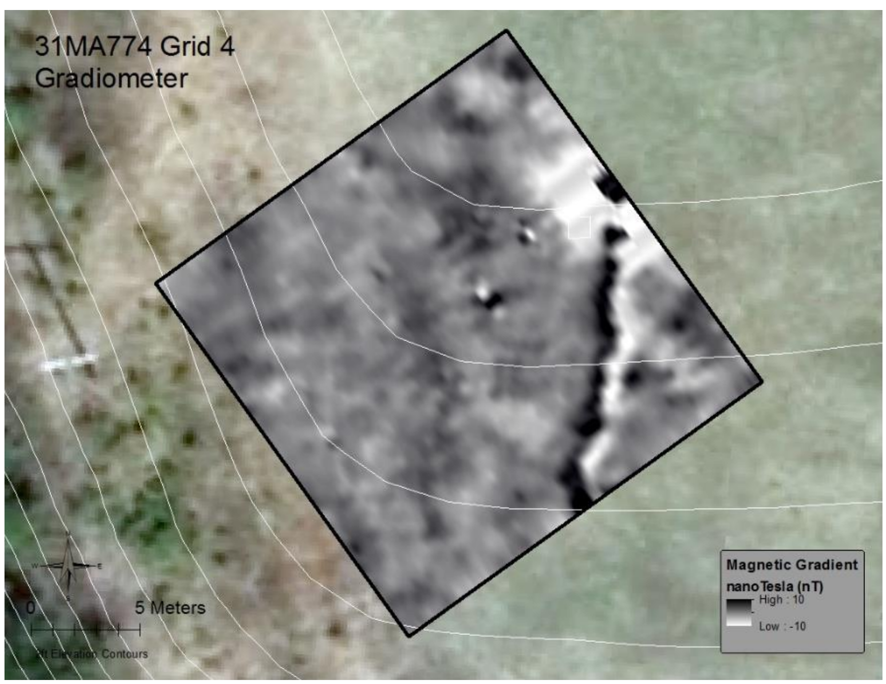

Figure 9. MA774 Grid 4 Gradiometer Results

Figure 10. Bartington 601 Dual Magnetic Gradiometer

Figure 11. GSSI 3000 Ground-Penetrating Radar (GPR) with a 400 MHz Antenna

CHAPTER IV

RESULTS

One or both of the instruments were able to positively identify 15 cultural features (3.73%) and 51 (12.69%) of the cultural features were placed in the maybe ‘m’ category (Figure 12 and 13). TRC archaeologists categorized the excavated features within the remote sensing grids into six classes, with two additional items, a vessel and a feature referred to as a smoke hole (which will be discussed later), classified independently (Figure 14). Of the 402 features examined by TRC following plow zone removal in the remote sensing grids, 15 could be positively identified in the remote sensing data using one or both instruments (Figure 15). There were a total of 95 features classified as ‘non-cultural’ (code 0), of those, three were positively identified. The remaining 307 features located by TRC were all associated with cultural processes. For a complete listing of all features refer to Appendix A.

Within the cultural features a total of 221 were classified by TRC as ‘unassigned post/post associated with structure’ (Code 1). Three posts were positively identified, solely by the GPR. The posts ranged in diameter from 4 cm to 35.5 cm. They were positively detected in GPR profile and 3D cube views as deep as 40 cm below the surface, with the shallowest reading at approximately 21 cm below the surface. The largest positively identified post, feature 563, was clearly visible at the edge of the floor midden of structure 1. There were several smaller reflections directly before and after the location of feature 563 visible in the GPR profile that may be indicative of other post features (Figure 16). The next category as specified by TRC was 'maybe post/maybe post associated with structure' (code 2). TRC identified 67 features falling into this class. Only one 'maybe post' was detected during the geophysical examination and the only instrument to do so was the gradiometer. Both the instruments had trouble locating the features in the post category.

The magnetometer proved to be the most efficient instrument for locating features from the 'pit, real/ambiguous,' (code 3) category. The pit group contained 12 associated features. The GPR and magnetometer were collectively able to locate five of this class. Three pits were identifiable with both the GPR and magnetometer, two of which, features 339 and 350, were situated close to one another in grid three (Figure 17). One additional pit was discernable with the GPR only (Figure 18) and two with the magnetometer only (Figure 19). The pit feature (feature 567) that was missed by the magnetometer was also described as a rock cluster by the archaeologists. It is highly likely the rocks produced the reflections seen in the GPR profile (Figure 18). The pits range in size from 30-145 cm wide and 47-172 cm long.

The gradiometer was the only instrument that could determine the approximate location of the category classified as Grave (code 4). A faint anomaly was detected in the GPR profile and 3D view, however due to the amount of noise present and relatively small contrast between the grave and the surrounding soil, a positive identification was not possible. There were 3 graves present across both sites; the gradiometer was able to successfully find one (Figure 20). Due the sensitive nature of Cherokee burials the exact location of the graves cannot be divulged.

The last classification ‘hearth’ (code 5) had a total of two features associated with it. The geophysical instruments were both able to detect one of the two hearths. This was feature 569, which was associated with the winter house. The hearth measured 86x86 cm (Figure 21).

Fifty-one (12.69%) of the 402 excavated features that are given an ‘m’ (maybe) in either the GPR or Mag heading in the attribute table. These features show potential evidence for a feature location in the geophysical data, but not enough to confidently identify them. There were a total of 15 features within the remote sensing grids that were categorized as ‘non-cultural’ (code 0) with an ‘m’ classification. The GPR was able to potentially detect 14 of these features, while the gradiometer was able to potentially identify one. The classification that makes up the largest portion of the ‘m’ geophysical survey category was the ‘unassigned post/post associated with structure’ (code 1) which contained 221individual locations from the TRC archaeology maps. In the analysis 27 features were given a ‘maybe’ for the code 1 ‘unassigned posts/posts associated with structure’ category. The GPR can potentially identify 25 of these. The posts ranged in diameter from 11 to 29.5 cm and range in depth from 15 to 62 cm below the surface. In GPR profile 20, from Grid 2, post feature 528 appears to be faintly visible near the edge of the floor midden in structure 1. However due to the undulating surface caused from continuous plowing there are coupling errors present distorts potentially masking and/or giving false readings with in the data (Figure 22). The two remaining unassigned posts were seen as faint magnetic monopoles in the gradiometer survey grid.

Of the 67 features that were given a ‘maybe post/maybe post associated with structure’ code 2 category by TRC, seven are potentially visible in the geophysical data sets. Enough evidence was present in the GPR profiles for six of these features to warrant a classification of ‘m’. In GRP profile 21, grid 2, a faint trace of feature 530 can be seen (Figure 23). This GPR return also contained the coupling errors, mentioned in Figure 22, caused by the antenna movement over the plow zone. The depth, seen in the GPR profile view, ranges from 15-55 cm below the surface. The gradiometer revealed a faint monopole within structure 2, feature 74 possible post (code 2) and feature 70 unassigned post (code 1) (Figure 24). These posts range in diameter from 10-31 cm.

The final classification where any evidence of a feature’s location was interpreted as an ‘m’ by one or both of the geophysical instruments is the ‘pit, real/ambiguous,’ (code 3) category. Of the 12 pit features excavated, two were given an ‘m’ by the GPR. The GPR and the gradiometer agreed that feature 508 in Grid 3 rated an ‘m’ (Figure 25). The gradiometer has what appears to be a monopolar anomaly associated with the feature location and the GPR shows faint hyperbolas. The location of feature 508 was on western edge of the remote sensing Grid 3 and extended out of the survey area so there was not enough of the feature to make a positive identification.

The remaining 336 (85.58 percent), features, which include the ceramic vessel, located within the remote sensing grids and excavated by TRC were undetectable by either the GPR or gradiometer. A prime example of this comes from Grid 4 where at the location of an excavated post, feature 372, there is no evidence of any anomaly. The GPR profiles 34 and 35 contain very little noise or coupling errors; yet no posthole feature can be detected (Figure 26). There are several considerations one must take into account when doing this type of survey that could explain this lack of evidence and the discrepancies between geophysical and archaeological results.

A bulk density analysis was also undertaken to determine if any significant difference in soil density existed between the features in question and the surrounding soil. In general, it was found the surrounding soil matrix retained slightly more moisture and had a higher bulk density than the sampled post features. The difference was not statistically significant.

For postholes, features 44-222, the dry weight (Figure 27) within the feature was consistently less than the dry weight outside the feature. The bulk density (Figure 28) was also consistently less inside the feature than outside the feature. The soil bulk density ranged from 0.92 g/cm^3 to 1.5 g/cm^3 inside the feature to 1.46 g/cm^3 to 1.73 g/cm^3 outside the feature. The differences ranged from a low of 0.11 g/cm^3 to a high of 0.58 g/cm^3, with an average of about 0.40 g/cm^3. The posthole samples used for bulk density analysis came solely from the flood plain (site 31MA684) due to the vast majority of post holes that were recovered from there. Neither of the geophysical equipment were able to detect these features.

The smokehole daub (feature 324) displayed similar results to those of the post features. The feature's dry weight and bulk density within the feature were less than the dry weight and bulk density outside the feature with a difference in bulk density of about 0.17

g/cm^3. The soil outside the feature revealed a bulk density of 1.57 g/cm^3. However, unlike the post features, this feature was able to be detected by both the GPR and the gradiometer.

The remaining features (337, 339, and 393) were pit features located on the hilltop (site 31MA774). The hilltop area was predominately Braddock clay loam, eroded with 2 to 8 percent slopes (http://websoilsurvey.sc.egov.usda.gov). Feature 337 was located outside the geophysical survey grids. Features 339 and 393 were both located in geophysical survey Grid 4 with feature 339 detected by both geophysical instruments. Feature 393 would likely have been detected with the gradiometer had the grid (Grid 4) been extended to the east-southeast and the linear dipole feature that ran south-southwest through the grid not been present (Figure 9). The pits differed from the post features in that the bulk densities were greater inside the feature matrix than outside the feature matrix. The soil outside these features showed a bulk density that ranged from 1.12 g/cm^3 to 1.54 g/cm^3. Of the pit features, features 337 and 339 displayed the greatest difference in bulk density between the inside and outside soil matrix; 0.09 g/cm^3 and 0.06 g/cm^3 respectively. Feature 393 also exhibited a greater difference in bulk density inside versus outside the feature but to a much lesser degree; 0.006 g/cm^3.

Soil moisture content of the sampled features were also looked at to determine if any correlation existed between it and bulk density, and by association, the ability of the GPR to distinguish features from the surrounding soil matrix. It was assumed that as bulk density increased, soil moisture would decrease. To test this relationship between bulk density and soil moisture a simple regression analysis **(**Figure 29**)** was conducted using the Data Analysis module in Microsoft Excel. Bulk density was input as the independent variable (x) and water content as the dependent variable (y). Based on the results it was found that no such relationship existed (R^2=0.05, Significance F=0.34). However, when a scatter plot (Figure 30**)** was created from the data and fitted with a line of best fit, a weak negative relationship was observed. As expected, when bulk density increased soil moisture decreased. A probable cause for these conflicting results is likely due to water not being uniformly applied to all samples taken in the field.

The following section will discuss a variety of geophysical features, both cultural and geologic in origin. It will address possible causes of the successes and misses of the survey, as well as elaborate on the capabilities of the instruments and the factors that hinder or facilitate the detection of features and objects.

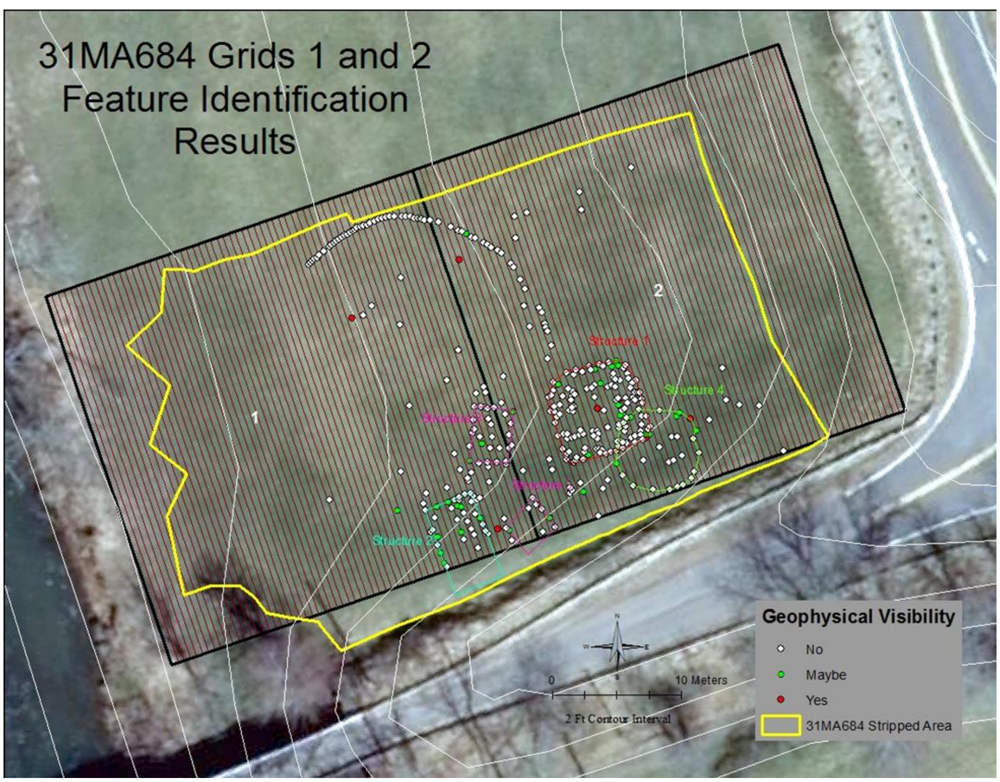

Figure 12. Feature Identification Results 31MA684

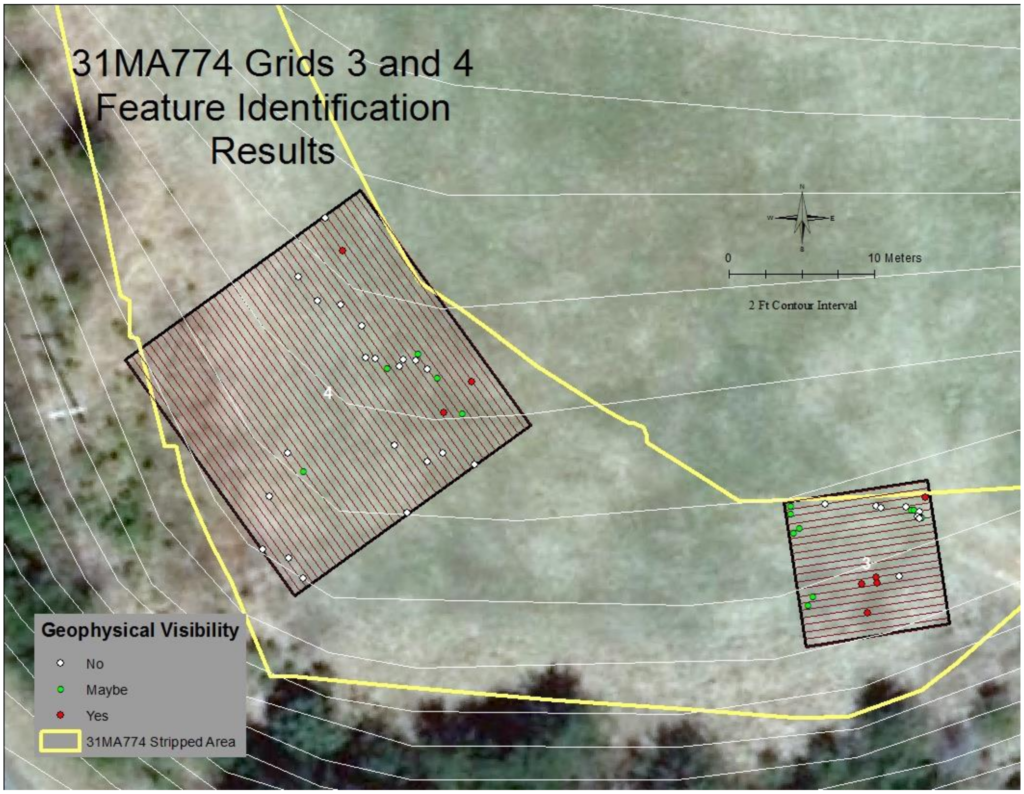

Figure 13. Feature Identification Results 31MA774

Code	Description	Total
0	Non-cultural	95
1	Unassigned post/post associated with structure	221
2	Maybe post/maybe post associated with structure	67
3	Pit (real, ambiguous)	12
4	Grave	3
5	Hearth	2
N/A	Smokehole	1
N/A	Vessel	1

Figure 14. Code Description Developed by TRC Archaeologists

Code	Feat. No.	GPR	Mag	Post Diam.	Pit Length	Pit Width	GPR Depth	Site	Type
0	21	y	n	X	X	X	35	31MA684	post-noncultural
0	460	m	y	X	X	X	25	31MA774	post-noncultural
0	507	m	y	X	X	X	28	31MA774	post-noncultural
1	214	y	n	X	X	X	21	31MA684	post-real
1	563	y	n	19.5	X	X	40	31MA684	post-real
1	570	y	n	15.5	X	X	31	31MA684	post-real
2	444	n	y	11	X	X	X	31MA774	post-ambiguous
3	**339**	**y**	**y**	**X**	**120**	**112**	**31**	**31MA774**	**pit-real**
3	510	n	y	X	47	32	X	31MA774	pit-real
3	511	n	y	X	49	30	X	31MA774	pit-real
3	**350**	**y**	**y**	**X**	**145**	**145**	**19**	**31MA774**	**pit-real**
3	**301**	**y**	**y**	**X**	**172**	**125**	**52**	**31MA684**	**pit-real**
3	567	y	n	X	60	42	24	31MA684	rock cluster
4	340	n	y	X	130	70	70	31MA774	grave
5	**569**	**y**	**y**	**X**	**86**	**86**	**20**	**31MA684**	**Hearth**
Total Yes		9	10						

Figure 15. Archaeological Features Identified by Geophysical Instruments: Features in Bold Identified by both Instruments

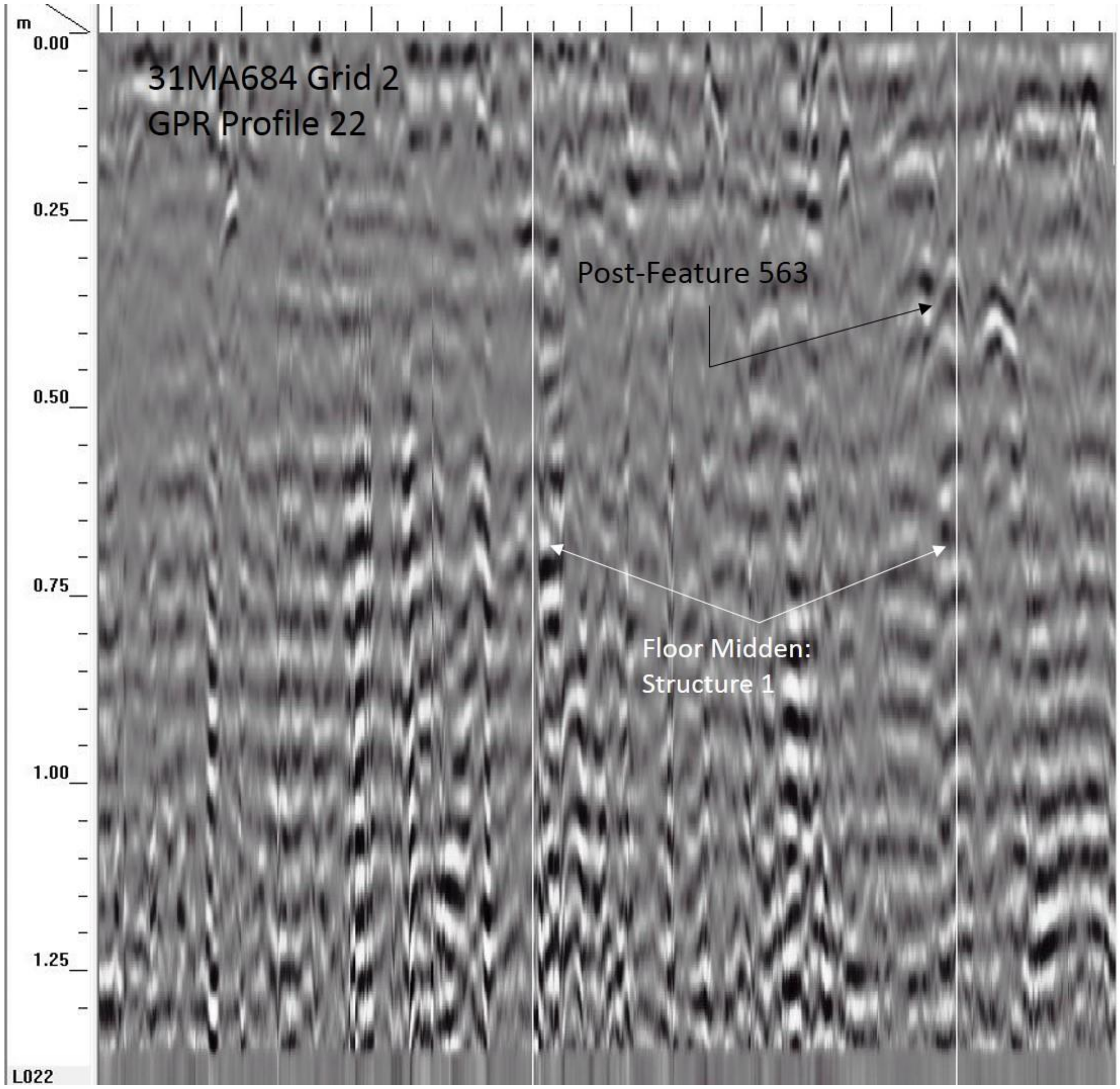

Figure 16. Feature 563: Post Associated with Structure 1

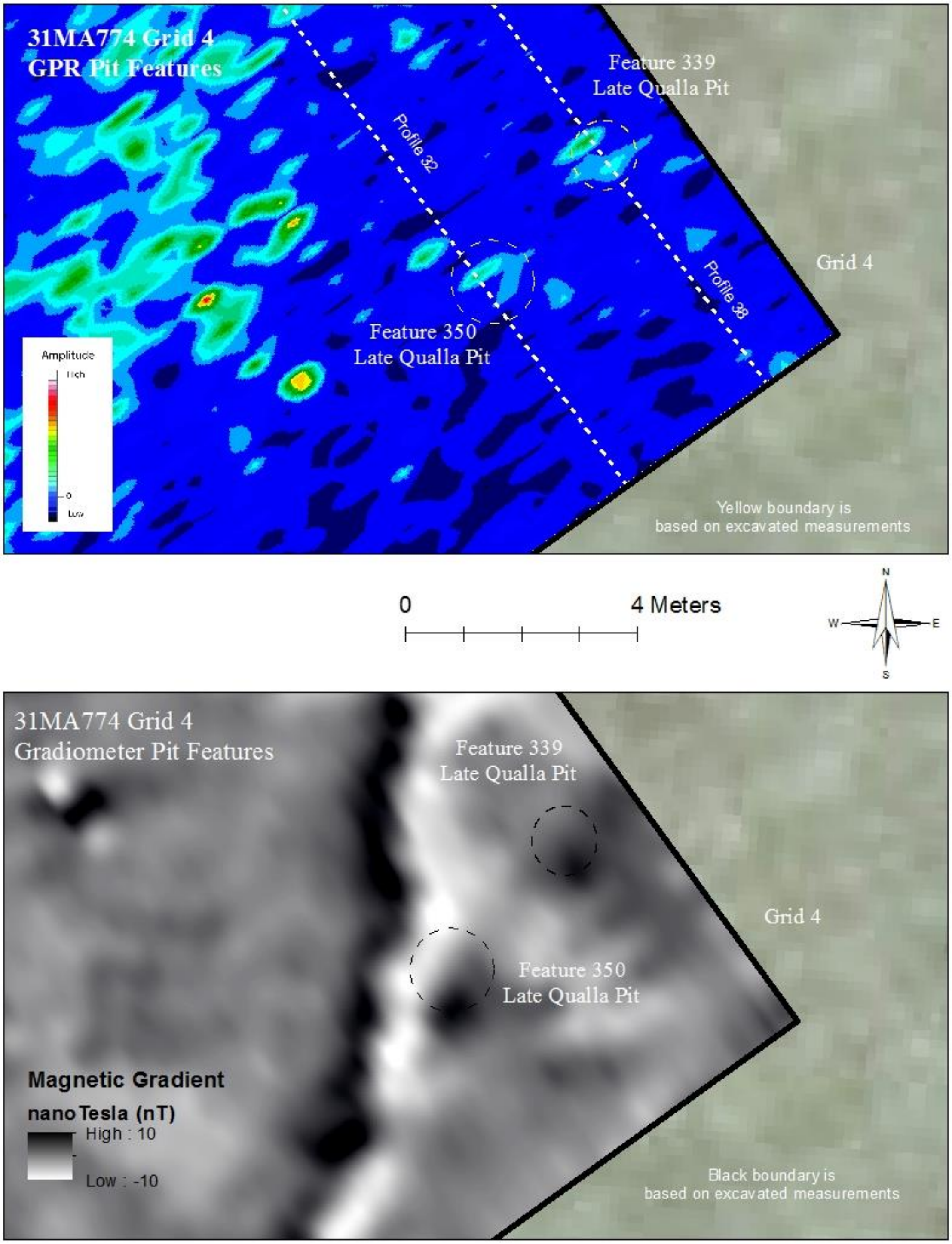

Figure 17. Grid 4 Pit Features 339 and 350

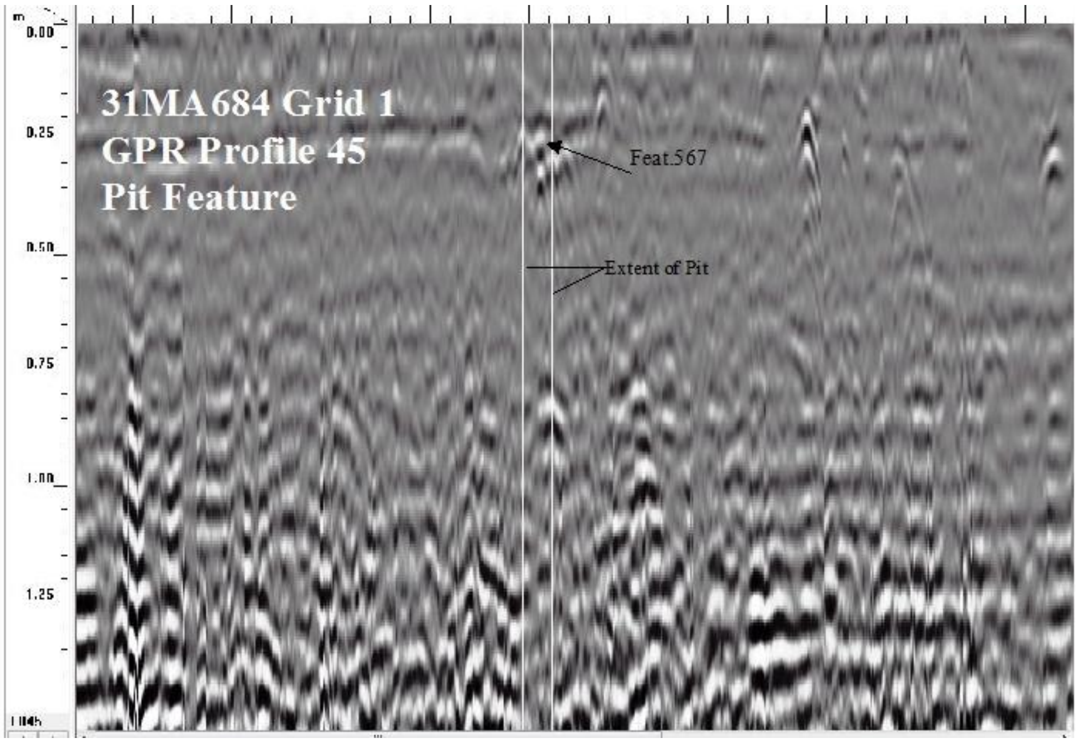

Figure 18. **Pit Feature 567**

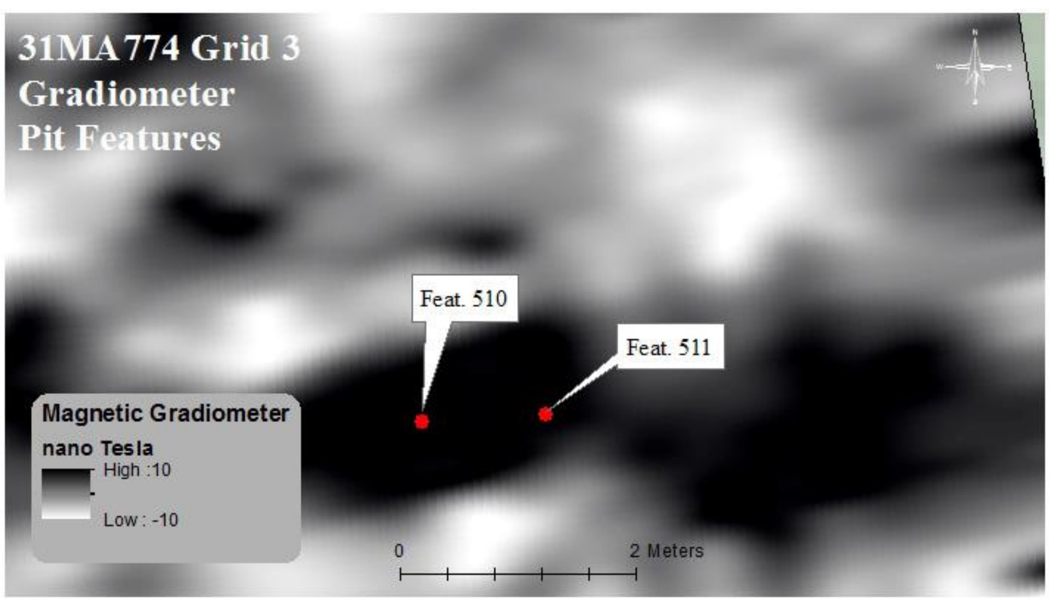

Figure 19. **Pit Features 510 and 511**

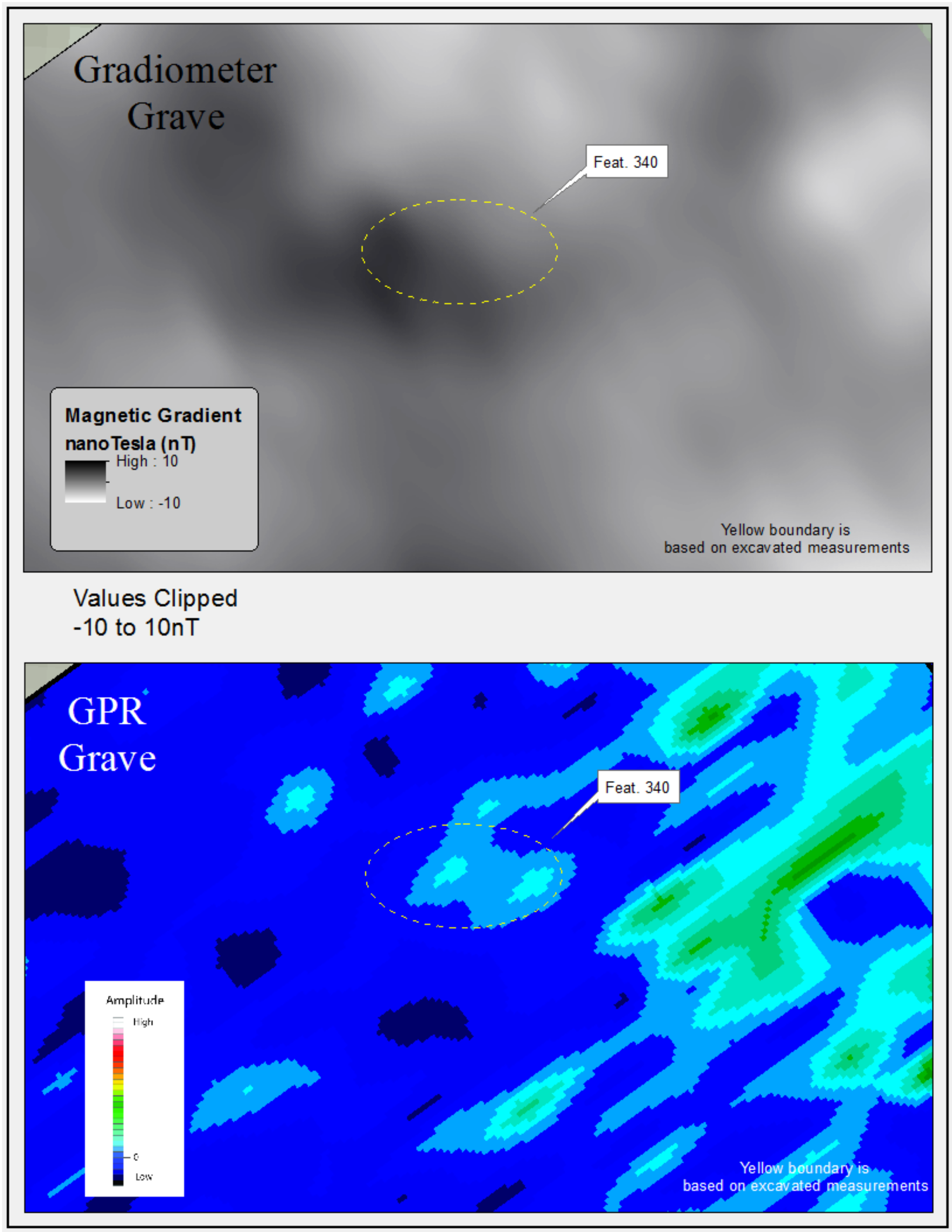

Figure 20. **Grave Feature 340**

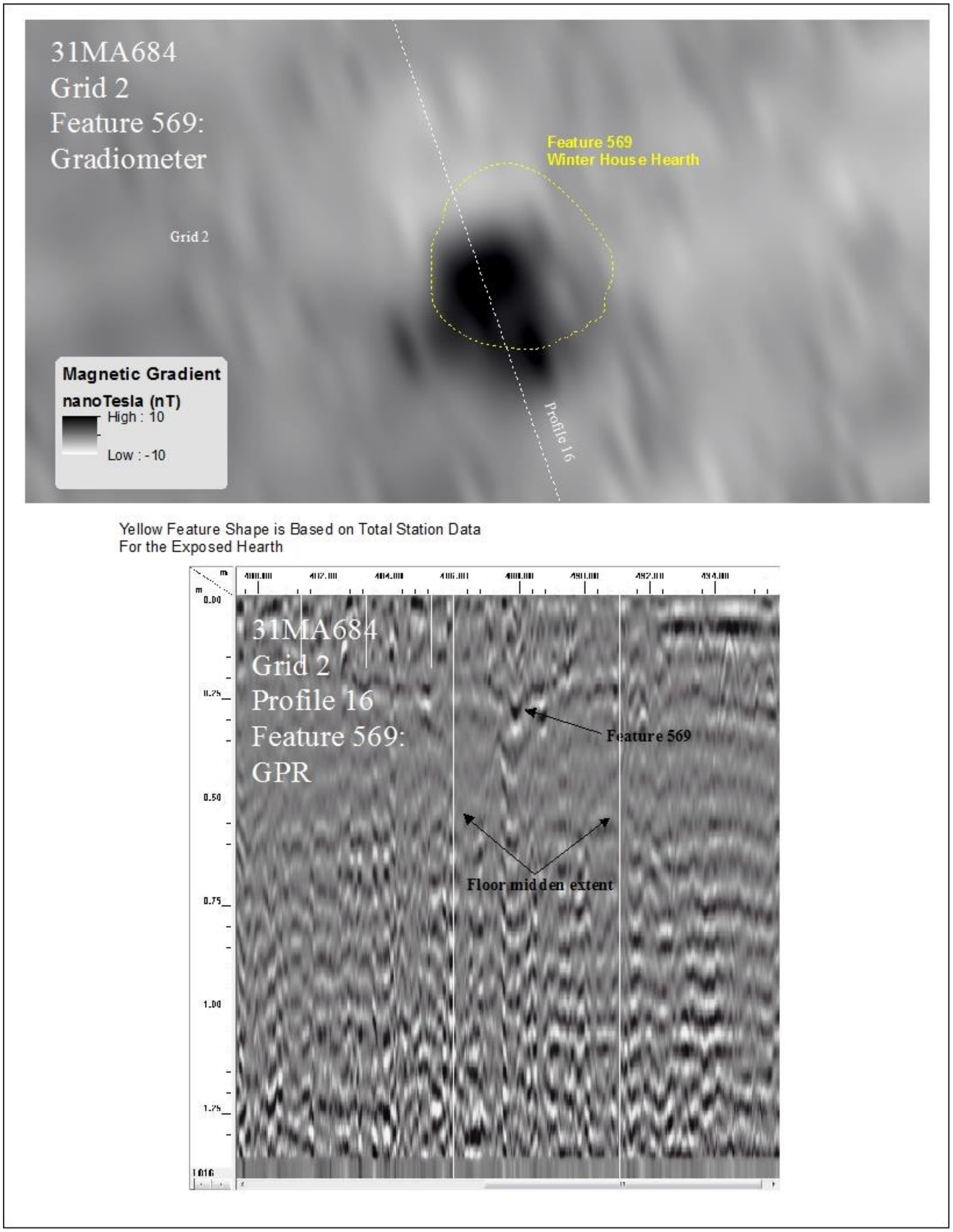

Figure 21. Feature 596 Winter House Hearth

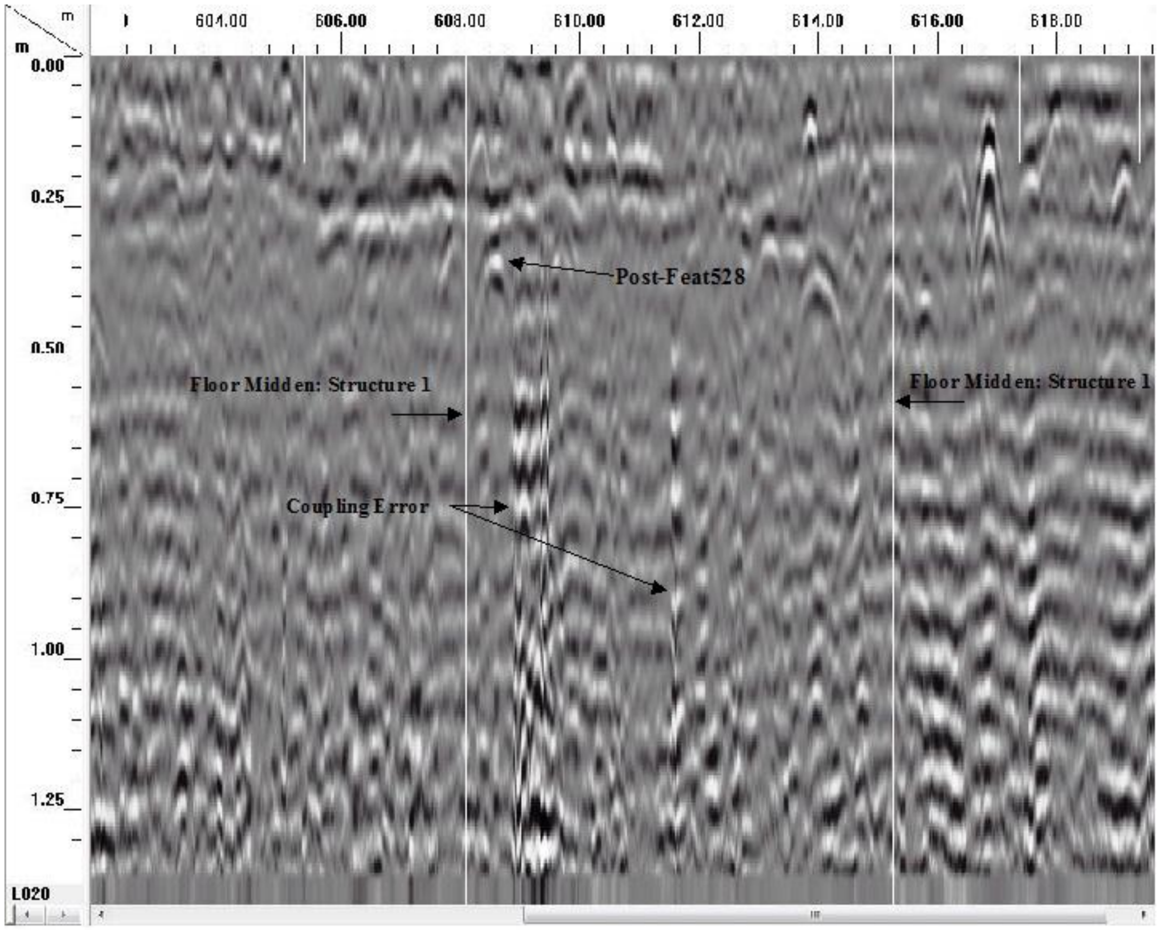

Figure 22. **Post Feature 528**

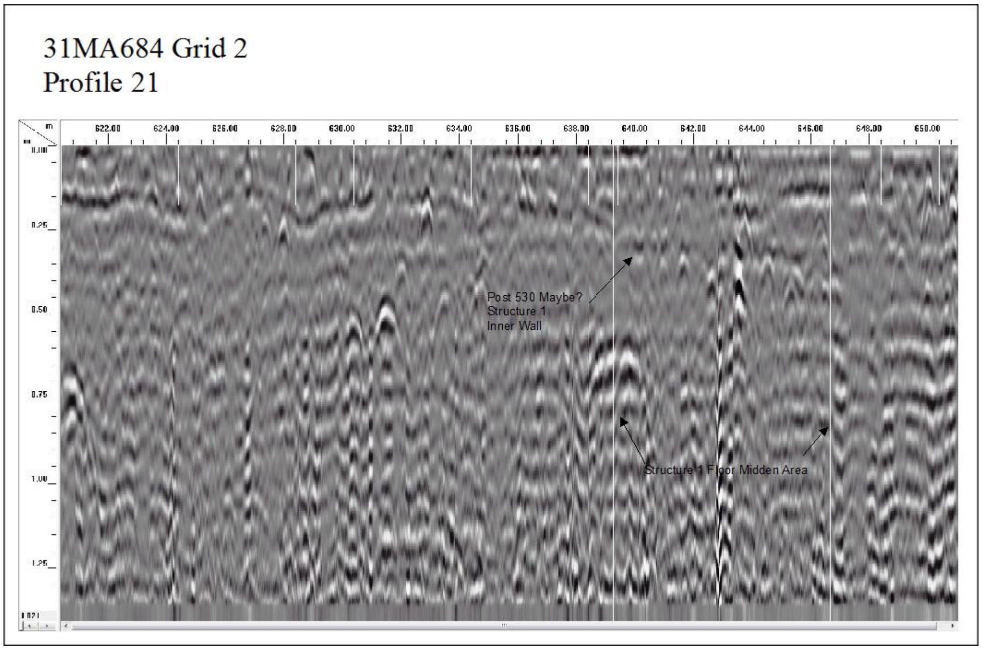

Figure 23. Possible Post Feature 530

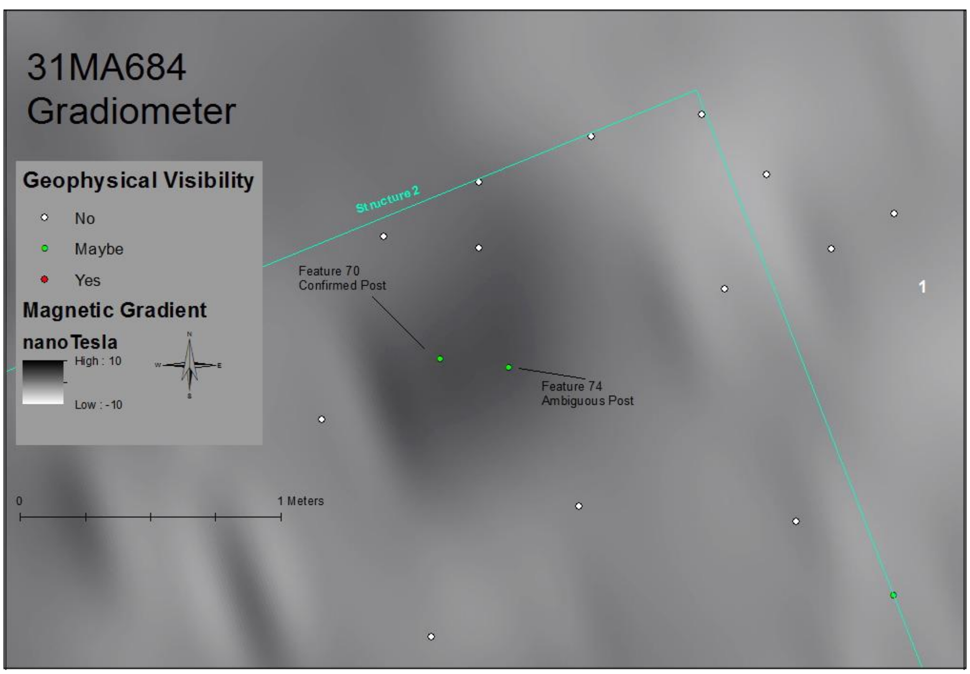

Figure 24. Structure 2 with Possible Post Feature 74 and Unassigned Post Feature 70

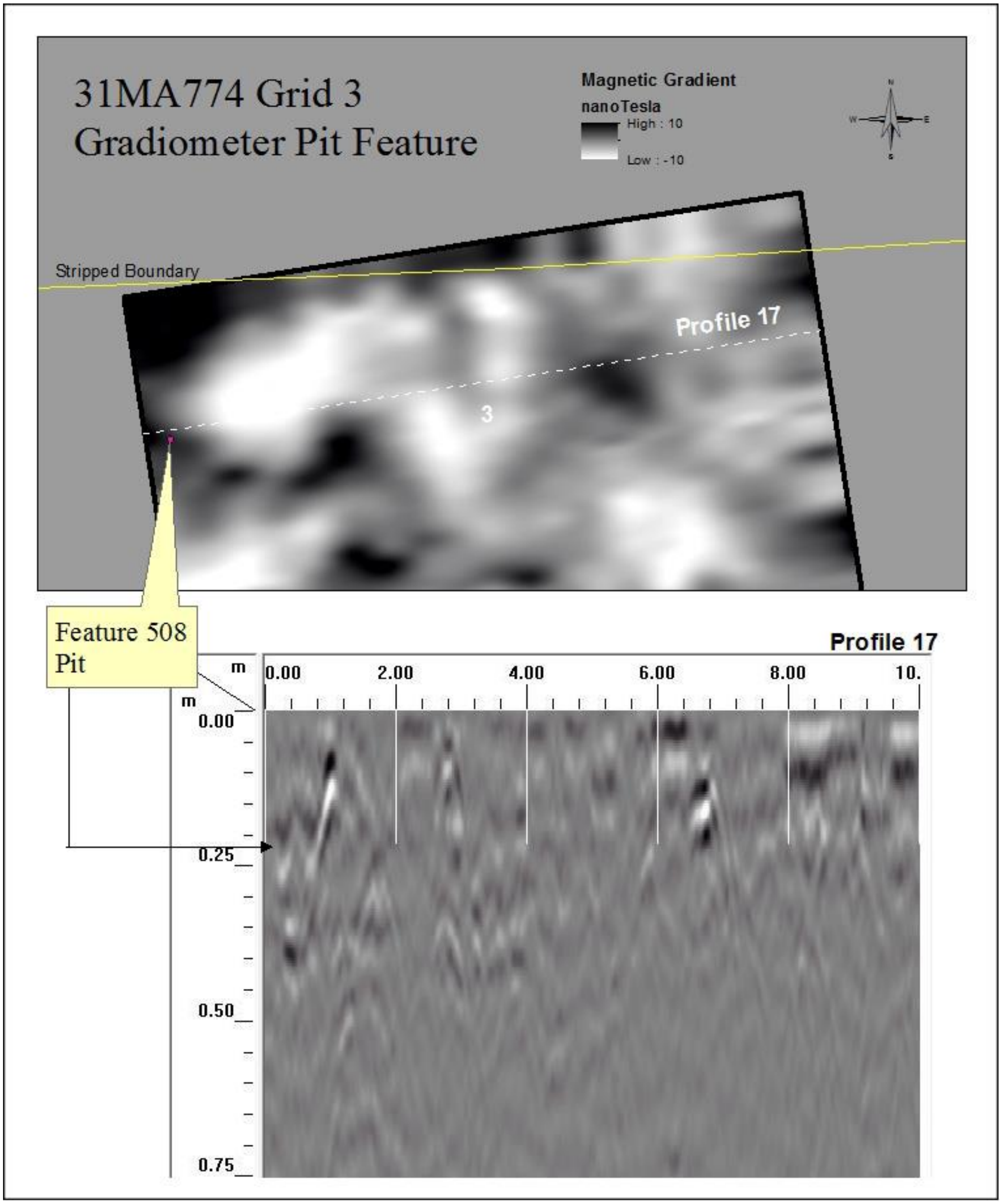

Figure 25. Possible Pit Feature 508

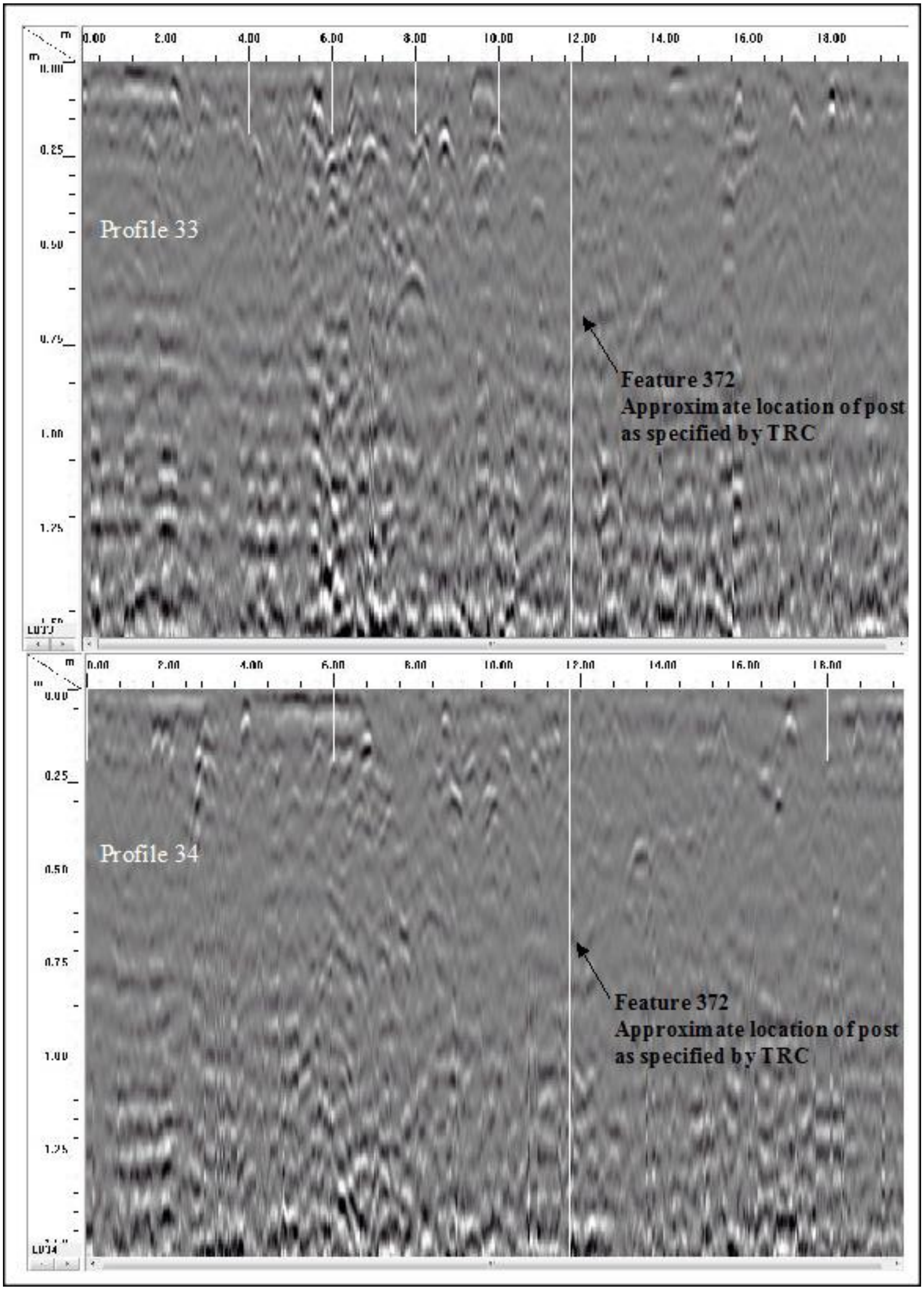

Figure 26. No GPR Return for a Known Post. Feature 372

Tin Wght	IN			Tin Wght	OUT		
	Wet	Dry	Difference		Wet	Dry	Difference
3.921	30.557	25.414	5.143	4.575	38.969	32.901	6.068
3.514	35.729	30.908	4.821	5.033	42.332	35.649	6.683
5.269	35.835	30.616	5.219	3.679	38.578	32.875	5.703
3.225	30.882	26.233	4.649	4.891	40.581	33.72	6.861
3.809	21.979	18.903	3.076	4.629	35.95	30.211	5.739
5.688	26.279	22.305	3.974	3.295	38.178	34.103	4.075
3.795	33.45	28.791	4.659	5.113	39.319	32.338	6.981
4.468	39.664	33.682	5.982	4.738	38.444	31.806	6.638
4.963	29.205	24.387	4.818	4.777	28.394	23.209	5.185
4.529	31.059	25.61	5.449	4.339	31.661	25.513	6.148

Figure 27. McCoy Bridge Soil Samples Wet/Dry Weights

Fea	DW-in	DW-out	B_Den-inside feature	B_Den-outside feature
44 post hole	25.414	32.901	1.230463833	1.592960201
52 post hole	30.908	35.649	1.496465576	1.72600949
72 post hole	30.616	32.875	1.482327878	1.591701365
117 post hole	26.233	33.72	1.270117169	1.632613537
171 post hole	18.903	30.211	0.915222233	1.462719086
222 post hole	22.305	34.103	1.07993609	1.651157161
324 hearth	28.791	32.338	1.39396727	1.565701559
337 pit	33.682	31.806	1.6307737	1.539943837
339 pit	24.387	23.209	1.180739808	1.123704851
393 pit	25.61	25.513	1.23995352	1.235257093

Figure 28. McCoy Bridge Soil Samples Bulk Density Rates

Regression Statistics	
Multiple R	0.224741399
R Square	0.050508696
Adjusted R Square	-0.002240821
Standard Error	0.01967108
Observations	20

ANOVA

	df	SS	MS	F	Significance F
Regression	1	0.000370514	0.000370514	0.957519599	0.340782029
Residual	18	0.006965125	0.000386951		
Total	19	0.007335639			

	Coefficients	Standard Error	t Stat	P-value	Lower 95%	Upper 95%	Lower 95.0%	Upper 95.0%
Intercept	0.184539599	0.028234486	6.535964402	3.83192E-06	0.125221144	0.243858054	0.125221144	0.24385805
bulk density inside and outs	-0.01946452	0.019891607	-0.978529304	0.340782029	-0.061255236	0.022326195	-0.061255236	0.0223262

RESIDUAL OUTPUT

Observation	Predicted water content	Residuals
1	0.16058921	0.007719197
2	0.155411614	-0.020479206
3	0.155686797	-0.01004706
4	0.159817377	-0.009276609
5	0.166725237	-0.026773465
6	0.163519161	-0.01229575
7	0.157406694	-0.018124183
8	0.152797371	-0.001980509
9	0.161557064	0.003414687
10	0.160404498	0.015035793
11	0.153533392	0.002180124
12	0.150943652	0.006927462
13	0.153557895	-0.005727525
14	0.152761559	0.01630771
15	0.156068473	0.003569914
16	0.152400616	-0.045663752
17	0.154063969	0.023483782
18	0.15456533	0.018101406
19	0.162667223	0.019941779
20	0.160495912	0.033686205

Figure 29. Simple Regression Analysis Results

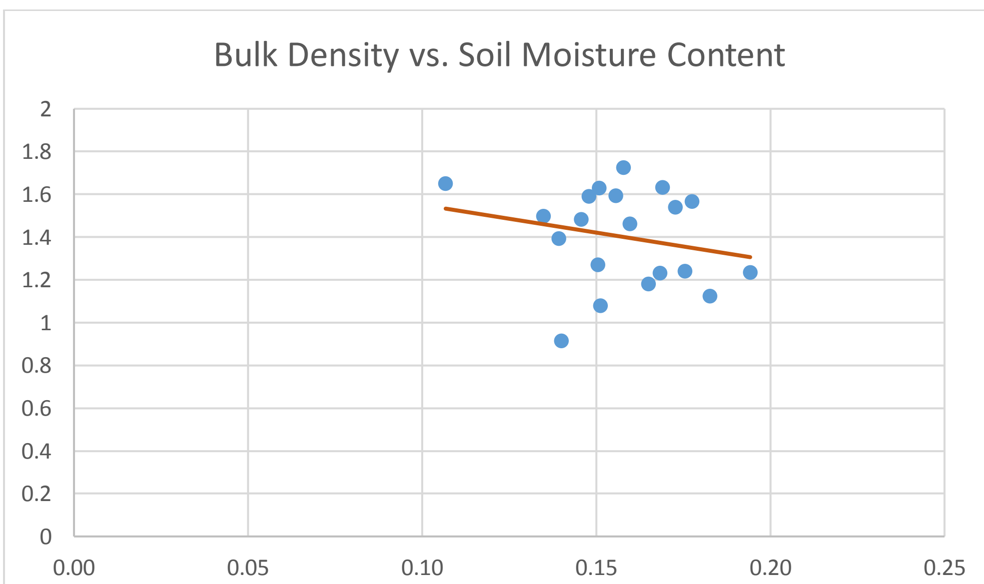

Figure 30. Linear Regression Line Chart Based on Simple Regression Analysis Displaying a Negative Relationship Between Bulk Density and Soil Moisture Content

CHAPTER V

DISCUSSION

Site 31MA684

Until the time of the geophysical survey Site 31MA684 has been used for agricultural purposes. Conyers (2004) notes that the mounds and furrows present in plowed fields can either scatter or focus radar energy, depending on the surface's orientation to the antenna. In most cases a convex surfaces (mound) tend to scatter radar energy, creating no to very low-amplitude reflections, while concave surfaces (furrow) tend to focus radar energy, creating false high-amplitude reflections in GPR slice maps (Conyers 2004). The rough surface of alternating mounds and furrows can also cause the antenna to be continuously jarred which can cause coupling errors to occur (Figure 22), potentially creating false high-amplitude anomalies in GPR slice maps. Evidence of plowing as well as coupling errors can be seen to some degree in nearly all vertical profiles and horizontal slice maps in Grids 1 and 2. These occurrences can significantly complicate the identification of culturally significant features, particularly posts, prior to fill and plow zone removal which varied on the floodplain from 24 cm to 51 cm thick (Idol 2017).

In addition to high-amplitude reflections being present in GPR data because of the above-mentioned phenomenon, high-amplitude reflections can also be caused by naturally occurring features; further complicating the identification of cultural features.

A large area of high amplitude reflections closest to the river in Grid 1(Figure 5) was assumed to be the combined effect of several potential factors. The stumps of freshly cut riparian vegetation were visible at the surface, and roots were also visible in the GPR profile and 3D data cube. Vertical profiles and slice maps of this area also suggested that a previously eroded portion of the bank may have been backfilled with soil and other solid objects as evident from the large amount of 'noise' present in the data.

The areas closest to Bryson City Road and Rose Creek Road were visibly sloped from construction of the road beds. Many high amplitude anomalies were present in the overburden in the southeastern corner of survey Grid 2 (Figure 5), making it difficult to determine if cultural features were present beneath the road bed soil. Overburden from road construction was less of an issue in Grids 1 and 2 where they bordered Rose Creek Road/McCoy Bridge.

There were several high-amplitude reflections present in the GPR profile and slice maps of Grid 2 that appeared to be culturally significant. The observed reflections were initially hypothesized to be pits or other similar cultural features. Once the plow zone was removed two of the reflections correlated to pit features documented by TRC; the others proved to be geological or non-cultural in nature. The highest amplitude reflections were the result of cobbles uncovered at the intersection of two plow scars (Figure 31), an elongated gravel or cobble bar (Figure 32) and a depressed, low lying area that was filled with a concentration of wet, clay rich soil (Figure 33) (Idol 2017). At first glance these reflections appeared as strong cultural returns. It was not until after mechanical stripping of the site were these returns determined to be natural; emphasizing the fact that while geophysical surveys are extremely useful in guiding researchers to areas of interest prior to digging, to truly understand a site's cultural context ground-truthing is still a necessary task.

The gradiometer survey of Grids 1 and 2 in the floodplain (Site 31MA684) were bounded to the south and east by a metal guard rail that distorted the magnetic survey data along the edges of the grids (Figure 4). A large linear dipole signature is evident in Grid 1; originating in the southwest, traversing northeast across the grid (Figure 34). Two similar magnetic features were excavated at Guilford Courthouse National Military (GUCO) Park by Stine and Stine (2013). Upon excavation at GUCO, a large outdoor fire with concentrations of charcoal, historic artifacts and bone were revealed. However, the TRC excavation of this area revealed 50 cm of modern fill soils, followed by red clay (Idol 2017). Similar magnetic features at Garden Creek were interpreted by Wright (2014) to be the product of lightning striking the ground. Other significant magnetic disturbances that were found to be non-cultural in nature are also evident in Grids 1 and 2: placement of a DOT right of way marker in the northeastern portion of Grid 2, a rebar site datum located in the southwest of Grid 1, and other modern refuse near or at the surface in the area near the datum below the bridge. A scattering of other isolated modern iron objects visible within each grid can also be seen.

As previously mentioned, survey Grids 1 and 2 were an agricultural field that had been repeatedly plowed up to the time of field investigations. As a result, a stripping effect due to plowing scars is visible throughout site 31MA684 (Figure 4). Plowing is common on sites selected for geophysical investigations, similar linear variations in magnetic susceptibility are noted on two of the three sites included in the literature review for this paper (Clay 2001b; Horsley and Wright 2014). When such striping is intense, it may mask weaker magnetic anomalies associated with archaeological features (Clay 2001b). Horsley and Wright (2014) suggest that even though this striping effect clutters magnetic maps, it may also indicate areas of intense cultural activity.

Site 31MA774

The surface area where the GPR survey was conducted was considerably eroded due to the lack of vegetation present. This surface erosion created data collection challenges similar to those caused by mounds and furrows discussed above. Similar to site 31MA664, high-amplitude reflections caused by naturally occurring features can also be observed (Figures 6 and 7).

In Grid 3 (Figure 6) there are several prominent high amplitude reflections; the largest can be observed slightly off-center in the grid. This was a large rock visible at the surface which created a high amplitude reflection in its corresponding depth slice map and profile view. Other high amplitude reflections near the surface were very likely similar objects. Due to the quantity of large rocks and cobbles, the identification of posts and pits was extremely challenging in this area. Grid 4 (Figure 7) presented a similar rocky substrate in its center, beginning at the crest of the hill in the northern corner and terminating at the southern corner. The rocky substrate can be seen at ground level in some profiles, predominately towards the south where erosion is most prominent. In most cases the rocky substrate is overlain with 5-30 cm of plow zone (Idol 2015). There were far fewer high amplitude reflections present in Grid 4 versus Grid 3; likely due to rock and cobble size being overall smaller in size. Regardless, the strong return created by the rocky substrate present throughout the site masked cultural features' reflections and made identification with the GPR challenging.

The gradiometer survey of Grids 3 (Figure 8) and 4 (Figure 9) exhibited few modern magnetic distortions. There are two prominent modern magnetic distortions that can be seen in Grid 4: a DOT benchmark located in the center of the northeastern boundary and a linear dipolar geophysical anomaly that appears to begin at the DOT benchmark, terminating in the center of the southeastern boundary of the grid. No evidence of this anomaly could be detected in either the profile or planar view in the GPR data. This area was closely examined post plow zone removal, as well as in the plow zone profile at the edge of the stripped area, and no evidence of a trench or transmission line could be found. This feature may have been caused by a small wire that was either at or just beneath the surface, possibly being removed during stripping. Grid 4 contained a few small modern magnetic distortions, such as bullet casings, but overall lacked any significant disturbances (Idol 2017; Turner, Stine and Lukas 2017).

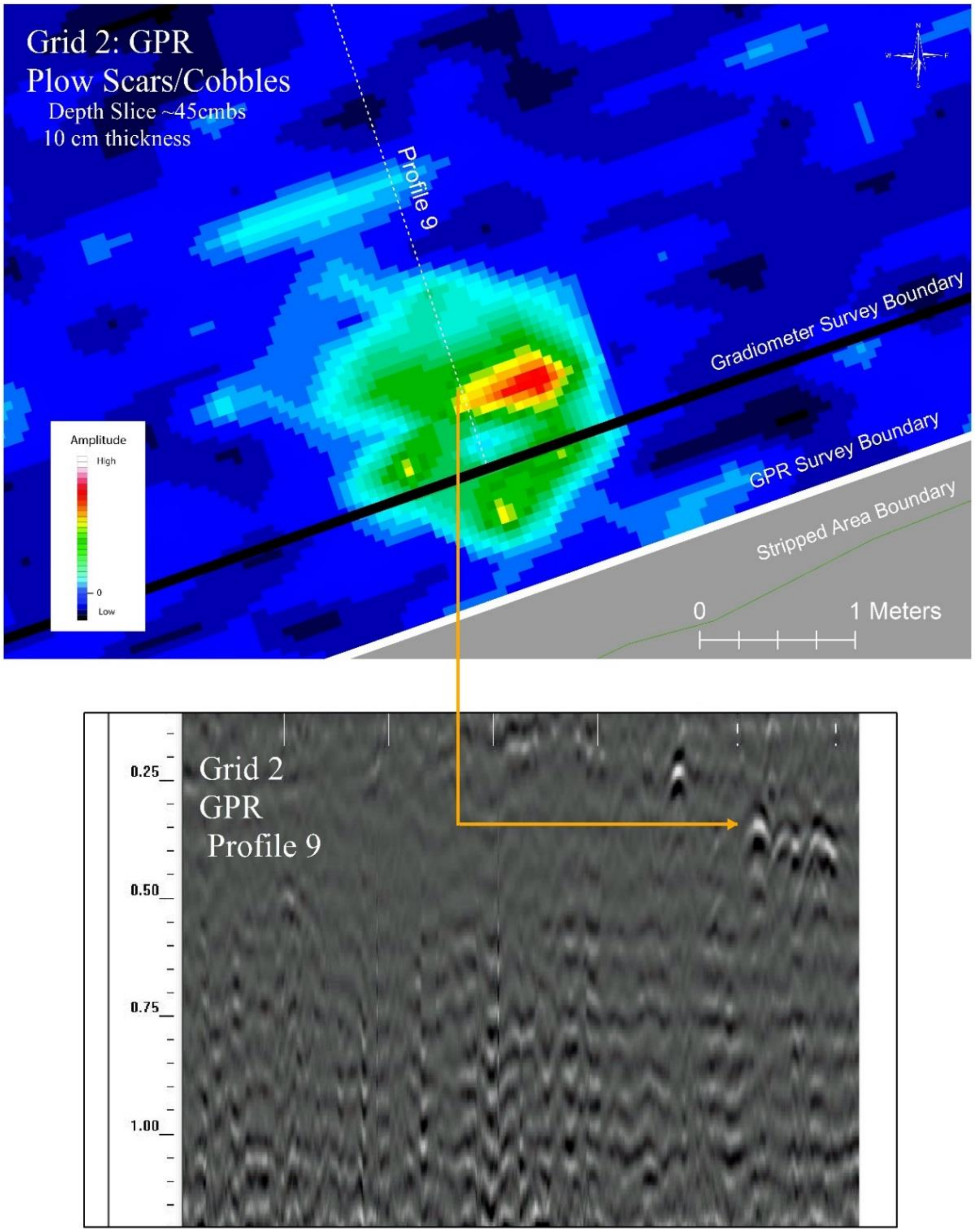

Figure 31. GPR Slice Map and Profile View of Plow Scar with Cobbles in Grid 2.

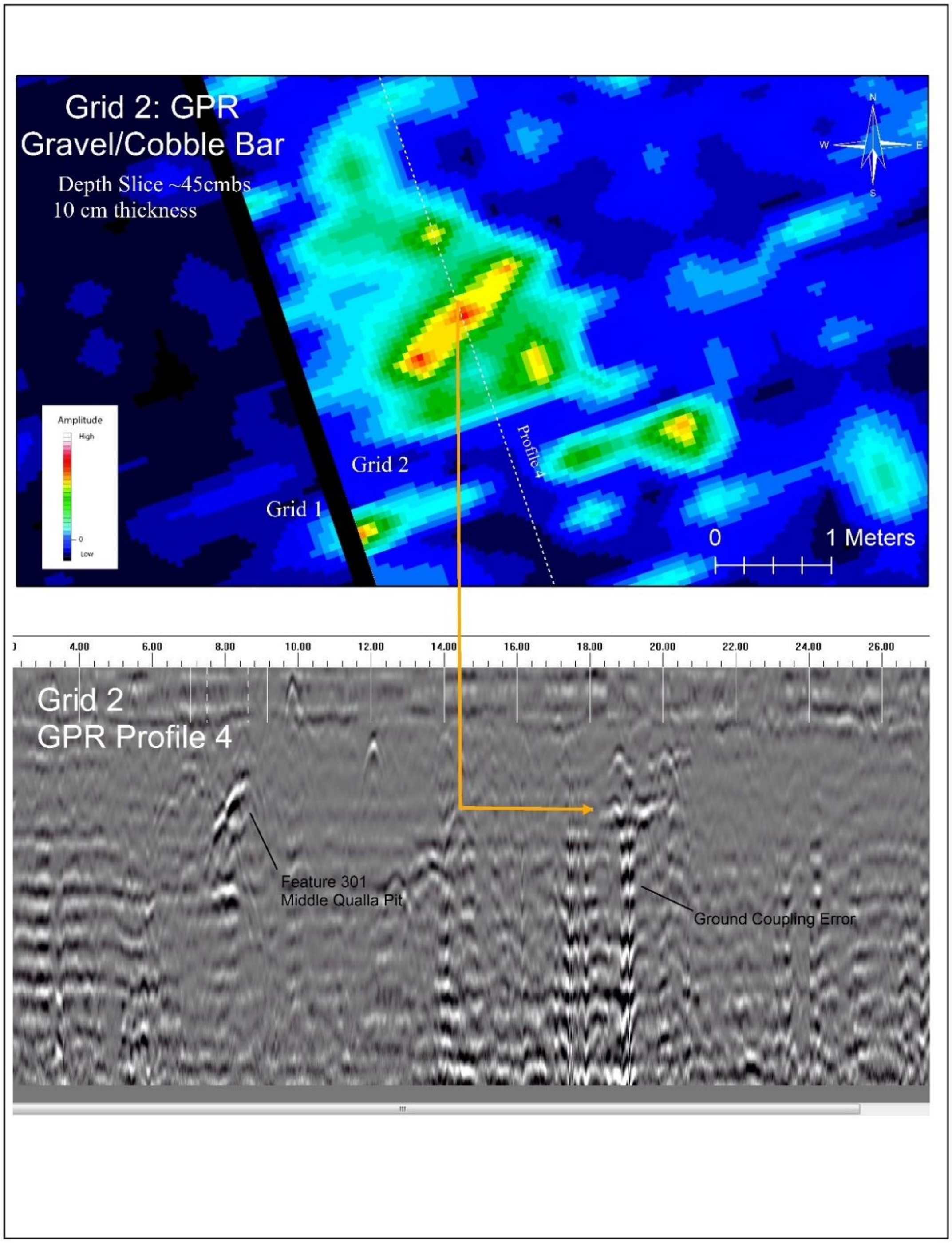

Figure 32. Site 31MA684 GPR Slice Map and Profile View of Gravel/Cobble Bar in Grid 2

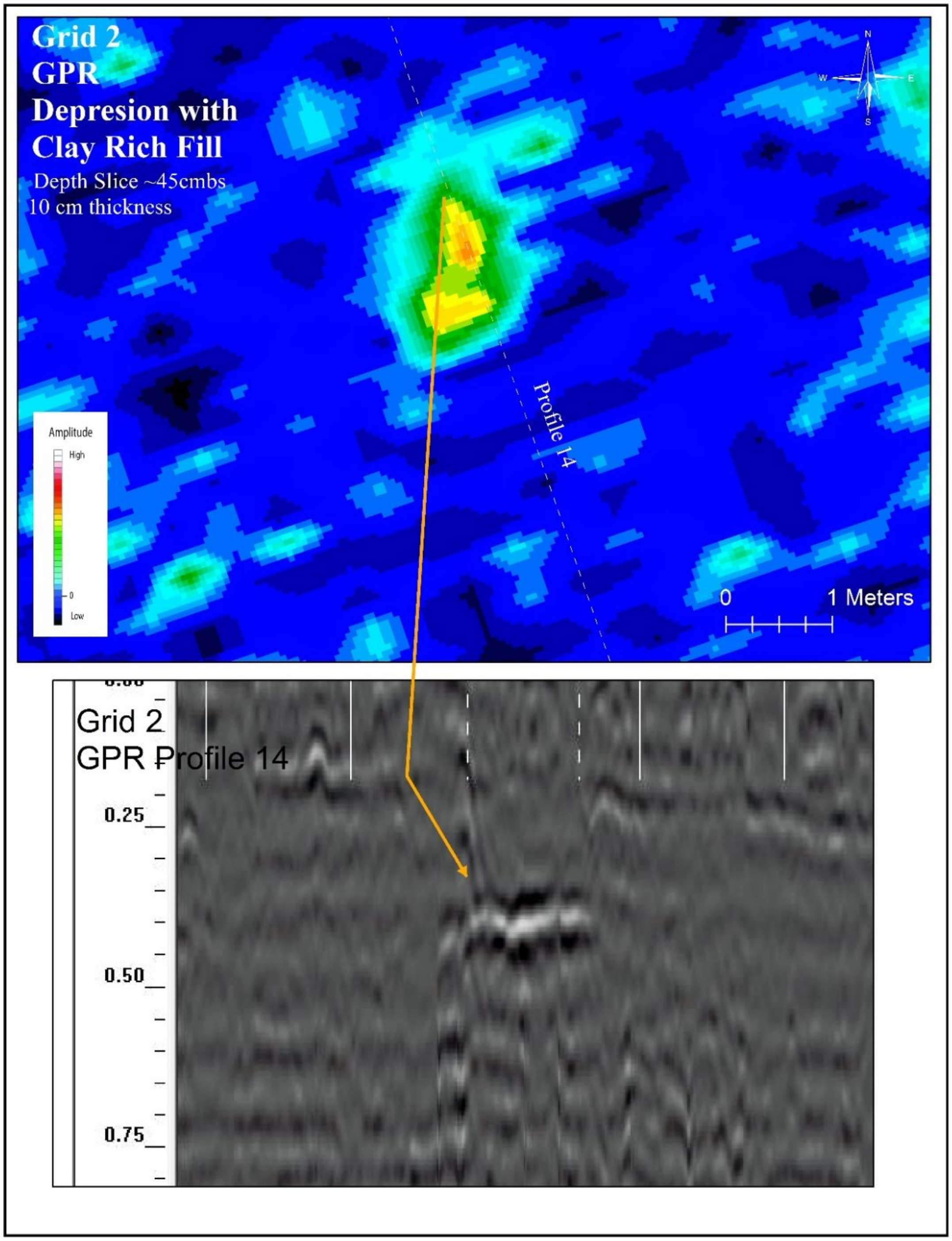

Figure 33. Site 31MA684 GPR Slice Map and Profile View of Clay Rich Depression in Grid 2

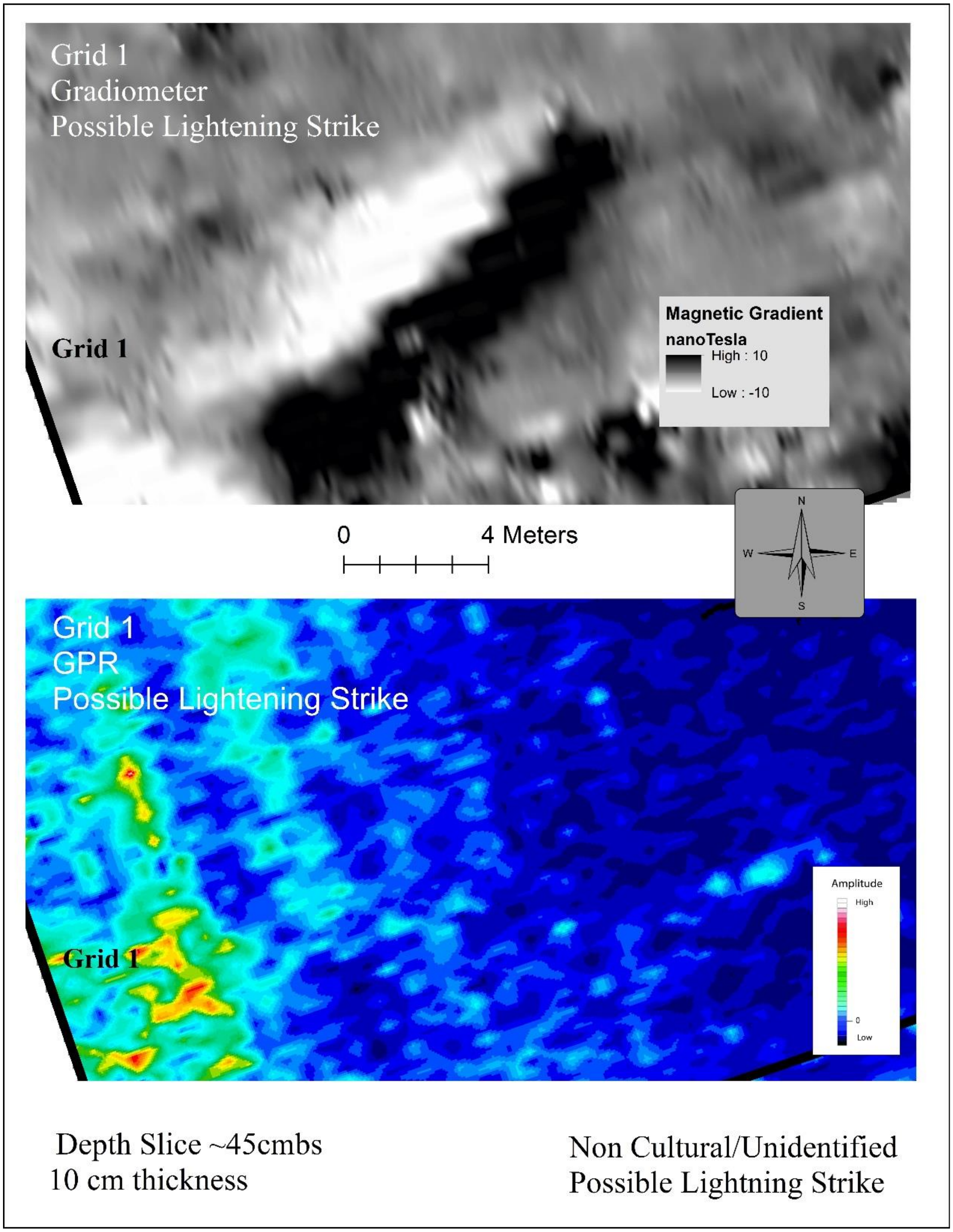

Figure 34. Site 31MA684 Gradiometer and GPR Lightening Strike in Grid 1

Features Positively Identified with Geophysical Equipment

There were a total of 95 features classified as non-cultural (Code 0), and three of those were positively identified. The identified features categorized as non-cultural were described by TRC as being post-sized in nature and as such were marked, mapped, and investigated; through either coring or by cross-sectioning (Idol 2017). It was determined no association existed between these features and any other features found on site; rather they were attributed to tree-related growth and decay processes or modern posts (Idol 2017). One of the positively identified non-cultural features was located on site 31MA684, the other two features were located on site 31MA774. There was an additional positively identified feature that was classified "maybe post/maybe post associated with structure" (Code 2). This feature was later found to be non-cultural in nature as well. An in-depth interpretation of the remaining 11 positively identified culturally significant features and the geophysical tools that could identify them is presented. Features positively identified are arranged for discussion by feature type and broken down by: those identified solely with the GPR, those identified solely with the gradiometer, and those identified with both the GPR and gradiometer.

Of the 11 positively identified culturally significant features, four (Features 214, 563, 567 and 570) were identified solely with the GPR. These features were detected on site 31MA684 in Grids 1 and 2. Features 214, 563 and 570 were all classified as "Unassigned post/post associated with structure (Code 1). Feature 567 was classified as "Pit (real, ambiguous)" (Code 3), but was described by archaeologist as an Archaic rock cluster.

Feature 214 was 1 of 17 outer wall posts associate with a Late Qualla structure (structure 4) in Grid 2 on the flood plain (31MA684). The GPR was the only geophysical tool that could identify this feature. It appeared in the GPR profile approximately 21 cm below the surface (cmbs) as a steep sided, high amplitude reflection in transect 29 of Grid 2 (Figure 35). There was no indication of this feature in the planar map; perhaps the coupling error observed directly before the feature or the multiple small reflections immediately after the feature helped to mask it.

Structure 4 was described as "…a circular, presumed winter house-type structure represented by a single wall post arc, four central support posts, and an oxidized area that represents a central hearth" (Idol 2017: 125). This post feature was the only post of structure 4 that was detectable with either geophysical tool. Once excavated, feature 214 was found to be 17.5 cm in diameter and 19 cmbs. The depth and location noted by archaeologists matches very closely with what was observed in the GPR profile view (Figure33); confirming the correlation of the observed hyperbolic reflection with this feature. Based on the overall layout of the posts and the ceramic sherds that were collected from within the post molds, structure 4 was dated to the Late Qualla phase. The steeply sloped sides observed in the hyperbolic reflection (Figure 35) may be attributed to a small highly reflective object, perhaps a rock or modern refuse such as metal, present in the fill of feature 214, which enabled the GPR to detect this feature.

Features 563 (outer wall post) and 570 (interior post of unidentified function) were both post features associated with a Middle Qualla phase structure (structure 1) in Grid 2 (site 31MA684). The GPR was the only geophysical tool capable of identifying these features. They could only be observed in their respective GPR profile views (Figures 16 and 36).

Feature 563 was observed in GPR profile 22 of Grid 2 (Figure 16) as a high amplitude reflection. There were several smaller reflections directly before and after the location of feature 563 (denoted by the provided feature point file from TRC) that were visible in the GPR profile that may be indicative of other post features. The hyperbolic reflection of feature 563 was noted by the analyst to begin at roughly 40 cmbs. Once excavated, feature 563 was determined by TRC to measure 19.5 cm in diameter and 43 cmbs.

Feature 570 was observed in the GPR profile view of transect 19 of Grid 2 (Figure 36). The hyperbolic reflection was determined to be roughly 32 cmbs. Once excavated this feature was determined by TRC to be 15.5 cm in diameter and 39 cmbs. While the hyperbolic reflection did not exhibit the same signal strength as the previously mentioned features (features 214 and 563), its location (denoted by TRC feature point file) and depth combined with the presence of a high amplitude reflection, provided enough evidence to confidently identify the observed reflection in the GPR profile with feature 570. There are several posts in the proximity of features 563 and 570. It is probable the close proximity of these posts to features 563 and 570 helped to produce the high amplitude reflections observed in the GPR profiles.

Feature 567 was in Grid 1 on the boundary of the upper and lower terrace of the flood plain (31MA684). A moderate-amplitude reflection was associated with this feature in the GPR planar map but due to the large amount of noise caused from recent plowing, feature 567 was largely obscured. However, in the GPR profile a series of small, point-source hyperbolic reflections could be observed (Figure 18). Due to multiple hyperbolic reflections at this location it was difficult to determine the exact depth of this feature but it appeared to be located approximately 25 cmbs.

Archaeologists described feature 567 as a ‘rock or cobble cluster’ (Idol 2017:156) made up of up to 27 unmodified and fragmented cobbles (Figure 37) and measured 60 x 42 cm; dating to the Middle Archaic to Late Archaic period. This was based on the associated Late Archaic artifacts, B horizon contexts, and Qualla phase feature fill (Idol 2017). Idol (2017) notes that features similar to this have been documented throughout the Appalachian Summit region in North Carolina and eastern Tennessee; primarily in Late Archaic contexts. There was not an exact depth given by Idol (2017) for this feature, but it was noted that it appeared at the surface of the B horizon during mechanized stripping, which ranged from 24 cmbs (upper flood plain terrace) to over 1 meter below the surface (lower terrace flood plain terrace) (Idol 2017).

The various cobbles that composed feature 567 were what most likely caused the clustered, high amplitude reflections to be observed in the GPR profile (Figure 37). Conyers (2012) describes similar reflections seen in association with historic midden piles where each small reflection was produced from individual objects contained within the pile; much like the individual cobbles associated with this feature. Idol (2017) notes that there was little to no evidence of continuous burning associated with this feature which explains why it effectively remained ‘invisible’ to the gradiometer.

Three features (340, 510 and 511) could be detected solely with the gradiometer. Feature 340 was classified as "Grave" (Code 4). Feature 340 (Figure 20**)** was one of three graves located by archaeologist on this project. The magnetic gradiometer was the only geophysical instrument that was capable of locating a grave feature with any level of confidence. A faint positive monopole which measured 130 x 70 cm, once the over-lying soil was removed, was detected in the magnetic map (Idol 2017).

Respecting Cherokee wishes archaeologists did not excavate any grave features, therefore no definitively date was determined for this burial.

The faint monopole observed at Feature 340 was presumably the result of the grave being backfilled with topsoil; topsoil tends to exhibit higher magnetic qualities than the surrounding subsoil. This is due to the natural tendency of insoluble iron minerals to accumulate in top soil while other minerals, such as calcites and silicates, tend to be filtered out (Kvamme 2007). Though the precise location of features observed in the gradiometer data may not be as accurate as the GPR, the magnetic signature enables the analyst to determine the subsurface feature's relative location. This combined with the data collected by archaeologists, allowed the analyst to confidently identify feature 340 in the gradiometer map.

Features 510 and 511were Qualla series pits located in Grid 3 (31MA774). The proximity of the two features were so close they appeared as one large magnetic signature (Figure 19). The signature appears initially as a strong positive monopolar anomaly but upon closer inspection the negative portion is weakly visible; offset slightly to the north and west. Such a strong positive signature observed may be a result of the proximity of feature 510 and 511 to one another. These features could not be detected with the GPR due to the rocky matrix in which they were located.

Upon excavation, feature 510 measured 47 x 32 cm. and feature 511 measured 49 x 30 cm. Both contained several Qualla sherds, with feature 510 producing an additional chert flake and feature 511 an additional serrated chert point. The origin of feature 510 (Figure 38) and 511(Figure 39) were both reported to be ‘ambiguous’ in nature as it could be a very small pit or simply a natural depression with ‘midden-like fill’ (Idol 2017). Several factors could have contributed to the magnetic signature produced by features 510 and 511. The most probable cause stems from the high temperatures produced during firing episodes that introduced thermoremanent magnetism (TRM) into the soil. Features 510 and 511 may also have become filled with topsoil upon their abandonment, making them easily detectable because of the magnetically enhanced topsoil (Kvamme 2008). Additionally, the presence of ceramic sherds found within the pits may have contributed to the magnetic signature observed due to the firing process that ceramics undergo (Kvamme 2008).

The remaining four positively identified features (Features 301, 339, 350 and 569) could be detected by both the GPR and the gradiometer. These were classified as “Pit (real/ambiguous)” (Code 3). Feature 301 was located on site 31MA684 in Grid 2. Features 339, 350 and 596 were located on site 31MA774 in Grids 3 and 4.

Feature 301was a Middle Qualla pit located in Grid 2 on the flood plain (31MA684). The GPR and gradiometer were both able to detect this feature with varying degrees of success. It appeared in the gradiometer map as a weak dipole that was slightly offset south and west of a high amplitude reflection seen on the corresponding GPR slice map **(**Figure 40**)**. Feature 301 was also detected in GPR profile 4 (Figure 41); appearing as a steeply sloping high amplitude surface. This was corroborated by archaeologists who described this feature as having "irregular, in sloping sides with a rounded uneven base…charcoal-flecked fill with numerous unmodified cobbles…" (Idol 2017:140). Feature 301 appeared at the base of the plow zone, which measured 40 cm in thickness in the test units, measuring 172 x 125 cm (excavated measurements) and extended 30 cm into the subsoil (Idol 2017). The fill was classified as a dark yellowish brown (10 YR 4/4) sandy loam in the Munsell color chart and upon excavation was found to contain a Qualla series sherd, several fragments of debitage, and trace animal bone (Idol 2017). The numerous cobbles see in the southern the fill of feature 301 (Figure 42) are what likely caused the high amplitude reflections seen in the GPR profile and amplitude slice map. The presence of charcoal flecks indicates that burning occurred in this location, causing thermoremanent anomalies to be introduced into the soil, allowing the gradiometer to recognize this feature as well.

Feature 339 was a Late Qualla pit located on the hill top (31MA774) in Grid 4 (Figure 17). A high amplitude reflection can be seen in the GPR slice map that roughly matches the excavated pit's shape; however, it appears most distinctly in GPR profile 38 in Grid 4 **(**Figure 43**)**. Feature 339 appeared as a concave surface, approximately one meter wide, with a maximum depth of 31 cm. In the gradiometer data, an associated weak positive monopole can also be observed, slightly to the south of the excavated feature boundary. Hargrave (2006) notes that such monopolar positive anomalies often identify the locations of pits.

The excavated measurements of feature 339 were 120 x 112 cm and exhibited both in sloping and straight sides with a relatively flat floor **(**Figure 44**)**. The feature fill was up to 21 cm thick and contained numerous Late Qualla sherds as well as three glass beads found within the fill (Idol 2017). The shape and width of the reflection observed in the GPR profile matched closely with excavation of the feature. The concave reflection observed in the GPR profile was likely caused by multiple firing events that baked the floor of this pit feature, creating a surface that retained water, which in turn produced a good radar reflective surface (Conyers 2012). A single, discrete high amplitude reflection was also detected in the GPR profile slightly above the base of the concave surface. It is highly probable the large stone (Figure 44) located within the pit feature's fill was the source of the observed reflection. The magnetic signature that was visible in the gradiometer map could be the effect of thermoremanent magnetism. The numerous ceramic sherds, which are known to be magnetically detectable in large concentrations, may have also caused the positive monopole seen in the gradiometer map (Aspinall, Gaffney, and Schmidt 2008; Kvamme 2008).

Feature 350 was a Late Qualla pit located three meters south of feature 339 on the hill top (31MA774) in Grid 4 (Figure 17). While feature 350 appeared most prominently in the gradiometer map, a strong reflection could be observed in GPR profile 32 **(**Figure 45**)**. The GPR profile had a concave like surface with a high amplitude reflection near the base of the floor and defined walls that sloped inwards towards the bottom of the feature.

There was also a high amplitude reflection observed in the GPR amplitude slice map in the location marked by archaeologists to be the pit's approximate center. Similar to feature 339, the horizontal amplitude slice map did not reveal the shape of the excavated pit feature. Feature 350 appears as a moderately strong positive monopole in the gradiometer map. The magnetic signature may have appeared stronger and matched the shape of the excavated feature more closely had it not been distorted by the linear magnetic anomaly spanning the eastern and southern portions of the grid (Figure 17).

Excavation of feature 350 **(**Figure 46**)** revealed a circular pit that measured 145 x 145 cm and extended 35 cm into the subsoil. This feature was initially believed to be larger than noted above but upon closer inspection a separate pit, feature 349, appeared to be conjoined by a thin layer of overlapping shared fill (Idol 2017). Idol (2017) noted feature 350 exhibited in sloping walls with a relatively flat floor; closely matching what was observed in the GPR profile. The fill was described as a sequence of layered soils that were undistinguishable from one another in cross-section; representing multiple episodes of refilling with soils from comparable sources. In general, the soil was classified from the Munsell color chart as dark brown (7.5YR 3/4) sandy loam with varying charcoal content. Several Late Qualla sherds, a few lithic artifacts, and ten peach pits were recovered within the fill. Six unmodified large cobbles were also observed at or near the floor of this pit feature (Idol 2017).

Two main factors helped the GPR detect feature 350. Indications of burning were present in the form of charcoal recovered from within the fill. High heat associated with periods of burning has been seen to create a surface that can retain water, which in turn produced a good radar reflective surface (Conyers 2012). The floor of feature 350 does not appear as defined as that of feature 339. This may be due in part to the six cobbles that were recovered from within feature 350. However, it was these cobbles that further assisted the GPR to detect this feature. There was not a single discrete high amplitude reflection observed near the base of the concave reflection; rather it appears as a series of closely packed small reflections, indicative of what one would see in a midden pile. As discussed above, the magnetic signature that was visible in the gradiometer map could be the result of thermoremanent magnetism. However, the multiple refilling episodes that feature 350 underwent was doubtlessly the primary cause of the strong positive monopole observed in the gradiometer map.

Feature 569 was in Grid 2 (31MA684). This feature, associated with structure 1 (winter house), was detected by both geophysical instruments. The hearth appeared most prominently in the gradiometer map, with a slight indication visible in the GPR profile (Figure 21). The magnetic signature of the hearth appears at first glance as a strongly positive monopole, but upon closer examination, a weak negative portion is slightly visible. The GPR data did not indicate the hearth as clearly as the gradiometer, however, in profile 16 of Grid 2 (Figure 21) the hearth appears to be visible “as a sharp depression within a broader subterranean house floor” (Turner, Stine, and Lukas 2015:32).

Excavation of the hearth confirmed the depression seen in the GPR profile. An 86 cm diameter reddened circle that was 15 cm deep with a hardened surface constructed at its base was uncovered. The hearth contained two burned logs and pieces of the fallen smokehole daub, hardened clay likely mixed with soil or sand and fibrous material to line the smokehole to keep it from catching fire, were found within this feature (Figure 47) (Idol 2017). Conyers (2012) notes that the heat from a fire tends to bake the bottoms of hearths/fire pits, which creates a surface that retains water and as a result produces a strong reflective surface. The signal generated by the hearth may have appeared more prominent in the GPR profile if not for the amount of disturbance seen above its location; likely caused from recent plowing. The fallen daub found within and next to may have also contributed to the noise observed above this feature. However, the smokehole daub (Figure 47) likely contributed to the strength of the hearth's magnetic signature seen in the gradiometer maps; though the presence of burned material within the hearth was likely the leading cause.

General Discussion

There were a total of 402 features examined by TRC following plow zone removal in the remote sensing grids, of which, 15 could be positively identified in the remote sensing data using one or both instruments. There were a variety of reasons as to why many of the examined features could not be resolved with either geophysical tool. First, the bulk of the features examined were post holes (n=288), with the vast majority recovered in the floodplain. These features proved the most difficult for either tool to detect for their own unique reasons. The average RDP calculated for the floodplain, site 31MA684, was 19.5 for Grid 1 and 22.9 for Grid 2 (Figure 1). This coincides with numbers noted by Conyers (2012) for average RDP in organic rich agricultural fields (15) and in saturated sands (20-30). The soil description for the floodplain is Rosman fine sandy loam, 0 to 2 percent slope, frequently flooded (websoilsurvey.sc.egov.usda.gov). RDP values were generated in the lab using Radan7 software once the field data were collected. These values are averages that change with soil depth. As the radar waves move downward through the soil the signal attenuates, losing its strength. As a result, the amount of radar energy that can be returned diminishes; lowering the GPR's ability to resolve features. Conyers (2004) notes that the strength of the cone is greatest directly under the antenna and it weakens as it spreads outward. Using the equation below can give the analyst an indication of how the cone, which is more of an ellipse with the major axis occurring along the line of travel, or 'footprint' may appear. Conyers (2004:61) does urge caution stating that this equation can only be used as a "rough approximation of real-world conditions."

$$A = \lambda/4 + D/\sqrt{K+1}$$

Where:

A = approximate long dimension radius of footprint
λ = center frequency wavelength of radar energy
D = depth from ground surface to reflection surface
K = average relative dielectric permittivity (RDP) of material from ground surface to depth (D)
(Conyers 2004:62)

The fill and plow zone varied on the floodplain from as little as 24 cm up to 51 cm thick (Idol 2017). This increased the GPR footprint in certain areas which affected the amount of transmitted energy that came into contact with subsurface features; making them much more difficult to detect. Conyers (2004) states that if the desired target is much smaller than the footprint size, then only a small portion of the transmitted energy that intersects it will be transmitted to the surface. Using the above formula, the RDP of Grid 1 (19.51) with the 400 MHz antenna (converted to meters using Table 3.2 from Conyers 2004:60) and a depth of 24 cm below the fill and plow zone, the semi-major axis is 9.5 cm and the semi-minor axis is 4.8 cm. When 51 cm was input into the above equation, keeping the RDP and the antenna the same, a semi-major axis of 15.5 cm and a semi-minor axis of 7.75 cm was found. This created an illumination cone in Grid 1 that ranged from 19 x 9.6 cm to 31 x 15.5 cm. The above formula was also used to estimate the GPR's cone size for Grid 2 using the RDP (22.95) for Grid 2, the same antenna and same depth variations. The footprint for Grid 2 ranged from 17.64 x 8.82 cm to 28.68 x 14.34 cm. The average post size for the flood plain (site 31MA684) was 15.87 cm. These foot print estimates help to explain why many of the post features were undetected with the GPR and will be vital in future research endeavors of this type. The results indicate that researchers should drastically reduce transect spacing, as well as, employ a GPR antenna in the 500 to 900 MHz range.

Another major problem that occurred on the survey was the plowed fields. As previously mentioned, mounds and furrows present in plowed fields can either scatter or focus radar energy, depending on the surface's orientation to the antenna. This can create false high-amplitude reflections in GPR slice maps, as well as, create coupling errors (Figure 22) caused from the continuous up and down movement of the antenna as it travels across the field (Conyers 2004, 2012). The result of this phenomenon can obscure subsurface features completely. Plowed fields can also obscure data collected with the magnetic gradiometer; causing striping to occur in magnetic maps and masking of weak magnetic anomalies (Clay 2001b; Kvamme 2007; Wright 2009). Researchers who plan on conducting geophysical surveys on sites similar to the ones mentioned here should strongly considering having the field harrowed with a log dragged behind the harrow to smooth the surface prior to data collection.

The similarity of the soil within a feature and from the surrounding soil matrix also created difficulties in the geophysical survey. Statistically there were not enough samples to decisively determine the role bulk density, and to a lesser degree soil moisture, played in the detection of subsurface features using a GPR; confirmed by inspecting the results of the regression analysis; R^2 and Significance F=0.34. Conyers (2012) notes that reflections usually occur in areas where differences in bulk density differ at stratigraphic boundaries, though this may not always be the case. A study conducted by Miller et al. (2002) closely examined the effects of soil bulk density and soil particle density in relation to GPR radar responses; paying close attention to the contrast between the RDP of the soil and the target feature to determine the strength of the reflection. The study was conducted using a 900MHz antenna in two locations that exhibited similar bulk density to the soil found in the flood plain. The bulk densities in these locations ranged from a low of 1.6 g/cm^3 to a high of 1.8 g/cm^3. Miller et al. (2002) found that bulk density and soil particle density had only minor effects on the radar wave, with soil moisture content exhibiting the largest effect. This study demonstrates while a bulk density difference of 0.2 or greater may be substantial in terms of soil science, the variance is inconsequential concerning GPR surveys. Future research should include more soil samples so that a statistically significant relationship may be found.

Documenting the soil moisture content at the time of collection would also be beneficial. A more precise measurement of soil moisture may give researchers a better understanding of how the water content of soil impacts the amount of information garnered from the geophysical tools during a survey.

The variety of issues with the soil from high RDP values to plowing and small changes within the bulk density indicate the need for greater research in these areas. Considering the soils types and their high RDP values, coupled with the plowed fields, the geophysical survey was an overall success. Disregarding the posts, which neither geophysical tool could detect for the multitude of issues mentioned above, the geophysical survey successfully located approximately 50 percent of the larger features on the two sites.

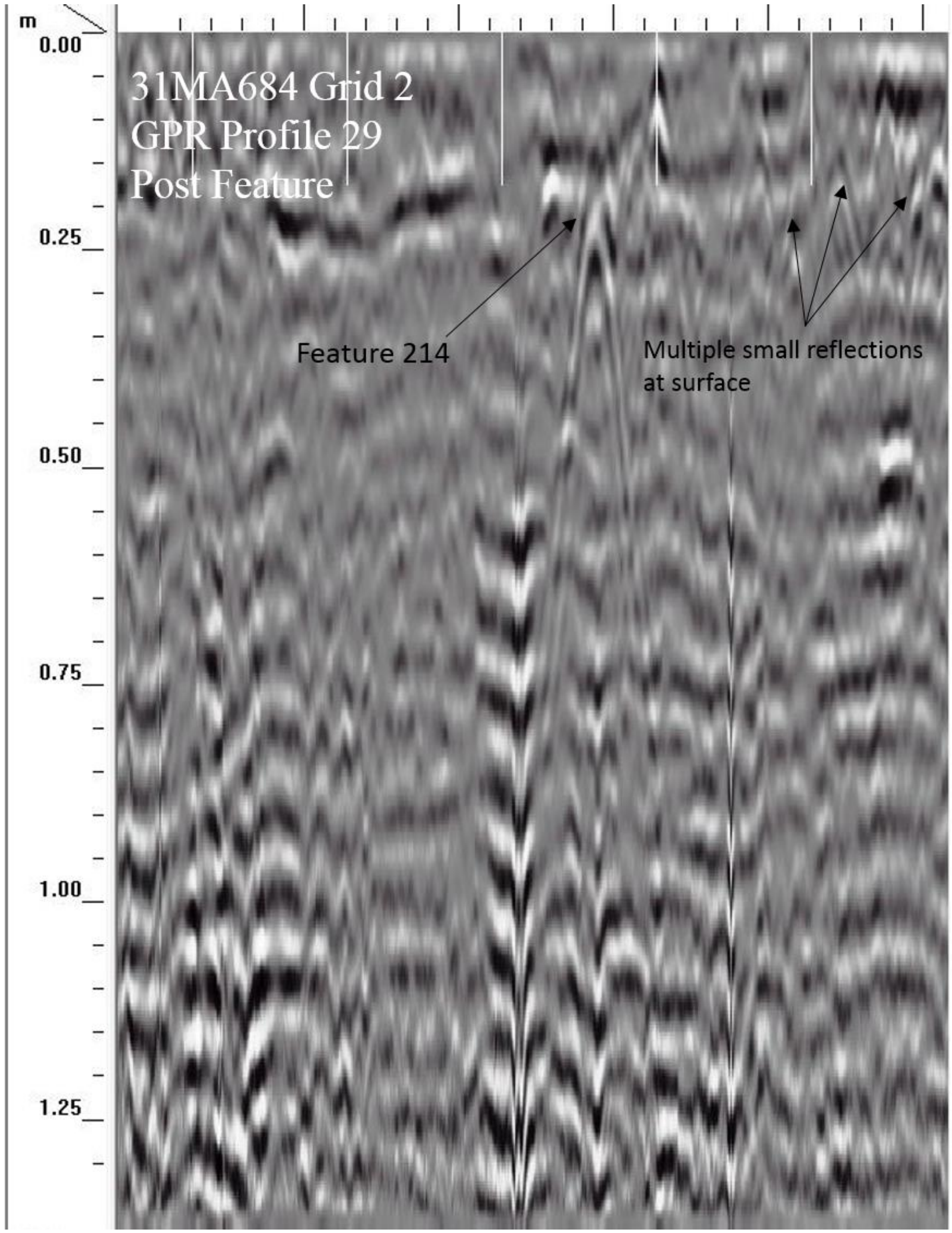

Figure 35. Site 31MA684 GPR Profile of Post Feature 214 in Grid 2

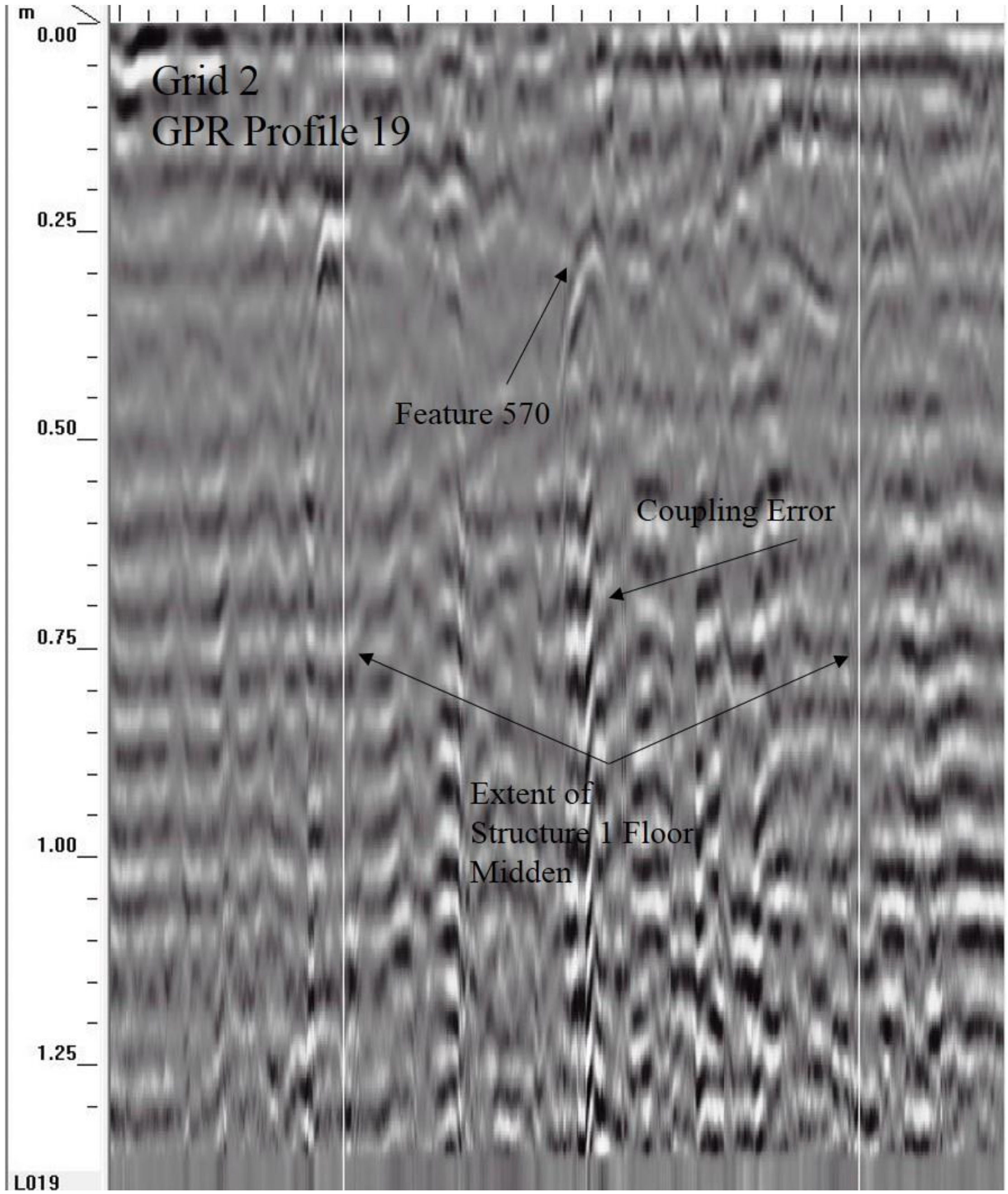

Figure 36. Site 31MA684 GPR Profile of Post Feature 570 in Grid 2

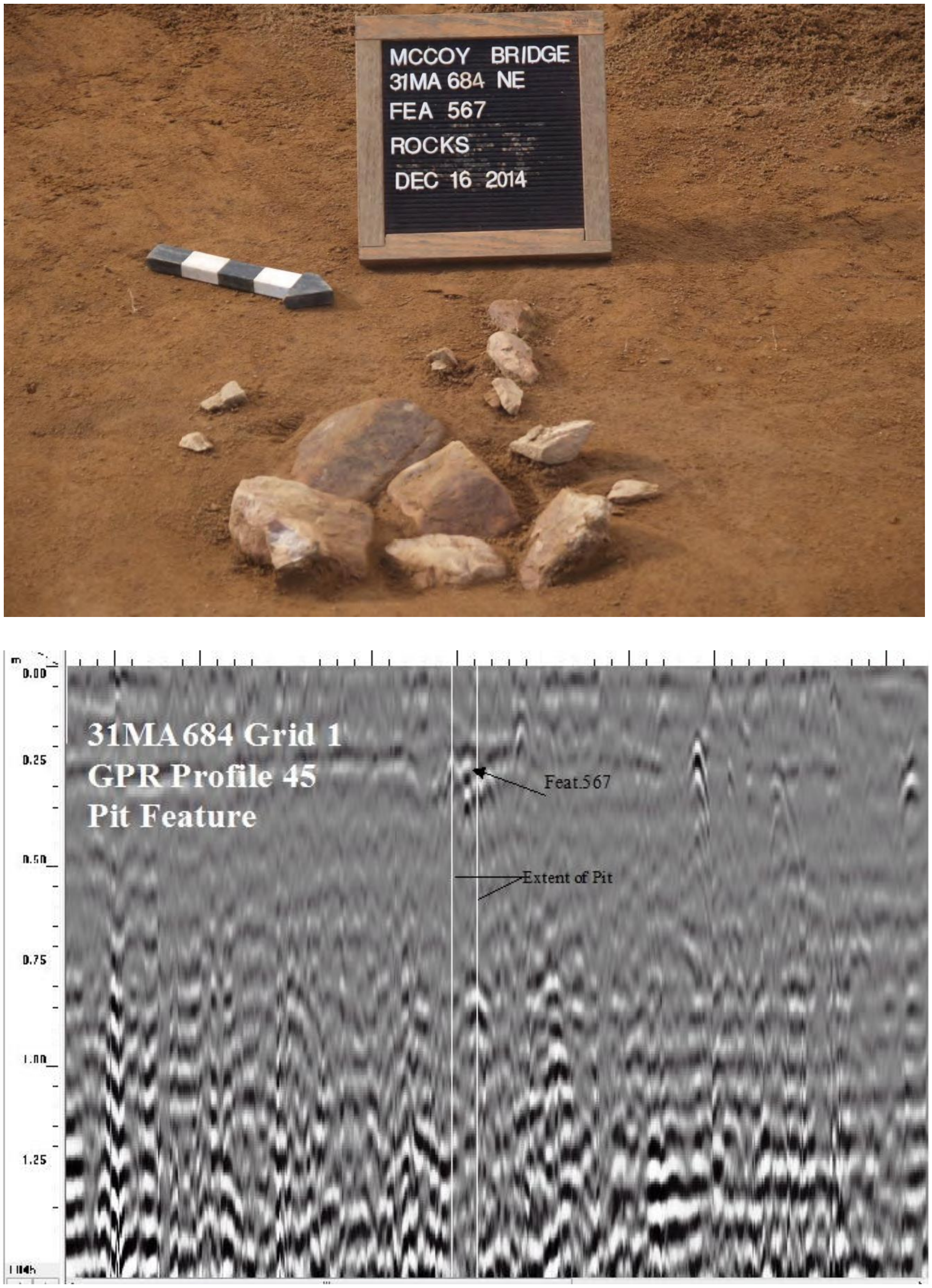

Figure 37. Feature 567 (Rock Cluster) at 31MA684, Plan View, With Associated GPR Profile. Photo Courtesy of TRC, INC

Figure 38. Pit Feature 510 at 31MA774, North Profile. Courtesy of TRC, INC

Figure 39. Pit Feature 511 at 31MA774, West Profile. Courtesy of TRC, INC

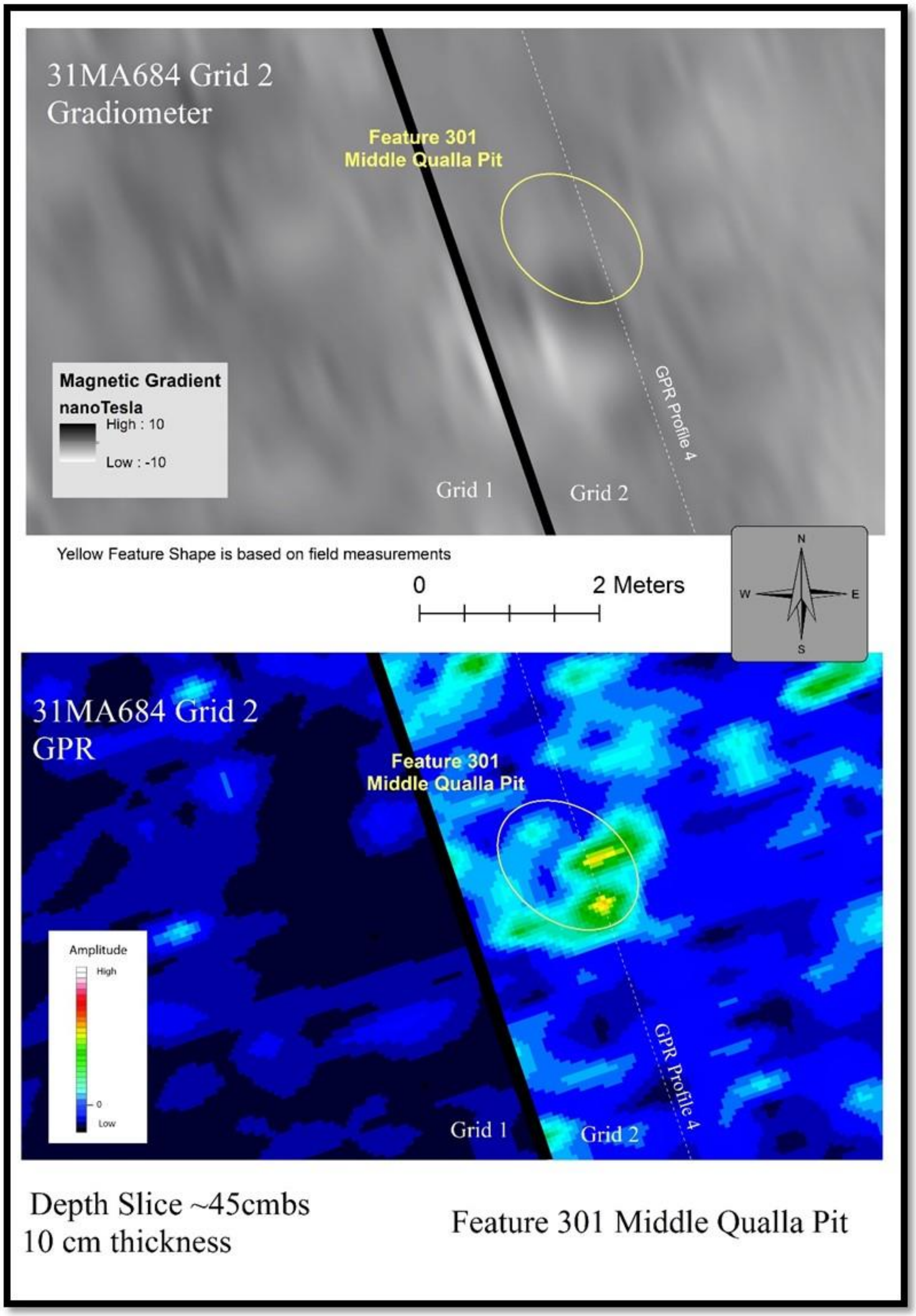

Figure 40. Site 31MA684 Gradiometer and GPR Slice Map of Middle Qualla Pit Feature 301in Grid 2

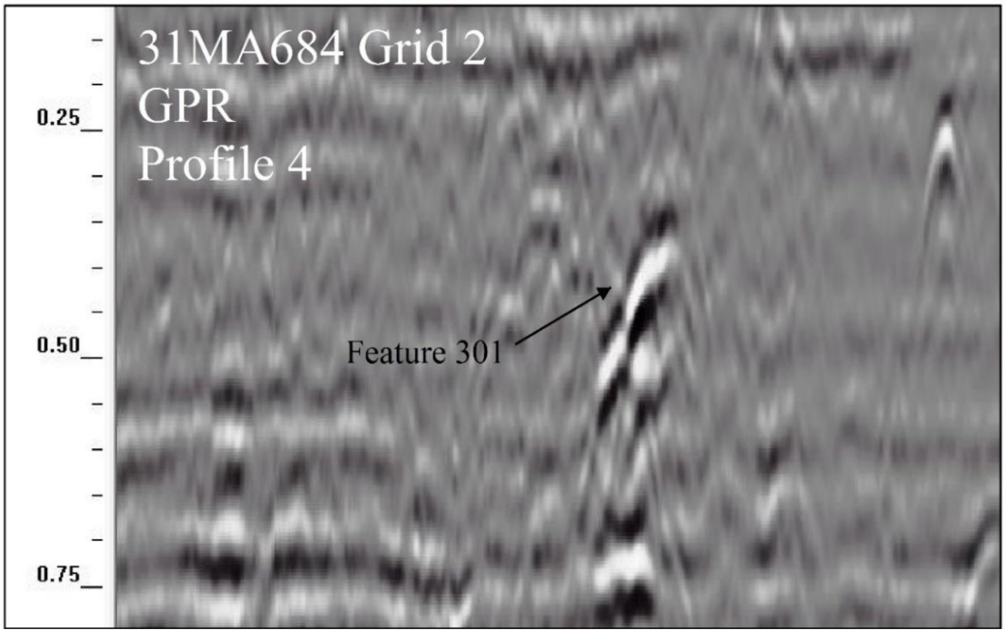

Figure 41. **Site 31MA684 GPR Profile of Middle Qualla Pit Feature 301**

Figure 42. **Feature 301 at 31MA684, East Profile. Cobbles Located to South in Facade. Courtesy of TRC, Inc**

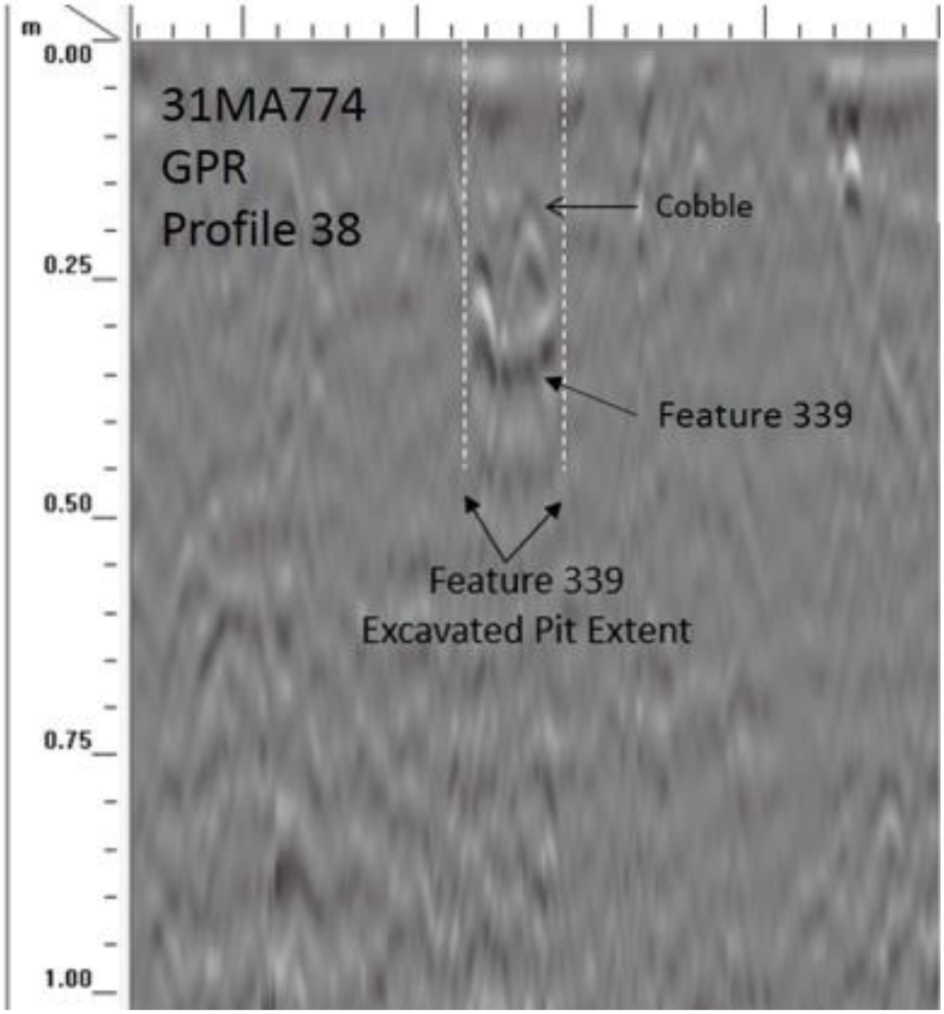

Figure 43. Late Qualla Pit Feature 339 Site 31MA774 GPR Profile in Grid 2

Figure 44. **Feature 339 at 31MA774, West Profile. Large Cobble Located in Northern Section of Fill in Facade of Pit. Courtesy of TRC, Inc**

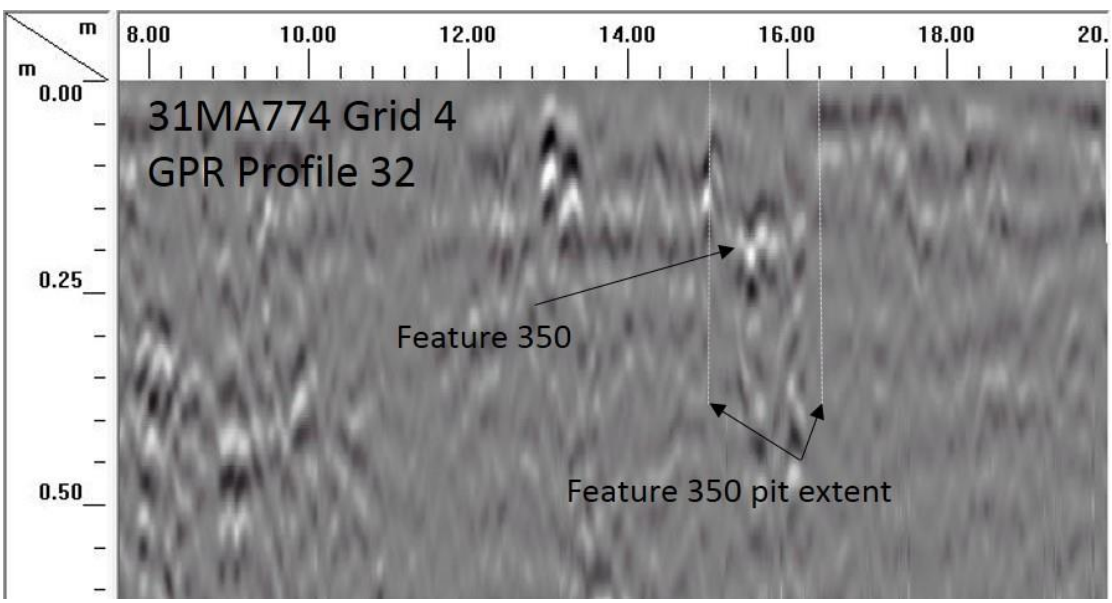

Figure 45. **Late Qualla Pit Feature 350. GPR Profile 32 in Grid 4**

Figure 46. Features 349 and 350 at 31MA774, North Profile. Courtesy of TRC, Inc

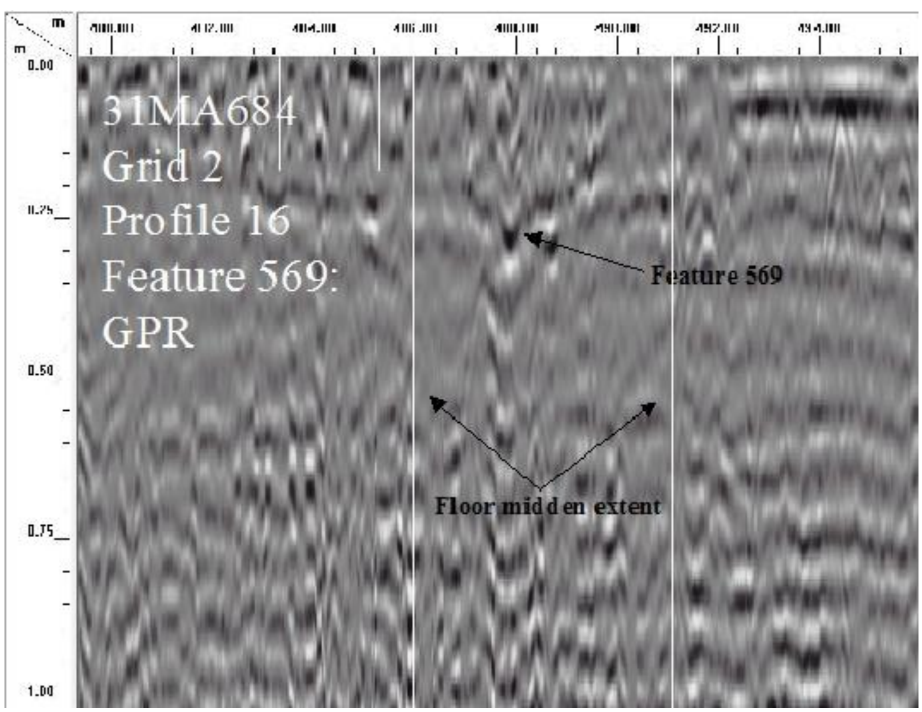

Figure 47. Feature 569 (Hearth) at 31MA684 With Associated GPR Profile. Feature 324 (Smokehole Daub) in Background; Facing East. Photo courtesy of TRC, Inc

CHAPTER VI

CONCLUSION

The geophysical research that took place in October and December of 2014, near McCoy Bridge, North Carolina demonstrated the ability of ground penetrating radar (GPR) and magnetic gradiometer to detect subsurface features. This project enabled researchers to compare the geophysical data collected prior to plow zone removal with feature location maps created by archaeologists. Researchers were then able to accurately determine the geophysical tools' ability to detect subsurface features found within the cultural landscape that once existed at sites 31MA684 and 31MA774.

Despite the many issues encountered across both sites, the geophysical survey positively identified 15 (3.73%) and possibly identified, with a lesser degree of certainty, an additional 51 (12.69%) of the cultural features. Removing real/ambiguous posts from the equation, as well as the 95 features classified as non-cultural, the geophysical equipment recovered approximately 50 percent of the larger culturally significant features across both sites: 5 of 12 pits, 1 of 3 graves, 1 of 2 hearths and one smoke hole. The features detected by the geophysical equipment provided evidence of continued habitation at sites 31MA684 and 31MA774 from the Late Archaic period to the Late Qualla phase.

A partial reason for the low recovery rate by the geophysical equipment stems from the fact that 95 of the features were non-cultural, meaning of natural origin (e.g.

stain in in the soil from a long dead tree) and 285 were real/ambiguous posts that only averaged 15.87 cm in diameter at the base of the plow zone, which varied greatly across both sites. Conyers (2012) states that the 400 MHz antenna is good at finding features of about 20 cm and larger; so even under the best of circumstances it would be very doubtful if many of the smaller features such as postholes would have been located.

The fill and plow zone overlaying site 31MA684 presented their own set of challenges as well. Until the geophysical survey Site 31MA684 has been used for agricultural purposes. Conyers (2004) notes that the mounds and furrows present in plowed fields can alternately scatter and focus radar energy, depending on the surface's orientation to the antenna. The rough surface of alternating mounds and furrows can also cause the antenna to be continuously jarred which can cause coupling errors to occur when the antenna loses contact with the ground surface. Additionally, the average RDP calculated for the floodplain was 19.5 for Grid 1 and 22.9 for Grid 2. The high RDP of the soil caused the signal to attenuate as it penetrated deeper into the soil. These occurrences can significantly complicate the identification of cultural features, particularly posts, prior to fill and plow zone removal which varied on the floodplain from 24 to 51 cm thick (Idol 2017). The fill and plow zone thickness increased the GPR footprint which decreased the amount of transmitted energy that came into contact with subsurface features, rendering them practically invisible. The bulk density analysis conducted on some of the features proved to be inconsequential; the difference was not substantial enough between the inside of the feature versus the surrounding matrix for the radar to distinguish any difference in signal. Other contributing factors that may have masked the returns of the gradiometer included: a metal guard rail along the southern edges of Grids 1 and 2, the placement of a DOT right of way marker in the northeastern portion of Grid 2, a rebar site datum located in the southwest of Grid 1, and other modern refuse near or at the surface.

Despite all the obstacles that were encountered on site 31MA684 the geophysical equipment located three posts, two pits (one a Late Archaic rock cluster and the other a Middle Qualla pit), one hearth and the smoke hole daub associated with the hearth. Two of the posts, the hearth and the smokehole daub were all associated with a Middle Qualla winter house. The Middle Qualla winter house was located without the typical circular or rectangular positive monopolar signatures associated with burned structures in magnetic maps or the presence of linear anomalies sometimes seen in GPR slice maps representative of structures (Hargrove and Beck 2001; Moore 2009; Perttula, Walker and Schultz 2008).

Likewise, many of the same challenges found on the floodplain could be found on site 31MA774, the hilltop. The surface where the geophysical survey was conducted was considerably eroded. Though the plow zone was thinner on the hilltop (5-30 cm thick) the surface erosion created data collection challenges similar to those caused by mounds and furrows discussed above. While the RDP and thick plow zone did not have the same effect on the GPR signal, the strong return created by the rocky substrate present throughout the site masked the features' reflections and made their identification with the GPR extremely challenging.

Regardless of the issues encountered on site 31MA774 the geophysical survey located four pits between Grids 3 and 4 and one grave. A partial cause for the low recovery rate were 39 features were determined to be non-cultural and three were real/ambiguous posts which were likely too small to be detected with the GPR. It is probable that an additional pit could have been detected with the gradiometer had a linear dipolar (Figure 9) that cuts south-southwest across Grid 4 not been present. No evidence of this anomaly could be detected in either the profile or planar view in the GPR data nor during excavation. This anomaly may have been caused by a small wire that was either at or just beneath the surface and was removed during stripping.

Bulk density analysis was conducted on various samples from both sites to determine what, if any, influence it had on the ability of the geophysical tools to detect subsurface features. It was determined that statistically there were not enough samples to decisively determine the role bulk density, and to a lesser degree soil moisture, played in the detection of subsurface features be these tools. The variety of issues observed with the soil such as high RDP values to plowing and small changes within the bulk density indicate the need for greater research in these areas. Data were collected in 50 cm transects by the GPR and gradiometer.

Researchers who plan on conducting geophysical surveys in the future on sites similar to 31MA684 and 31MA774 should strongly considering collecting data at smaller transect intervals so that a greater chance of detecting small features, such as posts, could be possible. The use of a higher frequency GPR antenna, in the 500 to 900 MHz range, in conjunction with the 400MHz antenna used here would be also be advised. Finally having the field harrowed with a log or chain harrow to smooth the surface prior to data collection would help to reduce coupling errors.

The benefits of conducting a geophysical survey before or in lieu of a full-scale excavation can be seen from the evidence presented in this report. A geophysical survey map, while highly effective at narrowing down the location of culturally significant features, should not be assumed to perfectly portray the subsurface features, and as such ground-truthing is, and for the foreseeable future will be, a necessary task to fully grasp a site's cultural landscape. The geophysical survey has proven its ability to give researchers a better understanding of where to focus research efforts before any digging takes place; saving time, money and most importantly the cultural integrity of the site.

REFERENCES

Aspinall, Arnold, Gaffney, Chris and Schmidt, Armin. 2008 Magnetometry For Archaeologists. Lanham: AltaMira Press.

Beck, Robin A, Moore, David G., and Rodning, Christopher B. 2006 Identifying Fort San Juan: A Sixteenth Century Spanish Occupation At the Berry Site, North Carolina. *Southeastern Archaeology* 25 (1): 65–77.

Bruseth, James E., Pierson, William T., & Johnson, Ross M. 2007 Large-Area Remote Sensing Coverage of Archaeological Sites with a Dual-Track Cart-Mounted Cesium Magnetometer. *Journal of Field Archaeology*, *32*(2), 133-148.

Campana, Stefano, and Piro, Salvatore. 2009 Seeing The Unseen: Geophysics and Landscape Archaeology. Preface. In *Seeing The Unseen: Geophysics and Landscape Archaeology*, xvii-xix. Boca Raton: CRC Press.

Clark, Anthony. 2001 *Seeing Beneath the Soil Prospecting Methods in Archaeology*. London: Routledge.

Clay, Berle R. 2001a Complementary geophysical survey techniques: Why two ways are always better than one. *Southeastern Archaeology* 20 (1): 31–43. 2001b Geophysical Survey Of Sites 31SW1 and 31SW2 Within the Kituhwa Archaeological District, Swain County, North Carolina. Report Prepared for the Cultural Resources Department, Eastern Band of Cherokee Indians. Lexington, Kentucky: Cultural Resource Analysts, Inc.

Conyers, Lawrence B. 2004 *Ground-Penetrating Radar for Archaeology*. Walnut Creek, CA: AltaMira Press. 2012 *Interpreting Ground-Penetrating Radar for Archaeology*. 1st ed. Walnut Creek, CA: Left Coast Press.

Goodman, Dean, and Piro, Salvatore. 2013 *GPR Remote Sensing in Archaeology*. Berlin: Springer.

Grossman, Tiffany. 2012 *Applying Geophysics and Geochemistry to Understand Middle Woodland Site Spatial Organization At the Northwood Site, Vigo County, Indiana* (Masters). Indiana State University.

Hargrave, Michael L. 2006 Ground Truthing The Results of Geophysical Surveys. Essay. In *Remote Sensing in Archaeology: an Explicitly North American Perspective*, 269–304. Tuscaloosa: University of Alabama Press.

Hargrave, Michael. L., Britt, T., & Reynolds, Matthew D. 2007 Magnetic evidence of ridge construction and use at Poverty Point. *American antiquity*, 757-769.

Hargrove, Thomas, and Beck, Robin A. 2001 Magnetometer and Auger Testing at the Berry Site, Burke County, North Carolina. In 58th Annual Meeting of the Southeastern Arcaheological Conference, Chattanooga, Tennessee.

Horsley, Timothy 2014 Notes on Geophysical Surveys Conducted Between 2011-2012 at the Garden Creek Site (31HW8), Haywood Co., North Carolina. Appendix A in Wright, Alice P. Inscribing Interaction: Middle Woodland Monumentality in the Appalachian Summit, 100 BC - AD 400. Unpublished PH. D. dissertation in Anthropology, The University Of Michigan, Ann Arbor.

Horsley, Timothy, Wright, Alice and Barrier, Casey. 2014 Prospecting For New Questions: Integrating Geophysics to Define Anthropological Research Objectives and Inform Excavation Strategies at Monumental Sites. *Archaeological Prospection Archaeol. Prospect.* 21 (1): 75–86.

Idol, Bruce. 2017 Archeological Survey and Testing at 31MA684 and Survey, Testing, and Data Recovery Excavations at 31MA684 and 31MA774 for the Replacement of Bridge No. 172 on SR 1456 Over the Little Tennessee River, Macon County, North Carolina. TRC Environmental Corporation, Chapel Hill, North Carolina. Submitted to North Carolina Department of Transportation Human Environment Section, Archaeological Group, Raleigh, North Carolina.

Jensen, John R. 2003 *Introductory Digital Image Processing: a Remote Sensing Perspective*. Upper Saddle River, NJ: Prentice Hall.

Keel, Bennie C. 1976 Cherokee Archaeology: A Study of the Appalachian Summit. University of Tennessee, Knoxville

King, Adam, Walker, Chester P., Sharp, Robert V., Reilly, F. Kent, and McKinnon, Duncan P. 2011 Remote sensing data from Etowah's Mound A: architecture and the re-creation of Mississippian tradition. American Antiquity, 76(2), 355-371.

Kvamme, Kenneth L. 2003 Geophysical Surveys As Landscape Archaeology. *American Antiquity* 68 (3): 435. 2006 Magnetometry: Nature's Gift to Archaeology. In Remote Sensing in Archaeology: An Explicitly North American Perspective, edited by Jay K. Johnson, pp. 205–234. University of Alabama Press, Tuscaloosa, Alabama. 2008 Remote Sensing Approaches To Archaeological Reasoning: Pattern Recognition and Physical Principles. Essay. In *Archaeological Concepts for the Study of the Cultural Past*, 65–84. Foundations Of Archaeological Inquiry. Salt Lake City, UT: The University of Utah Press.

Leckebusch, Jurg. 2003 Ground- penetrating radar: a modern three- dimensional prospection method. *Archaeological prospection*, *10*(4), 213-240.

Lockhart, Jami J., and Green, Thomas J. 2006 The Current and Potential Role of Archaeogeophysics in Cultural Resource Management in the United States. Essay. In *Remote Sensing in Archaeology: an Explicitly North American Perspective*, 17–31. Tuscaloosa: University of Alabama Press.

Miller, Timothy. W., Borchers, Brian, Hendrickx, Jan M., Hong, S., Dekker, Lois W., and Ritsema, Coen J. 2002 Effects of soil physical properties on GPR for landmine detection. In *Fifth International Symposium on Technology and the Mine Problem*.

Moore, Palmyra Arzaga. 2009 A Geophysical Survey Of the Kituhwa Mound (31Sw2) and Surrounding Area (31Sw1), Swain County, North Carolina. The University Of Tennessee, Knoxville.

Patch, Shawn, 2008 Ground Penetrating Radar (GPR) Survey of a Portion of Site 18TA315, Talbot County, Maryland. New South Associates, Stone Mountain, Georgia. Submitted to TRC Environmental Corporation, Chapel Hill, North Carolina. 2009 Identification of Unmarked Graves at B.F. Randolph Cemetery Using Ground Penetrating Radar (GPR) Richland County, South Carolina. New South Associates, Stone Mountain, Georgia. Submitted to Historic Columbia Foundation, Columbia, South Carolina. 2010 Geophysical Survey of the Boot Hill Site (LA32229), Eddy County, New Mexico. New South Associates, Stone Mountain, Georgia. Submitted to TRC Environmental Corporation, Albuquerque, New Mexico.

Patch, Shawn, and Lowry, Sarah. 2010 Conduct Geophysical Survey and Archaeological Assessment for Stanton House Property, Women's Rights NHP, Seneca Falls, New Your, Phase 1: Geophysical Survey; Accession Number WORI 00144. New South Associates, Stone Mountain, Georgia. Submitted to TRC Environmental Corporation, Albuquerque, New Mexico. 2013 Investigating Prehistoric Settlement In the Upper Guntersville Basin: Archaeological Geophysics Survey of the Raccoon Creek Wildlife Management Area. Technical Report 4309. Greensboro, NC: New South Associates.

Perttula, Timothy K., Walker, Chester P., and Schultz, T. Clay. 2008 A revolution in Caddo archaeology: The remote sensing and archaeological view from the Hill Farm site (41BW169) in Bowie County, Texas. Southeastern Archaeology, 93-107.

Radan 7. 2011 Users' Manual. Electronic document available at http://www.uvm.edu/~lewebb/CCLI/Manuals/Radan7UserManual.pdf.

Riggs, Brett H., and Shumate, Scott M. 2003 Archaeological Testing At Kituhwa: 2001 Investigations at Sites 31Sw1,31Sw2,31Sw287,31Sw316,31Sw317,31Sw318, and 31Sw320. Report Prepared for the Eastern Band of Cherokee Indians Cultural Resources Program. 2004 The Cherokee Town at Coweeta Creek. Unpublished Ph.D. dissertation, Department of Anthropology, University of North Carolina, Chapel Hill.

Rodning, Christopher B. 2004 The Cherokee Town at Coweeta Creek. Unpublished Ph.D. dissertation, Department of Anthropology, University of North Carolina, Chapel Hill.

Rogers, Michael, Leon, Jeffrey F., Fisher, Kevin D., Manning, Sturt W., and Sewell, David. 2012 Comparing Similar Ground-Penetrating Radar Surveys Under Different Moisture Conditions at Kalavasos- Ayios Dhimitrios , Cyprus. *Archaeological Prospection Archaeol. Prospect.* 19 (4): 297–305.

Stine, Linda, and Roy Stine. 2013 Archaeological and Geophysical Research at Guilford Courthouse National Military Park (GUCO) (31GF44**) Greensboro, North Carolina. The University of North Carolina at Greensboro. National Park Service Field Report.

Sturm, Jennie O., and Crown, Patricia L. 2015 Micro-scale Mapping Using Ground-Penetrating Radar: An Example From Room 28, Pueblo Bonito, Chaco Canyon, New Mexico. Advances in Archaeological Practice 3(2): 124-135.

Thompson, Victor D. 2014 Monumental Architecture, Households, and Archaeo-Geophysics in the American Southeast and Midwest. *Archaeological Prospection Archaeol. Prospect.* 21 (1): 1–3. doi:10.1002/arp.1478.

Turner, Jacob, Stine, Roy, and Lukas, Ari. 2015 Geophysical Investigation at 31MA684 Floodplain and 31MA774 Hilltop, Macon County, NC. Appendix A of Idol, Bruce. Archeological Survey and Testing at 31MA684 and Survey, Testing, and Data Recovery Excavations at 31MA684 and 31MA774 for the Replacement of Bridge No. 172 on SR 1456 Over the Little Tennessee River, Macon County, North Carolina. TRC Environmental Corporation, Chapel Hill, North Carolina. Submitted to North Carolina Department of Transportation Human Environment Section, Archaeological Group, Raleigh, North Carolina.

Watters, Margaret. 2012 Geophysical and Laser Scan Surveys at the Longfellow House – Washington's Headquarters National Historic Site. National Center for Preservation Technology Training.

Ward, H. Trawick, and Davis Jr., R.P. Stephen. 2004 The Cherokee Town at Coweeta Creek. Unpublished Ph.D. dissertation, Department of Anthropology, University of North Carolina, Chapel Hill.

Whiting, B., McFarland, D., & Hackenberger, S. 2001 Three-dimensional GPR study of a prehistoric site in Barbados, West Indies. *Journal Of Applied Geophysics*, *47*(3-4), 217-226.

Wright, Alice P. 2014 Inscribing Interaction: Middle Woodland Monumentality in the Appalachian Summit, 100 BC - AD 400. Unpublished PH. D. dissertation in Anthropology, The University Of Michigan, Ann Arbor.

APPENDIX A

TOTAL FEATURES COLLECTED BY TRC, INC WITH GEOPHYSICAL RESULTS

Site	No.	Point	N	E	Elev	Descrip.	Code	Type		GPR	Mag	GPR Comr	Mag Comr	GPR Dept	Northing	Easting	Post Diam	Post Dept	Pit Length	Pit Width	Pit Depth	Comment	Nearest T
31MA684	16	539	495.141	467.6933	96.71641	fea16post	0	post-noncultural		m	n	pro only, v	guard rail/	0.21	495.141	467.6933	N/A	N/A	N/A	N/A	N/A		17.6175
31MA684	21	544	495.7067	472.3191	96.97929	fea21post	0	post-noncultural		y	n	In pro anc		0.35	495.7067	472.3191	N/A	N/A	N/A	N/A	N/A		23.4225
31MA684	31	553	494.2195	470.8197	96.93809	fea31post	0	post-noncultural		n	n	very faint;	guard rail		494.2195	470.8197	N/A	N/A	N/A	N/A	N/A		16.7592
31MA684	34	556	496.2874	470.0084	96.84752	fea34post	0	post-noncultural		n	n				496.2874	470.0084	N/A	N/A	N/A	N/A	N/A		23.8383
31MA684	43	565	496.8818	470.5674	96.85135	fea43bio	0	post-noncultural		n	n				496.8818	470.5674	N/A	N/A	N/A	N/A	N/A		3.9642
31MA684	47	569	496.4769	472.8169	96.99982	fea47post	0	post-noncultural		n	n				496.4769	472.8169	N/A	N/A	N/A	N/A	N/A		4.4417
31MA684	51	573	495.4762	475.8005	97.05964	fea51post	0	post-noncultural		n	n	very faint;	washout c		495.4762	475.8005	N/A	N/A	N/A	N/A	N/A		4.8934
31MA684	66	588	498.4521	466.7823	96.62503	fea66post	0	post-noncultural		n	n	pro only;	very weak		498.4521	466.7823	N/A	N/A	N/A	N/A	N/A		10.7597
31MA684	67	590	496.4392	469.1664	96.786	fea67post	0	post-noncultural		n	n				496.4392	469.1664	N/A	N/A	N/A	N/A	N/A		0.8402
31MA684	96	621	498.9164	477.9072	97.22021	fea96post	0	post-historic		n	n	However,			498.9164	477.9072	20	22	N/A	N/A	N/A		6.2742
31MA684	100	625	498.7998	480.4342	97.33611	fea100pos	0	post-noncultural		n	n		wash out t		498.7998	480.4342	N/A	N/A	N/A	N/A	N/A	noncultur	8.5848
31MA684	104	627	499.2238	478.7174	97.25291	fea104pit	0	pit-noncultural		n	n	Take a clo	washed ou		499.2238	478.7174	N/A	N/A	N/A	N/A	N/A	noncultur	7.108
31MA684	110	631	499.3136	471.6547	96.88585	fea110pos	0	post-noncultural		n	n	very faint;			499.3136	471.6547	N/A	N/A	N/A	N/A	N/A	noncultur	22.0104
31MA684	115	635	500.7158	472.9522	96.99068	fea115pos	0	post-noncultural		n	n	very faint;			500.7158	472.9522	N/A	N/A	N/A	N/A	N/A	noncultur	3.6824
31MA684	119	639	502.1606	473.3783	97.02836	fea119pos	0	post-noncultural		n	n	very faint			502.1606	473.3783	N/A	N/A	N/A	N/A	N/A		16.3713
31MA684	137	670	501.7192	494.3722	97.39651	fea137pos	0	post-noncultural		n	n	signal dro			501.7192	494.3722	N/A	N/A	N/A	N/A	N/A		4.3483
31MA684	138	671	500.0901	464.8086	96.46279	fea138pos	0	post-noncultural		n	n	transition.	very faint		500.0901	464.8086	N/A	N/A	N/A	N/A	N/A		5.9337
31MA684	139	672	497.9714	459.3434	95.94221	fea139pos	0	post-noncultural		n	n				497.9714	459.3434	N/A	N/A	N/A	N/A	N/A		20.2124
31MA684	140	673	500.2749	469.4319	96.78176	fea140pos	0	post-historic		n	n				500.2749	469.4319	13	N/A	N/A	N/A	N/A		0.8957
31MA684	147	680	502.8033	470.9073	96.92972	fea147pos	0	post-noncultural		n	n				502.8033	470.9073	N/A	N/A	N/A	N/A	N/A		20.901
31MA684	153	685	499.4366	480.84	97.32209	fea153pos	0	post-noncultural		n	n	noise and			499.4366	480.84	N/A	N/A	N/A	N/A	N/A		0.511
31MA684	158	690	501.3844	486.5669	97.26831	fea158pos	0	post-noncultural		n	n				501.3844	486.5669	N/A	N/A	N/A	N/A	N/A		5.4176
31MA684	160	692	502.8062	486.1655	97.26551	fea160pos	0	post-noncultural		n	n	dist in Arc			502.8062	486.1655	N/A	N/A	N/A	N/A	N/A		13.7388
31MA684	166	697	505.2791	490.989	97.24268	fea166pos	0	post-noncultural		n	n				505.2791	490.989	N/A	N/A	N/A	N/A	N/A		0.3078
31MA684	167	698	505.2441	492.5124	97.27808	fea167pos	0	post-noncultural		n	n				505.2441	492.5124	N/A	N/A	N/A	N/A	N/A		6.7805
31MA684	170	699	504.5523	472.8867	96.98367	fea170pos	0	post-noncultural		n	n	hit at dist.			504.5523	472.8867	N/A	N/A	N/A	N/A	N/A		14.9931
31MA684	176	705	501.0523	476.28	97.12666	fea176pos	0	post-noncultural		n	n				501.0523	476.28	N/A	N/A	N/A	N/A	N/A	noncultur	21.9347
31MA684	212	737	504.424	486.0928	97.2576	fea212pos	0	post-noncultural		m	n	Moderate		.14-.15	504.424	486.0928	N/A	N/A	N/A	N/A	N/A		9.5259
31MA684	220	926	506.2506	471.3875	96.93508	fea220pos	0	post-noncultural		n	n	very faint;			506.2506	471.3875	N/A	N/A	N/A	N/A	N/A		21.4931
31MA684	221	927	509.4997	469.243	96.85474	fea221pos	0	post-noncultural		n	n	Y strong; s		0.2	509.4997	469.243	N/A	N/A	N/A	N/A	N/A		18.5131
31MA684	223	2393	511.2864	474.7547	97.16806	fea223pos	0	post-noncultural		n	n	may possi			511.2864	474.7547	N/A	N/A	N/A	N/A	N/A		10.7938
31MA684	225	1012	507.1848	468.4234	96.69504	fea225pos	0	post-noncultural		n	n				507.1848	468.4234	N/A	N/A	N/A	N/A	N/A	noncultur	21.3597
31MA684	232	1019	502.7045	480.0481	97.22799	fea232pos	0	post-noncultural		n	n		appears tc		502.7045	480.0481	N/A	N/A	N/A	N/A	N/A	noncultur	17.9992
31MA684	236	1023	501.5538	480.2114	97.246	fea236pos	0	post-noncultural		n	n				501.5538	480.2114	N/A	N/A	N/A	N/A	N/A	noncultur	9.9895

31MA684	280	1067	518.5167	469.8811	97.04662	fea280pos	0	post-noncultural		m	n	faint in bc		0.67	518.5167	469.8811	N/A	N/A	N/A	N/A	N/A		14.6992
31MA684	286	1073	517.1716	472.3431	97.18036	fea286pos	0	post-noncultural		n	n	faint pro c			517.1716	472.3431	N/A	N/A	N/A	N/A	N/A		24.3155
31MA684	297	1084	509.8391	476.4786	97.13847	fea297pos	0	post-noncultural		n	n	very faint,			509.8391	476.4786	N/A	N/A	N/A	N/A	N/A		23.3021
31MA684	302	1088	518.1334	473.6667	98.78472	fea302pos	0	post-noncultural		n	n				518.1334	473.6667	N/A	N/A	N/A	N/A	N/A		19.2332
31MA684	304	1090	520.1273	474.5327	98.72961	fea304pos	0	post-noncultural		n	n				520.1273	474.5327	N/A	N/A	N/A	N/A	N/A		22.4513
31MA684	305	1092	520.3502	478.801	98.71109	fea305pos	0	post-noncultural		n	n				520.3502	478.801	N/A	N/A	N/A	N/A	N/A		11.603
31MA684	306	1091	521.6821	478.6459	98.72543	fea306pos	0	post-noncultural		n	n	very faint			521.6821	478.6459	N/A	N/A	N/A	N/A	N/A		17.0827
31MA684	310	1299	504.9865	471.5269	96.89659	fea310pos	0	post-noncultural		n	n				504.9865	471.5269	N/A	N/A	N/A	N/A	N/A		0.5462
31MA684	312	1301	503.7778	471.8417	96.90862	fea312pos	0	post-noncultural		n	n	faint in pr			503.7778	471.8417	N/A	N/A	N/A	N/A	N/A		9.023
31MA684	313	1302	502.8188	471.8899	96.90013	fea313pos	0	post-noncultural		n	n	however,t			502.8188	471.8899	N/A	N/A	N/A	N/A	N/A		14.3142
31MA684	314	1303	501.9562	471.7588	96.86866	fea314pos	0	post-noncultural		n	n	very sligh			501.9562	471.7588	N/A	N/A	N/A	N/A	N/A		23.845
31MA684	315	1304	501.9209	472.4537	96.89515	fea315pos	0	post-noncultural		n	n	very faint;			501.9209	472.4537	N/A	N/A	N/A	N/A	N/A		11.5979
31MA684	319	1348	508.2779	480.4347	97.21875	fea319pos	0	post-noncultural		n	n				508.2779	480.4347	N/A	N/A	N/A	N/A	N/A	noncultur	0.0449
31MA684	483	1585	503.5107	480.7844	97.21003	fea483pos	0	post-noncultural		n	n		on edge o		503.5107	480.7844	N/A	N/A	N/A	N/A	N/A		22.1398
31MA684	488	1590	502.482	481.8398	97.22558	fea488pos	0	post-noncultural		n	n				502.482	481.8398	N/A	N/A	N/A	N/A	N/A	noncultur	5.8249
31MA684	502	1772	504.4512	481.7462	97.22739	fea502pos	0	post-noncultural		m	n	possible s			504.4512	481.7462	N/A	N/A	N/A	N/A	N/A	noncultur	0.5893
31MA684	516	1776	501.6868	479.0242	97.18898	fea516pos	0	post-noncultural		n	n				501.6868	479.0242	N/A	N/A	N/A	N/A	N/A	noncultur	2.0631
31MA684	517	1777	501.913	479.1009	97.17093	fea517pos	0	post-noncultural		n	n				501.913	479.1009	N/A	N/A	N/A	N/A	N/A	noncultur	16.6763
31MA684	518	1778	503.0429	477.6696	97.14826	fea518pos	0	post-noncultural		n	n			n	503.0429	477.6696	N/A	N/A	N/A	N/A	N/A	noncultur	18.1111
31MA684	541	2161	506.6004	482.5836	98.85675	feapost54	0	post-noncultural		n	n	mounded			506.6004	482.5836	N/A	N/A	N/A	N/A	N/A	noncultur	1.4585
31MA684	545	2165	506.2108	483.1214	98.84943	feapost54	0	post-noncultural		n	n				506.2108	483.1214	N/A	N/A	N/A	N/A	N/A	noncultur	13.2838
31MA684	550	2170	505.7384	483.4417	97.21338	feapost55	0	post-noncultural		n	n				505.7384	483.4417	N/A	N/A	N/A	N/A	N/A	noncultur	1.6285
31MA684	10	533	492.7839	468.4012	96.85147	fea10post	1	post-real		n	n	group of r	dipol pres		492.7839	468.4012	19	12	N/A	N/A	N/A	Structure	7.8381
31MA684	12	535	493.9076	467.8968	96.77724	fea12post	1	post-real		m	n	strong in p		0.25	493.9076	467.8968	18	5	N/A	N/A	N/A	Structure	3.2872
31MA684	13	536	494.4495	467.6903	96.73972	fea13post	1	post-real		n	n				494.4495	467.6903	21.5	36	N/A	N/A	N/A	Structure	5.1726
31MA684	14	537	495.4523	467.1432	96.69118	fea14post	1	post-real		n	n				495.4523	467.1432	22	13	N/A	N/A	N/A	Structure	24.2699
31MA684	15	538	495.5912	467.2845	96.71052	fea15post	1	post-real		n	n				495.5912	467.2845	15.5	13	N/A	N/A	N/A	Structure	6.3811
31MA684	24	547	495.4633	469.4709	96.85108	fea24post	1	post-real		m	n	Pro only; t		0.52	495.4633	469.4709	17	35	N/A	N/A	N/A	Structure	3.813
31MA684	32	554	495.2795	470.4895	96.91482	fea32post	1	post-real		n	n		faint circu		495.2795	470.4895	15.5	13	N/A	N/A	N/A	Structure	13.4818
31MA684	33	555	495.7284	470.2917	96.89018	fea33post	1	post-real		n	n				495.7284	470.2917	14	7	N/A	N/A	N/A	Structure	17.5711
31MA684	39	561	495.3618	471.5923	96.95614	fea39post	1	post-real		n	n				495.3618	471.5923	12.5	7	N/A	N/A	N/A	Structure	6.5283
31MA684	40	562	496.0397	471.1486	96.91977	fea40post	1	post-real		n	n				496.0397	471.1486	26	37	N/A	N/A	N/A	Structure	23.5855
31MA684	41	563	495.5562	471.3488	96.94422	fea41post	1	post-real		n	n	strong ref			495.5562	471.3488	19	29	N/A	N/A	N/A	Structure	23.2268
31MA684	42	564	496.5984	470.938	96.89841	fea42post	1	post-real		m	n	very faint		0.48	496.5984	470.938	17.5	18	N/A	N/A	N/A	Structure	21.8513

31MA684	45	567	495.7778	472.9877	97.00226	fea45post	1	post-real		n	n				495.7778	472.9877	24	28	N/A	N/A	N/A	Structure	11.0468
31MA684	46	568	495.6465	473.1699	97.01711	fea46post	1	post-real		m	n	very faint		0.22	495.6465	473.1699	27.5	37	N/A	N/A	N/A	Structure	1.9133
31MA684	53	575	495.8286	476.7595	97.14755	fea53post	1	post-real		n	n				495.8286	476.7595	25	34	N/A	N/A	N/A	Structure	2.7485
31MA684	54	576	496.5295	476.3305	97.13381	fea54post	1	post-real		m	n	very faint		0.4	496.5295	476.3305	26	27	N/A	N/A	N/A	Structure	20.4952
31MA684	55	577	497.2538	475.7632	97.10006	fea55post	1	post-real		n	n				497.2538	475.7632	25.5	26	N/A	N/A	N/A	Structure	0.5675
31MA684	56	578	497.5746	475.2745	98.69198	fea56post	1	post-real		n	n				497.5746	475.2745	19.5	26	N/A	N/A	N/A	Structure	13.6657
31MA684	57	579	498.0903	475.0383	97.08515	fea57post	1	post-real		n	n				498.0903	475.0383	19.5	37	N/A	N/A	N/A	Structure	8.1111
31MA684	63	585	497.1396	466.7236	96.67058	fea63post	1	post-real		n	n				497.1396	466.7236	24	22	N/A	N/A	N/A	Structure	9.0294
31MA684	64	586	497.6788	466.5532	96.64497	fea64post	1	post-real		n	n				497.6788	466.5532	29	32	N/A	N/A	N/A		7.5855
31MA684	65	587	497.4568	467.5872	96.74812	fea65post	1	post-real		m	n	Pro only; t		0.56	497.4568	467.5872	15	13	N/A	N/A	N/A	Structure	17.0456
31MA684	68	591	497.2732	468.745	96.81838	fea68post	1	post-real		n	n				497.2732	468.745	10	7	N/A	N/A	N/A	Structure	13.5395
31MA684	69	592	497.7662	468.4752	96.80766	fea69post	1	post-real		m	n	Pro only; t		0.32	497.7662	468.4752	24	39	N/A	N/A	N/A	Structure	23.0023
31MA684	70	593	497.5054	469.1972	96.84186	fea70post	1	post-real		n	m		faint mon		497.5054	469.1972	13.5	8	N/A	N/A	N/A	Structure	13.222
31MA684	71	594	497.9751	468.984	96.81738	fea71post	1	post-real		n	n	reflection			497.9751	468.984	20.5	14	N/A	N/A	N/A	Structure	18.0989
31MA684	72	595	498.9234	468.4104	96.75024	fea72post	1	post-real		n	n				498.9234	468.4104	19.5	30	N/A	N/A	N/A		8.5321
31MA684	75	598	497.929	469.3483	96.83156	fea75post	1	post-real		n	n				497.929	469.3483	17	12	N/A	N/A	N/A	Structure	14.8512
31MA684	76	599	497.7744	470.2927	96.87092	fea76post	1	post-real		n	n				497.7744	470.2927	17.5	15	N/A	N/A	N/A	Structure	0.8839
31MA684	79	602	498.4427	470.2053	96.91396	fea79post	1	post-real		n	n				498.4427	470.2053	22	33	N/A	N/A	N/A	Structure	12.6068
31MA684	88	611	496.702	480.0822	97.26901	fea88post	1	post-real		n	n				496.702	480.0822	17	29	N/A	N/A	N/A		10.1363
31MA684	93	2395	501.4163	479.3154	97.20981	fea93post	1	post-real		m	n	very faint		0.17	501.4163	479.3154	24	23	N/A	N/A	N/A	Structure	20.793
31MA684	94	619	498.4883	477.8792	97.24138	fea94post	1	post-real		n	n	however f			498.4883	477.8792	22	20	N/A	N/A	N/A		10.3125
31MA684	95	620	498.6435	478.0213	97.23601	fea95post	1	post-real		n	n	However,			498.6435	478.0213	24.5	20	N/A	N/A	N/A		8.1784
31MA684	97	622	499.179	477.7849	97.22046	fea97post	1	post-real		m	n	very faint		0.17-0.23	499.179	477.7849	17	10	N/A	N/A	N/A		3.2575
31MA684	99	624	500.8325	478.1413	97.19841	fea99post	1	post-real		n	n	Possible c			500.8325	478.1413	20	30	N/A	N/A	N/A	Structure	9.2251
31MA684	99	2312	500.8394	478.1915	97.13489	fea99post	1	post-real		n	n	possible c			500.8325	478.1413	20	30	N/A	N/A	N/A	Structure	4.2539
31MA684	101	626	501.0848	478.9225	97.25578	fea101pos	1	post-real		n	n				501.0848	478.9225	19.5	45	N/A	N/A	N/A	Structure	22.8446
31MA684	106	640	498.0616	470.9441	96.90608	fea106pos	1	post-real		n	n				498.0616	470.9441	12.5	13	N/A	N/A	N/A		20.0585
31MA684	108	629	499.5826	470.0137	96.84793	fea108pos	1	post-real		n	n				499.5826	470.0137	15	20.5	N/A	N/A	N/A		18.4162
31MA684	109	630	500.0663	470.2923	96.8496	fea109pos	1	post-real		n	n				500.0663	470.2923	20	7	N/A	N/A	N/A		23.6685
31MA684	111	632	500.4685	471.5567	96.91227	fea111pos	1	post-real		n	n				500.4685	471.5567	14.5	11	N/A	N/A	N/A		6.3175
31MA684	112	633	500.8027	470.895	96.86584	fea112pos	1	post-real		n	n				500.8027	470.895	16	2	N/A	N/A	N/A	Structure	4.625
31MA684	113	634	500.8309	472.254	96.96228	fea113pos	1	post-real		n	n	however f			500.8309	472.254	13	4	N/A	N/A	N/A	Structure	15.9572
31MA684	116	636	500.9165	472.9884	96.99182	fea116pos	1	post-real		n	n				500.9165	472.9884	24	17	N/A	N/A	N/A	Structure	6.2691
31MA684	117	637	500.1776	474.263	97.06936	fea117pos	1	post-real		n	n				500.1776	474.263	19	18	N/A	N/A	N/A		2.7403
31MA684	118	638	501.917	473.1889	97.02122	fea118pos	1	post-real		n	n	faint refle			501.917	473.1889	18	8	N/A	N/A	N/A	Structure	7.7938

31MA684	121	653	498.1836	469.3495	96.81643	fea121pos	1	post-real		n	n				498.1836	469.3495	19	16	N/A	N/A	N/A	Structure	23.2519
31MA684	122	654	498.36	469.7784	96.85706	fea122pos	1	post-real		n	n				498.36	469.7784	16.5	10	N/A	N/A	N/A	Structure	19.5401
31MA684	125	657	499.0692	482.7855	97.34437	fea125pos	1	post-real		n	n				499.0692	482.7855	18.5	22	N/A	N/A	N/A	Structure	22.5108
31MA684	126	658	498.7282	484.3303	97.34254	fea126pos	1	post-real		n	n	however			498.7282	484.3303	18	25	N/A	N/A	N/A	Structure	7.4845
31MA684	130	663	498.9438	486.227	97.33217	fea130pos	1	post-real		n	n				498.9438	486.227	19	20.5	N/A	N/A	N/A	Structure	6.1572
31MA684	134	667	499.6351	487.2949	97.28715	fea134pos	1	post-real		n	n				499.6351	487.2949	16.5	15	N/A	N/A	N/A	Structure	17.3248
31MA684	135	668	500.0894	487.5288	97.27355	fea135pos	1	post-real		n	n				500.0894	487.5288	16.5	30	N/A	N/A	N/A	Structure	4.223
31MA684	141	674	501.498	468.9743	96.77811	fea141pos	1	post-real		n	n				501.498	468.9743	12	2	N/A	N/A	N/A		4.3534
31MA684	142	675	500.9857	470.1209	96.87347	fea142pos	1	post-real		m	n	very faint		0.39	500.9857	470.1209	28	20	N/A	N/A	N/A	Structure	12.6086
31MA684	143	676	502.1008	470.1464	96.89186	fea143pos	1	post-real		n	n				502.1008	470.1464	14.5	4	N/A	N/A	N/A	Structure	23.9115
31MA684	144	677	503.0743	470.3642	96.87485	fea144pos	1	post-real		n	n	coupling e			503.0743	470.3642	22.5	20	N/A	N/A	N/A	Structure	21.6316
31MA684	145	678	500.8858	471.531	96.928	fea145pos	1	post-real		n	n				500.8858	471.531	20	16	N/A	N/A	N/A	Structure	17.4672
31MA684	149	743	504.1024	470.4313	96.86982	fea149pos	1	post-real		n	n				504.1024	470.4313	19.5	13	N/A	N/A	N/A	Structure	18.1728
31MA684	150	682	505.1591	470.4847	96.93993	fea150pos	1	post-real		n	n				505.1591	470.4847	27	21	N/A	N/A	N/A	Structure	7.6203
31MA684	151	683	505.0778	471.2953	96.96084	fea151pos	1	post-real		n	n				505.0778	471.2953	12.5	6	N/A	N/A	N/A	Structure	18.3832
31MA684	152	684	502.9456	473.1977	97.02159	fea152pos	1	post-real		n	n	coupling e			502.9456	473.1977	22.5	25	N/A	N/A	N/A	Structure	7.8981
31MA684	154	686	500.7503	481.4827	97.32927	fea154pos	1	post-real		m	n	faint refle		0.28	500.7503	481.4827	22.5	38	N/A	N/A	N/A	Structure	4.0393
31MA684	155	687	500.9913	483.5502	97.3447	fea155pos	1	post-real		n	n	series of s			500.9913	483.5502	25.5	42	N/A	N/A	N/A	Structure	7.3845
31MA684	156	688	500.8375	485.5101	97.31918	fea156pos	1	post-real		n	n				500.8375	485.5101	24.5	40	N/A	N/A	N/A	Structure	12.309
31MA684	159	691	502.8002	485.7511	97.30434	fea159pos	1	post-real		n	n	however,			502.8002	485.7511	25.5	41	N/A	N/A	N/A	Structure	24.3607
31MA684	161	693	501.5658	487.8693	97.25549	fea161pos	1	post-real		n	n				501.5658	487.8693	20.5	19	N/A	N/A	N/A	Structure	15.5262
31MA684	162	694	502.6766	487.4066	97.21336	fea162pos	1	post-real		n	n				502.6766	487.4066	18	34	N/A	N/A	N/A	Structure	23.1261
31MA684	163	695	503.3469	487.6193	97.25062	fea163pos	1	post-real		m	n	very faint		0.37	503.3469	487.6193	18	42	N/A	N/A	N/A	Structure	18.8018
31MA684	169	745	503.8608	473.3445	96.9626	fea169pos	1	post-real		n	n	however,			503.8608	473.3445	19.5	8	N/A	N/A	N/A	Structure	14.2281
31MA684	171	700	505.4064	472.5813	96.99243	fea171pos	1	post-real		n	n	possible c			505.4064	472.5813	18.5	4	N/A	N/A	N/A		13.9115
31MA684	172	701	504.7731	473.5004	97.04454	fea172pos	1	post-real		m	n	Y In pro ar		0.29	504.7731	473.5004	29.5	18	N/A	N/A	N/A	Structure	19.7975
31MA684	173	702	504.7885	476.3645	97.12274	fea173pos	1	post-real		n	n				504.7885	476.3645	10.5	24	N/A	N/A	N/A	Structure	1.5256
31MA684	174	703	504.724	476.7166	97.16181	fea174pos	1	post-real		n	n				504.724	476.7166	14.5	17	N/A	N/A	N/A	Structure	17.2803
31MA684	177	706	501.0784	477.5869	97.17621	fea177pos	1	post-real		n	n				501.0784	477.5869	17	20	N/A	N/A	N/A	Structure	3.6439
31MA684	178	707	501.8972	477.2975	97.1741	fea178pos	1	post-real		n	n				501.8972	477.2975	21.5	40	N/A	N/A	N/A	Structure	4.3578
31MA684	179	708	502.8822	476.9852	97.17128	fea179pos	1	post-real		n	n				502.8822	476.9852	16.5	29	N/A	N/A	N/A	Structure	1.8326
31MA684	180	709	503.8847	476.757	97.15447	fea180pos	1	post-real		n	n		on rim of		503.8847	476.757	19	33	N/A	N/A	N/A	Structure	9.2203
31MA684	181	710	504.3183	476.8621	97.17292	fea181pos	1	post-real		n	n	possible c	edge of ci		504.3183	476.8621	14.5	19	N/A	N/A	N/A	Structure	16.7331
31MA684	182	711	504.5726	477.1227	97.20515	fea182pos	1	post-real		n	n				504.5726	477.1227	11.5	18	N/A	N/A	N/A	Structure	16.1839
31MA684	183	746	502.9998	477.4246	97.14615	fea183pos	1	post-real		n	n				502.9998	477.4246	14	25	N/A	N/A	N/A	Structure	6.4538

31MA684	184	712	502.6718	477.7174	97.2008	fea184pos	1	post-real		n	n				502.6718	477.7174	12.5	10	N/A	N/A	N/A	Structure	10.5546
31MA684	186	714	502.8381	478.305	97.2191	fea186pos	1	post-real		n	n				502.8381	478.305	13.5	11	N/A	N/A	N/A	Structure	21.529
31MA684	187	747	502.9843	478.6654	97.16665	fea187pos	1	post-real		n	n				502.9843	478.6654	11	11	N/A	N/A	N/A	Structure	10.364
31MA684	188	715	501.3562	477.6054	97.15043	fea188pos	1	post-real		n	n				501.3562	477.6054	17	30	N/A	N/A	N/A	Structure	7.1444
31MA684	189	716	501.4951	477.6964	97.14062	fea189pos	1	post-real		n	n				501.4951	477.6964	17.5	26	N/A	N/A	N/A	Structure	20.2715
31MA684	191	748	503.0156	478.9286	97.17917	fea191pos	1	post-real		n	n				503.0156	478.9286	24.5	55	N/A	N/A	N/A	Structure	13.7312
31MA684	192	749	503.3132	478.7016	97.17735	fea192pos	1	post-real		n	n				503.3132	478.7016	17.5	26	N/A	N/A	N/A	Structure	24.4876
31MA684	193	718	505.1148	476.6566	97.14874	fea193pos	1	post-real		n	n				505.1148	476.6566	17	31	N/A	N/A	N/A	Structure	10.239
31MA684	194	719	505.8487	476.2061	97.15274	fea194pos	1	post-real		n	n	extrmly fa			505.8487	476.2061	19	36	N/A	N/A	N/A	Structure	21.0546
31MA684	197	722	504.878	477.8415	97.23912	fea197pos	1	post-real		n	n				504.878	477.8415	11	15	N/A	N/A	N/A	Structure	5.9103
31MA684	198	723	505.9222	477.3208	97.19712	fea198pos	1	post-real		n	n				505.9222	477.3208	10	8	N/A	N/A	N/A	Structure	21.1583
31MA684	199	724	507.0591	476.5862	97.17711	fea199pos	1	post-real		n	n				507.0591	476.5862	18	31	N/A	N/A	N/A	Structure	3.6072
31MA684	200	725	506.885	476.9853	97.18417	fea200pos	1	post-real		m	n	faint in pr		0.29	506.885	476.9853	20	26	N/A	N/A	N/A	Structure	21.5391
31MA684	201	726	504.7545	478.0944	97.22921	fea201pos	1	post-real		n	n				504.7545	478.0944	14.5	22	N/A	N/A	N/A		13.987
31MA684	202	727	505.1058	478.2131	97.24386	fea202pos	1	post-real		n	n				505.1058	478.2131	19.5	26	N/A	N/A	N/A	Structure	13.354
31MA684	203	728	505.9601	478.0788	97.22082	fea203pos	1	post-real		n	n				505.9601	478.0788	28.5	46	N/A	N/A	N/A	Structure	1.749
31MA684	205	730	506.5034	477.7311	97.20738	fea205pos	1	post-real		n	n				506.5034	477.7311	16	25	N/A	N/A	N/A		13.4418
31MA684	206	731	507.7622	477.6123	97.22602	fea206pos	1	post-real		n	n	soil strata			507.7622	477.6123	20	49	N/A	N/A	N/A	Structure	16.2947
31MA684	207	732	507.6383	478.1861	97.24051	fea207pos	1	post-real		n	n	soil strata			507.6383	478.1861	16.5	6	N/A	N/A	N/A	Structure	16.5168
31MA684	208	733	507.9707	478.3759	97.27528	fea208pos	1	post-real		n	n	soil strata			507.9707	478.3759	21	42	N/A	N/A	N/A	Structure	4.7114
31MA684	209	734	506.5092	479.2299	97.27544	fea209pos	1	post-real		n	n				506.5092	479.2299	18.5	20	N/A	N/A	N/A	Structure	21.5377
31MA684	210	735	507.8563	478.8481	97.28486	fea210pos	1	post-real		n	n	soil strat c			507.8563	478.8481	15.5	30	N/A	N/A	N/A	Structure	13.7954
31MA684	211	736	504.8435	484.8097	97.29732	fea211pos	1	post-real		n	n				504.8435	484.8097	20	26	N/A	N/A	N/A	Structure	1.8482
31MA684	213	738	504.7134	486.3323	97.23864	fea213pos	1	post-real		m	n	faint in pr		0.15	504.7134	486.3323	14	18	N/A	N/A	N/A	Structure	8.4183
31MA684	214	739	504.187	487.2265	97.26522	fea214pos	1	post-real		y	n	Strong in		0.21	504.187	487.2265	17.5	19	N/A	N/A	N/A	Structure	9.0014
31MA684	217	923	505.2301	465.4857	96.54031	fea217pos	1	post-real		n	n				505.2301	465.4857	14.5	25	N/A	N/A	N/A		12.7538
31MA684	218	924	506.1882	470.6695	96.90043	fea218pos	1	post-real		n	n				506.1882	470.6695	19.5	12	N/A	N/A	N/A		8.5909
31MA684	219	925	506.6936	471.2227	96.93186	fea219pos	1	post-real		n	n				506.6936	471.2227	20	9	N/A	N/A	N/A		22.6524
31MA684	222	928	507.4955	472.7384	96.99439	fea222pos	1	post-real		n	n	possible c			507.4955	472.7384	14	11	N/A	N/A	N/A		3.2399
31MA684	226	1013	508.2671	479.3604	97.23081	fea226pos	1	post-real		n	n	possible c			508.2671	479.3604	21	48	N/A	N/A	N/A	Structure	1.9837
31MA684	227	1014	506.7792	479.78	97.25716	fea227pos	1	post-real		n	n	however r			506.7792	479.78	22	30	N/A	N/A	N/A	Structure	10.7277
31MA684	228	1015	506.574	479.5972	97.24524	fea228pos	1	post-real		n	n				506.574	479.5972	16.5	16	N/A	N/A	N/A	Structure	15.3103
31MA684	229	1016	503.2581	479.6401	97.20645	fea229pos	1	post-real		n	n	however s			503.2581	479.6401	22	29	N/A	N/A	N/A	Structure	11.4366
31MA684	231	1018	503.0447	480.0604	97.21955	fea231pos	1	post-real		n	n				503.0447	480.0604	16.5	19	N/A	N/A	N/A	Structure	5.7649
31MA684	234	1021	501.8498	480.1808	97.24388	fea234pos	1	post-real		n	n		faint linea		501.8498	480.1808	22	20	N/A	N/A	N/A	Structure	16.7338

31MA684	237	1024	501.5052	480.677	97.24591	fea237pos	1	post-real		n	n				501.5052	480.677	16	26	N/A	N/A	N/A	Structure	2.4299
31MA684	238	1025	516.1004	457.7335	96.40255	fea238pos	1	post-real		n	n				516.1004	457.7335	9	8	N/A	N/A	N/A	Palisade/s	8.0365
31MA684	239	1026	516.2731	457.8395	96.38595	fea239pos	1	post-real		n	n				516.2731	457.8395	9	11	N/A	N/A	N/A	Palisade/s	23.6816
31MA684	244	1031	517.1604	458.8548	96.32032	fea244pos	1	post-real		n	n				517.1604	458.8548	6.5	7	N/A	N/A	N/A	Palisade/s	1.4362
31MA684	245	1032	517.5011	459.297	96.38999	fea245pos	1	post-real		n	n				517.5011	459.297	8.5	13	N/A	N/A	N/A	Palisade/s	1.4616
31MA684	248	1035	517.9445	459.8333	96.40591	fea248pos	1	post-real		n	n	coupling e			517.9445	459.8333	7.5	12	N/A	N/A	N/A	Palisade/s	16.6043
31MA684	249	1036	518.055	460.0377	96.39478	fea249pos	1	post-real		n	n	coupling e			518.055	460.0377	8	13	N/A	N/A	N/A	Palisade/s	10.4759
31MA684	250	1037	518.1865	460.2458	96.39932	fea250pos	1	post-real		n	n				518.1865	460.2458	7	5	N/A	N/A	N/A	Palisade/s	13.4838
31MA684	251	1038	518.3418	460.4723	96.4228	fea251pos	1	post-real		n	n				518.3418	460.4723	8	7	N/A	N/A	N/A	Palisade/s	10.0482
31MA684	252	1039	518.4415	460.6916	96.44576	fea252pos	1	post-real		n	n				518.4415	460.6916	7.5	7	N/A	N/A	N/A	Palisade/s	13.938
31MA684	253	1040	518.566	460.8956	96.46638	fea253pos	1	post-real		n	n	possible c			518.566	460.8956	7	10	N/A	N/A	N/A	Palisade/s	12.7196
31MA684	254	1041	518.6996	461.1112	96.47629	fea254pos	1	post-real		n	n	possible c			518.6996	461.1112	7.5	14	N/A	N/A	N/A	Palisade/s	12.0134
31MA684	255	1042	518.8206	461.2852	96.48981	fea255pos	1	post-real		n	n				518.8206	461.2852	8.5	13	N/A	N/A	N/A	Palisade/s	17.6032
31MA684	256	1043	518.9274	461.4523	96.50117	fea256pos	1	post-real		n	n				518.9274	461.4523	8.5	13	N/A	N/A	N/A	Palisade/s	1.6833
31MA684	259	1046	519.1584	462.186	96.56835	fea259pos	1	post-real		n	n				519.1584	462.186	8	7	N/A	N/A	N/A	Palisade/s	21.4326
31MA684	260	1047	519.3222	462.4324	96.59245	fea260pos	1	post-real		n	n				519.3222	462.4324	6.5	7	N/A	N/A	N/A	Palisade/s	7.2015
31MA684	261	1048	519.454	462.7822	96.59963	fea261pos	1	post-real		n	n				519.454	462.7822	7.5	8	N/A	N/A	N/A	Palisade/s	5.4352
31MA684	265	1052	519.8174	463.9827	96.69548	fea265pos	1	post-real		n	n				519.8174	463.9827	6.5	4	N/A	N/A	N/A	Palisade/s	19.9049
31MA684	266	1053	519.8283	464.2996	96.72349	fea266pos	1	post-real		n	n	possible c			519.8283	464.2996	7	7	N/A	N/A	N/A	Palisade/s	0.2306
31MA684	267	1054	519.8227	464.911	96.74372	fea267pos	1	post-real		n	n				519.8227	464.911	6.5	10	N/A	N/A	N/A	Palisade/s	7.8568
31MA684	268	1055	519.8091	465.1893	96.76524	fea268pos	1	post-real		n	n	however,			519.8091	465.1893	6	9	N/A	N/A	N/A	Palisade/s	16.2714
31MA684	270	1057	519.6984	465.8235	96.82634	fea270pos	1	post-real		n	n	possible c			519.6984	465.8235	4	6	N/A	N/A	N/A	Palisade/s	9.9047
31MA684	271	1058	519.6983	466.1126	96.83052	fea271pos	1	post-real		n	n	possible c			519.6983	466.1126	8	11	N/A	N/A	N/A	Palisade/s	17.4208
31MA684	273	1060	519.6086	466.4001	96.84471	fea273pos	1	post-real		n	n	very faint		0.34	519.6086	466.4001	5	6	N/A	N/A	N/A	Palisade/s	8.3103
31MA684	278	1065	518.7394	469.2947	97.01614	fea278pos	1	post-real		n	n				518.7394	469.2947	6.5	8	N/A	N/A	N/A	Palisade/s	12.8988
31MA684	283	1070	517.8028	471.26	97.12787	fea283pos	1	post-real		n	n	In pro and		0.2	517.8028	471.26	8	10	N/A	N/A	N/A	Palisade/s	7.5536
31MA684	284	1071	517.6624	471.525	97.14873	fea284pos	1	post-real		n	n	very faint		0.2	517.6624	471.525	6	11	N/A	N/A	N/A	Palisade/s	12.9309
31MA684	288	1075	516.1881	473.3521	97.18054	fea288pos	1	post-real		n	n				516.1881	473.3521	8.7	18	N/A	N/A	N/A	Palisade/s	12.2857
31MA684	289	1076	515.9002	473.5255	97.17707	fea289pos	1	post-real		n	n				515.9002	473.5255	7	15	N/A	N/A	N/A	Palisade/s	5.2687
31MA684	290	1077	514.9517	474.0451	97.19396	fea290pos	1	post-real		n	n				514.9517	474.0451	8	16	N/A	N/A	N/A	Palisade/s	12.9986
31MA684	291	1078	514.2139	474.3886	97.21605	fea291pos	1	post-real		n	n				514.2139	474.3886	6	18	N/A	N/A	N/A	Palisade/s	21.4596
31MA684	292	1079	512.7368	475.5404	97.19558	fea292pos	1	post-real		n	n	very faint		0.18	512.7368	475.5404	7.5	13	N/A	N/A	N/A	Palisade/s	17.7033
31MA684	293	1080	512.4183	475.7172	97.18498	fea293pos	1	post-real		n	n	Y Strong ir		0.33	512.4183	475.7172	8	13	N/A	N/A	N/A	Palisade/s	11.3533
31MA684	298	1085	508.8517	476.16	97.14016	fea298pos	1	post-real		n	n				508.8517	476.16	8	9	N/A	N/A	N/A	Palisade/s	14.4309
31MA684	299	1086	505.0391	472.0381	96.92222	fea299pos	1	post-real		n	n	however t			505.0391	472.0381	18	21	N/A	N/A	N/A	Structure	0.601

31MA684	300	1087	499.8586	481.9745	97.26989	fea300pos	1	post-real		n	n	coupling e			499.8586	481.9745	16	18	N/A	N/A	N/A	Structure -	21.5239
31MA684	316	1345	507.9688	479.5235	97.20002	fea316pos	1	post-real		n	n	however r			507.9688	479.5235	18.5	29	N/A	N/A	N/A	Structure	3.7355
31MA684	317	1346	508.0328	479.7955	97.2361	fea317pos	1	post-real		m	n	Pro only; t		0.21	508.0328	479.7955	16	16	N/A	N/A	N/A	Structure	18.4689
31MA684	318	1347	508.4146	480.1634	97.2376	fea318pos	1	post-real		n	n	soil strata			508.4146	480.1634	20	47	N/A	N/A	N/A	Structure	21.2537
31MA684	321	1350	505.8695	479.8231	97.2281	fea321pos	1	post-real		n	n				505.8695	479.8231	10	5	N/A	N/A	N/A	Structure	13.7356
31MA684	322	1351	506.6978	480.8058	97.25021	fea322pos	1	post-real		n	n	pit feature			506.6978	480.8058	27	45	N/A	N/A	N/A	Structure	16.3827
31MA684	323	1352	506.8005	481.1309	97.25723	fea323pos	1	post-real		n	n	strata chai			506.8005	481.1309	35.5	67	N/A	N/A	N/A	Structure	17.694
31MA684	325	1353	505.1077	471.0323	96.87194	fea325pos	1	post-real		n	n				505.1077	471.0323	12	6	N/A	N/A	N/A		7.7241
31MA684	343	1404	507.4135	481.2185	97.25622	fea343pos	1	post-real		n	n	strata chai			507.4135	481.2185	28.5	37	N/A	N/A	N/A	Structure	4.0723
31MA684	344	1405	505.6505	481.4774	97.22752	fea344pos	1	post-real		n	n	coupling e			505.6505	481.4774	27.5	51	N/A	N/A	N/A	Structure	13.0324
31MA684	345	1406	505.8263	481.642	97.21114	fea345pos	1	post-real		n	n	strata chai			505.8263	481.642	20.5	35	N/A	N/A	N/A	Structure	15.6871
31MA684	352	1417	501.6369	481.0116	97.25453	fea352pos	1	post-real		n	n	possible s			501.6369	481.0116	17	55	N/A	N/A	N/A	Structure	11.6448
31MA684	353	1418	505.0922	478.029	97.18777	fea353pos	1	post-real		n	n				505.0922	478.029	15	30	N/A	N/A	N/A	Structure	18.7913
31MA684	484	1586	502.8937	479.7521	97.20874	fea484pos	1	post-real		n	n				502.8937	479.7521	11	19	N/A	N/A	N/A	Structure	10.1684
31MA684	485	1587	501.7191	481.4451	97.2511	fea485pos	1	post-real		n	n	soil strata			501.7191	481.4451	20.5	21	N/A	N/A	N/A	Structure -	17.9813
31MA684	486	1588	502.0711	481.611	97.23184	fea486pos	1	post-real		n	n				502.0711	481.611	15	14	N/A	N/A	N/A	Structure	9.1665
31MA684	487	1589	502.453	481.5772	97.21424	fea487pos	1	post-real		n	n				502.453	481.5772	16.5	35	N/A	N/A	N/A	Structure -	18.3991
31MA684	489	1591	501.9636	481.9988	97.22532	fea489pos	1	post-real		n	n				501.9636	481.9988	19.5	42	N/A	N/A	N/A	Structure	7.6649
31MA684	490	1592	502.3474	482.943	97.21018	fea490pos	1	post-real		n	n	strata chai			502.3861	482.9884	19	53	N/A	N/A	N/A	Structure	5.8981
31MA684	491	1593	502.339	482.2687	97.21435	fea491pos	1	post-real		n	n				502.339	482.2687	12	13	N/A	N/A	N/A	Structure	19.9335
31MA684	492	1594	502.3884	481.9962	97.23548	fea492pos	1	post-real		n	n	soil strata			502.3884	481.9962	13	25	N/A	N/A	N/A	Structure	5.9138
31MA684	493	1595	502.7377	482.6251	97.21624	fea493pos	1	post-real		n	n	series of s			502.7377	482.6251	18	35	N/A	N/A	N/A	Structure	23.2471
31MA684	494	1596	503.2765	482.1547	97.22822	fea494pos	1	post-real		n	n				503.2765	482.1547	14.5	17	N/A	N/A	N/A	Structure	0.1944
31MA684	495	1597	503.6369	482.2316	97.24498	fea495pos	1	post-real		n	n	strata chai			503.6369	482.2316	21	36	N/A	N/A	N/A	Structure -	18.8038
31MA684	497	1599	503.7294	481.7187	97.22691	fea497pos	1	post-real		n	n	pit like fea			503.7294	481.7187	10.5	6	N/A	N/A	N/A	Structure	23.3175
31MA684	498	1600	503.8941	482.021	97.2521	fea498pos	1	post-real		n	n	possible c			503.8941	482.021	34	55	N/A	N/A	N/A	Structure	7.269
31MA684	499	1601	504.3008	482.2705	97.24785	fea499pos	1	post-real		n	n	series of s			504.3008	482.2705	18.5	32	N/A	N/A	N/A	Structure	5.9078
31MA684	500	1602	504.8218	481.9374	97.22699	fea500pos	1	post-real		n	n				504.8218	481.9374	15.5	24	N/A	N/A	N/A	Structure	20.4508
31MA684	501	1771	504.5422	481.9492	97.22205	fea501pos	1	post-real		m	n	ambigious		0.25	504.5422	481.9492	13	20	N/A	N/A	N/A	Structure	21.5659
31MA684	513	1773	505.3148	481.6492	97.19599	fea513pos	1	post-real		m	n	faint in pr		0.28	505.3148	481.6492	26	26	N/A	N/A	N/A	Structure	18.3499
31MA684	514	1774	501.0284	478.314	97.14625	fea514pos	1	post-real		n	n				501.0284	478.314	18	29	N/A	N/A	N/A	Structure	13.4737
31MA684	515	1775	501.2399	478.4491	97.14877	fea515pos	1	post-real		n	n				501.2399	478.4491	13	19	N/A	N/A	N/A	Structure	16.864
31MA684	527	2147	508.5703	480.9224	98.86184	feapost52	1	post-real		n	n				508.5703	480.9224	17	50	N/A	N/A	N/A	Structure	5.5786
31MA684	528	2148	508.2942	481.0996	98.8498	feapost52	1	post-real		m	n	Pro and 3D		0.33	508.2942	481.0996	19	21	N/A	N/A	N/A	Structure	13.3552
31MA684	529	2149	508.6965	481.4952	98.85094	feapost52	1	post-real		m	n	faint in pr		.62-.63	508.6965	481.4952	18.5	46	N/A	N/A	N/A	Structure	13.8463

31MA684	530	2150	508.3443	481.6263	98.84247	feapost53	1	post-real		m	n	faint in pr		0.62	508.3443	481.6263	19.5	30	N/A	N/A	N/A	Structure	14.7807
31MA684	532	2152	508.1209	482.0596	98.84067	feapost53	1	post-real		n	n				508.1209	482.0596	16	33	N/A	N/A	N/A	Structure	1.5126
31MA684	533	2153	508.3508	482.1759	98.83689	feapost53	1	post-real		n	n	coupling e			508.3508	482.1759	22.5	29	N/A	N/A	N/A	Structure	16.9599
31MA684	536	2156	507.1991	483.0056	98.8365	feapost53	1	post-real		n	n				507.1991	483.0056	25.5	52	N/A	N/A	N/A	Structure	7.9336
31MA684	537	2157	506.9499	482.7049	98.84418	feapost53	1	post-real		n	n				506.9499	482.7049	15	30	N/A	N/A	N/A	Structure	21.3873
31MA684	538	2158	507.1668	481.79	98.85354	feapost53	1	post-real		n	n				507.1668	481.79	24	24	N/A	N/A	N/A	Structure	8.0607
31MA684	539	2159	507.2443	481.377	98.8645	feapost53	1	post-real		n	n				507.2443	481.377	15.5	19	N/A	N/A	N/A	Structure	5.4119
31MA684	540	2160	506.6895	481.4073	98.86659	feapost54	1	post-real		n	n	strata cha			506.6895	481.4073	18	37	N/A	N/A	N/A	Structure	9.7797
31MA684	542	2162	505.7657	482.2063	98.84525	feapost54	1	post-real		n	n				505.7657	482.2063	16.5	24	N/A	N/A	N/A	Structure	14.3021
31MA684	543	2163	505.8796	482.7764	98.83559	feapost54	1	post-real		n	n				505.8796	482.7764	11	19	N/A	N/A	N/A	Structure	6.684
31MA684	544	2164	506.2214	482.9143	98.85831	feapost54	1	post-real		n	n				506.2214	482.9143	20	30	N/A	N/A	N/A	Structure	17.4757
31MA684	546	2166	506.2331	483.3018	98.84485	feapost54	1	post-real		n	n				506.2331	483.3018	15.5	27	N/A	N/A	N/A	Structure	4.4977
31MA684	549	2169	505.6725	482.9591	97.2289	feapost54	1	post-real		n	n				505.6725	482.9591	13.5	25	N/A	N/A	N/A	Structure	3.8457
31MA684	551	2171	505.4133	483.4882	97.22042	feapost55	1	post-real		n	n	coupling e			505.4133	483.4882	20.5	48	N/A	N/A	N/A	Structure	4.5566
31MA684	552	2172	504.9092	483.2382	97.21416	feapost55	1	post-real		n	n	coupling e			504.9092	483.2382	17	25	N/A	N/A	N/A	Structure	5.3969
31MA684	553	2173	504.3634	482.5272	97.25158	feapost55	1	post-real		m	n	In Pro, ver		0.24	504.3634	482.5272	14	27	N/A	N/A	N/A	Structure	20.4059
31MA684	554	2174	503.7496	483.4524	97.2127	feapost55	1	post-real		n	n				503.7496	483.4524	16.5	35	N/A	N/A	N/A	Structure	12.0945
31MA684	555	2175	504.4293	483.4641	97.2056	feapost55	1	post-real		n	n	coupling e			504.4293	483.4641	16	24	N/A	N/A	N/A	Structure	11.1352
31MA684	556	2176	504.4483	483.7953	97.23139	feapost55	1	post-real		n	n	coupling e			504.4483	483.7953	14	35	N/A	N/A	N/A	Structure	6.9331
31MA684	557	2177	502.8664	482.9426	97.23304	feapost55	1	post-real		n	n	series of s			502.8664	482.9426	21	27	N/A	N/A	N/A	Structure	10.9558
31MA684	558	2178	503.2198	483.356	97.22767	feapost55	1	post-real		n	n				503.2198	483.356	27	11	N/A	N/A	N/A	Structure	11.5481
31MA684	559	2179	502.9863	483.37	97.24174	feapost55	1	post-real		n	n				502.9863	483.37	10.5	19	N/A	N/A	N/A	Structure	5.2724
31MA684	561	2181	503.0025	483.8263	97.2622	feapost56	1	post-real		m	n	In Pro, fai		0.37	503.0025	483.8263	22.5	42	N/A	N/A	N/A	Structure	1.0508
31MA684	562	2182	502.5921	483.5221	97.24044	feapost56	1	post-real		n	n	however r			502.5921	483.5221	19.5	22	N/A	N/A	N/A	Structure	6.8254
31MA684	563	2183	502.706	483.772	97.24279	feapost56	1	post-real		y	n	Pro only; t		0.4	502.706	483.772	19.5	43	N/A	N/A	N/A	Structure	15.8371
31MA684	564	2184	503.1828	483.9299	97.2488	feapost56	1	post-real		m	n	faint in pr		0.36	503.1828	483.9299	11	7	N/A	N/A	N/A	Structure	14.6094
31MA684	565	2185	503.3907	483.9666	97.2585	feapost56	1	post-real		n	n				503.3907	483.9666	18.5	6	N/A	N/A	N/A	Structure	24.8443
31MA684	566	2186	503.5952	484.0517	97.22504	feapost56	1	post-real		n	n				503.5952	484.0517	20	50	N/A	N/A	N/A	Structure	10.4522
31MA684	568	2304	503.0091	484.0158	97.21862	fea568pos	1	post-real		m	n	Pro only; t		0.3	503.0091	484.0158	15	20	N/A	N/A	N/A	Structure	17.0759
31MA684	570	2309	505.6026	481.5862	97.20329	fea570pos	1	post-real		y	n	in pro only		0.31	505.6026	481.5862	15.5	39	N/A	N/A	N/A	Structure	21.7578
31MA684	571	2387	506.0765	478.302	97.16048	fea571pos	1	post-real		n	n	However,			506.0765	478.302	13	40	N/A	N/A	N/A	Structure	23.3552
31MA684	11	534	493.0496	468.1929	96.79773	fea11post	2	post-noncultural		m	n	faint in pr		0.15	493.0496	468.1929	N/A	N/A	N/A	N/A	N/A		3.2146
31MA684	52	574	497.2561	474.7319	97.07947	fea52post	2	post-ambiguous		n	n				497.2561	474.7319	N/A	N/A	N/A	N/A	N/A		1.9943
31MA684	73	596	496.939	469.7335	96.84073	fea73post	2	post-ambiguous		n	n	however p			496.939	469.7335	14.5	7	N/A	N/A	N/A	Structure	19.0509
31MA684	74	597	497.4728	469.4621	98.44303	fea74post	2	post-ambiguous		n	m		circular m		497.4728	469.4621	18	12	N/A	N/A	N/A	Structure	10.7568

31MA684	77	600	497.9278	470.7024	96.89573	fea77post	2	post-ambiguous	n	n				497.9278	470.7024	17.5	23	N/A	N/A	N/A	may be m	7.1546
31MA684	78	601	498.2116	470.4517	96.89827	fea78post	2	post-ambiguous	n	n				498.2116	470.4517	10.5	8	N/A	N/A	N/A	Structure	21.6226
31MA684	98	623	498.6332	478.9071	97.26701	fea98post	2	post-ambiguous	m	n	faint in pr		0.16	498.6332	478.9071	31	13	N/A	N/A	N/A		8.4024
31MA684	107	628	499.4293	470.0881	98.43463	fea107pos	2	post-ambiguous	n	n	strata char			499.4293	470.0881	16	25	N/A	N/A	N/A		16.3741
31MA684	120	2396	497.1171	464.5104	96.23949	fea120pos	2	post-ambiguous	m	n	faint in Pr	square sig	0.55	497.1171	464.5104	23.5	12	N/A	N/A	N/A		19.0295
31MA684	129	662	498.7805	485.5849	97.33704	fea129pos	2	post-ambiguous	n	n				498.7805	485.5849	14.5	3	N/A	N/A	N/A	Structure	22.187
31MA684	132	665	499.1175	486.647	97.31921	fea132pos	2	post-ambiguous	n	n	tran 25/ 2			499.1175	486.647	15.5	19	N/A	N/A	N/A		10.7854
31MA684	146	679	502.2922	471.1146	96.93147	fea146pos	2	post-ambiguous	m	n	faint in pr		0.33	502.2922	471.1146	13	17	N/A	N/A	N/A	Structure	23.8728
31MA684	148	681	503.3779	470.5351	96.91067	fea148pos	2	post-ambiguous	n	n				503.3779	470.5351	10.5	2	N/A	N/A	N/A	Structure	4.4101
31MA684	157	689	500.9703	485.9106	97.29823	fea157pos	2	post-ambiguous	n	n	tran 21/ 2			500.9703	485.9106	11	5	N/A	N/A	N/A	Structure	20.1178
31MA684	165	696	505.6622	489.9692	97.24313	fea165pos	2	post-noncultural	n	n	tran 35/24			505.6622	489.9692	29.5	55	N/A	N/A	N/A		16.3486
31MA684	175	704	500.2755	476.5561	97.16292	fea175pos	2	post-ambiguous	n	n	however,			500.2755	476.5561	17.5	45	N/A	N/A	N/A		22.757
31MA684	185	713	502.7253	478.0373	97.21232	fea185pos	2	post-ambiguous	n	n	coupling e			502.7253	478.0373	10	10	N/A	N/A	N/A	Structure	7.4516
31MA684	190	717	501.6695	477.8079	97.15627	fea190pos	2	post-ambiguous	n	n				501.6695	477.8079	9.5	9	N/A	N/A	N/A	Structure	13.5133
31MA684	195	720	505.2718	477.1374	97.21843	fea195pos	2	post-ambiguous	n	n				505.2718	477.1374	17.5	4	N/A	N/A	N/A	Structure	9.66
31MA684	196	721	506.3659	476.5745	97.1909	fea196pos	2	post-ambiguous	n	n				506.3659	476.5745	15	20	N/A	N/A	N/A	Structure	22.7159
31MA684	204	729	506.3086	478.0949	97.20343	fea204pos	2	post-ambiguous	n	n				506.3086	478.0949	15.5	18	N/A	N/A	N/A	Structure	14.613
31MA684	215	740	504.11	488.6748	97.17595	fea215pos	2	post-ambiguous	n	n				504.11	488.6748	24	15	N/A	N/A	N/A		6.5557
31MA684	216	922	508.0951	489.6675	97.02304	fea216pos	2	post-ambiguous	n	n	tran 36/22			508.0951	489.6675	16	16	N/A	N/A	N/A		17.0064
31MA684	230	1017	503.2283	479.9869	97.22049	fea230pos	2	post-ambiguous	n	n	coupling e			503.2283	479.9869	14	25	N/A	N/A	N/A	Structure	6.7369
31MA684	233	1020	501.9025	479.9712	97.23531	fea233pos	2	post-ambiguous	n	n				501.9025	479.9712	13	15	N/A	N/A	N/A	Structure	1.3722
31MA684	235	1022	501.8245	480.4036	97.23655	fea235pos	2	post-ambiguous	n	n				501.8245	480.4036	10	21	N/A	N/A	N/A	Structure	13.0255
31MA684	240	1027	516.4262	457.9835	96.37675	fea240pos	2	post-ambiguous	n	n	strata char			516.4262	457.9835	8.5	10	N/A	N/A	N/A	Palisade/s	7.7225
31MA684	241	1028	516.5327	458.1446	96.35667	fea241pos	2	post-ambiguous	n	n				516.5327	458.1446	8	5	N/A	N/A	N/A	Palisade/s	10.9769
31MA684	242	1029	516.6402	458.3728	96.33964	fea242pos	2	post-ambiguous	n	n				516.6402	458.3728	7.5	N/A	N/A	N/A	N/A	Palisade/s	13.9484
31MA684	243	1030	516.8611	458.5328	96.31938	fea243pos	2	post-ambiguous	n	n	coupling e			516.8611	458.5328	7.5	2	N/A	N/A	N/A	Palisade/s	8.3733
31MA684	246	1033	517.6241	459.4404	96.38725	fea246pos	2	post-ambiguous	n	n				517.6241	459.4404	9	12	N/A	N/A	N/A	Palisade/s	19.0208
31MA684	247	1034	517.7918	459.6669	96.40243	fea247pos	2	post-ambiguous	n	n				517.7918	459.6669	3.5	N/A	N/A	N/A	N/A	Palisade/s	4.096
31MA684	257	1044	519.02	461.6872	96.53043	fea257pos	2	post-ambiguous	n	n				519.02	461.6872	8	11	N/A	N/A	N/A	Palisade/s	23.0952
31MA684	258	1045	519.0847	461.9568	96.54268	fea258pos	2	post-ambiguous	n	n				519.0847	461.9568	8	9	N/A	N/A	N/A	Palisade/s	4.5
31MA684	262	1049	519.5744	463.0629	96.61927	fea262pos	2	post-ambiguous	n	n				519.5744	463.0629	6.5	2	N/A	N/A	N/A	Palisade/s	24.975
31MA684	263	1050	519.6943	463.3524	96.64184	fea263pos	2	post-ambiguous	n	n				519.6943	463.3524	7.5	5	N/A	N/A	N/A	Palisade/s	6.2978
31MA684	264	1051	519.7291	463.6487	96.66995	fea264pos	2	post-ambiguous	n	n				519.7291	463.6487	9.5	2	N/A	N/A	N/A	Palisade/s	14.5507
31MA684	269	1056	519.7978	465.529	96.81054	fea269pos	2	post-ambiguous	n	n	reflection			519.7978	465.529	9	N/A	N/A	N/A	N/A	Palisade/s	15.482
31MA684	272	1059	519.689	466.3782	96.84274	fea272pos	2	post-ambiguous	n	n				519.689	466.3782	7	10	N/A	N/A	N/A	Palisade/s	7.767

31MA684	274	1061	519.5454	466.6612	96.86912	fea274pos	2	post-ambiguous		n	n				519.5454	466.6612	10	N/A	N/A	N/A	N/A	Palisade/s	14.3199
31MA684	275	1062	519.492	467.05	96.89757	fea275pos	2	post-ambiguous		n	n	strata chai			519.492	467.05	8	N/A	N/A	N/A	N/A	Palisade/s	0.6586
31MA684	276	1063	519.3715	467.7109	96.92778	fea276pos	2	post-ambiguous		n	n	very faint		0.48	519.3715	467.7109	6.5	N/A	N/A	N/A	N/A	Palisade/s	7.9126
31MA684	277	1064	518.9957	468.6864	96.99816	fea277pos	2	post-ambiguous		n	n	faint in pr		0.42	518.9957	468.6864	6.5	7	N/A	N/A	N/A	Palisade/s	12.0796
31MA684	279	1066	518.6509	469.5608	97.03869	fea279pos	2	post-ambiguous		n	n	coupling e			518.6509	469.5608	6.5	10	N/A	N/A	N/A	Palisade/s	9.3818
31MA684	281	1068	518.253	470.2703	97.0684	fea281pos	2	post-ambiguous		n	n	Pro and 3D		0.69	518.253	470.2703	9	10	N/A	N/A	N/A	Palisade/s	13.514
31MA684	282	1069	518.1436	470.5774	97.08082	fea282pos	2	post-ambiguous		n	n	however			518.1436	470.5774	6.5	8	N/A	N/A	N/A	Palisade/s	11.0066
31MA684	285	1072	517.43	471.8348	97.17057	fea285pos	2	post-ambiguous		n	n	pro and 3D		0.67	517.43	471.8348	7	6	N/A	N/A	N/A	Palisade/s	15.3351
31MA684	287	1074	516.9742	472.5964	97.17804	fea287pos	2	post-ambiguous		n	n				516.9742	472.5964	9.5	9	N/A	N/A	N/A	Palisade/s	8.1561
31MA684	294	1081	511.5504	475.979	97.16014	fea294pos	2	post-ambiguous		n	n	Y Pro and		0.36	511.5504	475.979	6.5	9	N/A	N/A	N/A	Palisade/s	14.8452
31MA684	295	1082	511.2373	476.0556	97.16034	fea295pos	2	post-ambiguous		n	n	Y Pro and		0.37	511.2373	476.0556	7	8	N/A	N/A	N/A	Palisade/s	17.7927
31MA684	296	1083	510.9366	476.1605	97.16295	fea296pos	2	post-ambiguous		n	n	Y Pro and		0.36	510.9366	476.1605	8.5	9	N/A	N/A	N/A	Palisade/s	17.6619
31MA684	303	1089	519.8314	473.6556	98.73867	fea303pos	2	post-ambiguous		n	n				519.8314	473.6556	16.5	23	N/A	N/A	N/A		15.0092
31MA684	307	2397	512.2089	461.9497	96.44573	fea307pos	2	post-ambiguous		n	n	Pro only; t		0.25	512.2089	461.9497	8.5	4	N/A	N/A	N/A		19.9551
31MA684	308	2398	512.8876	462.5934	96.51314	fea308pos	2	post-ambiguous		n	n				512.8876	462.5934	10.5	3	N/A	N/A	N/A		12.9952
31MA684	309	2399	511.4291	464.7722	96.64119	fea309pos	2	post-ambiguous		n	n				511.4291	464.7722	18	9	N/A	N/A	N/A		21.5404
31MA684	311	1300	504.1654	471.5681	96.90592	fea311pos	2	post-ambiguous		n	n	tran 60/ 20			504.1654	471.5681	10.5	7	N/A	N/A	N/A	Structure	22.2855
31MA684	320	1349	506.9824	480.2217	97.22553	fea320pos	2	post-ambiguous		m	n	Pro only; t		0.18	506.9824	480.2217	10	4	N/A	N/A	N/A	Structure	12.3512
31MA684	354	1419	505.646	477.9655	97.17544	fea354pos	2	post-ambiguous		n	n				505.646	477.9655	18	31	N/A	N/A	N/A	Structure	19.1889
31MA684	496	1598	503.4774	481.6917	97.24061	fea496pos	2	post-ambiguous		n	n	flat surfac			503.4774	481.6917	18.5	16	N/A	N/A	N/A	Structure	12.5664
31MA684	519	1779	506.0091	476.472	97.07022	fea519pos	2	post-ambiguous		n	n				506.0091	476.472	14.5	17	N/A	N/A	N/A	Structure	1.4107
31MA684	531	2151	507.689	481.2408	98.85892	feapost53	2	post-ambiguous		n	n	coupling e			507.689	481.2408	15	9	N/A	N/A	N/A	Structure	7.0049
31MA684	534	2154	507.6944	482.3231	98.82516	feapost53	2	post-ambiguous		n	n				507.6944	482.3231	18.5	31	N/A	N/A	N/A	Structure	9.5182
31MA684	535	2155	507.3307	482.4392	98.8295	feapost53	2	post-ambiguous		n	n	tran 22/ 20			507.3307	482.4392	20	5	N/A	N/A	N/A	Structure	8.6637
31MA684	547	2167	505.4062	482.3237	97.24488	feapost54	2	post-ambiguous		n	n	coupling e			505.4062	482.3237	23.5	7	N/A	N/A	N/A	Structure	14.8998
31MA684	548	2168	505.0205	482.1232	97.23652	feapost54	2	post-ambiguous		n	n				505.0205	482.1232	22.5	37	N/A	N/A	N/A	Structure	3.5898
31MA684	560	2180	502.8814	483.4991	97.24993	feapost56	2	post-ambiguous		m	n	Pro only; t		0.37	502.8814	483.4991	11.5	6	N/A	N/A	N/A	Structure	14.0617
31MA684	301	1415	516.4861	469.3522	96.69933	fea301cen	3	pit-real		y	y	point clos		0.52	516.4861	469.3522	N/A	N/A	172	125	32	Middle Qu	19.1987
31MA684	351	1457	512.912	474.364	97.18278	fea351sm	3	smudge pit		n	n	coupling e			512.9575	474.4007	N/A	N/A	59	66	14	Middle Qu	23.2422
31MA684	523	2146	523.5617	482.5987	98.43443	fea523 cer	3	pit-real		n	n	coupling e			523.5617	482.5987	N/A	N/A	66	46	23	Middle Qu	2.0155
31MA684	567	2242	511.9747	461.028	96.4919	fea567cer	3	rock cluster		y	n	Pro and 3D		0.24	511.9747	461.028	N/A	N/A	60	42	6	Late Archa	14.7341
31MA684	103	617	496.5829	467.426	96.73925	fea103pit	4	grave		n	n				496.5829	467.426	N/A	N/A	84	60	n/a	Middle Qu	10.7325
31MA684	224	1010	515.0723	464.8004	96.74663	fea224pit	4	grave		n	n	coupling e			515.0723	464.8004	N/A	N/A	126	79	n/a	Middle Qu	7.2199
31MA684	168	1456	502.0372	484.7842	97.33777	fea168hea	5	Hearth		n	n	possible c			502.0372	484.7842	N/A	N/A	52	35	6	Structure	8.1052
31MA684	569	2388	504.9926	480.019	97.22993	fea569cnt	5	Hearth		y	y	faint in Pr	dipolar sig	0.2	504.9926	480.019	N/A	N/A	86	86	15	Structure	3.719

31MA684	29	486	494.8768	469.7101	96.86866	fea29vess	19	ceramic vessel	n	n				494.8768	469.7101	N/A	N/A	N/A	N/A	N/A	inside Stru	0.2814
31MA684	324	2305	504.8536	480.5225	97.2492	fea324cen	19	smokehole daub	n	n				504.8093	480.4988	N/A	N/A	N/A	N/A	N/A	Structure	3.1992
31MA774	363	1534	557.1422	540.2859	109.1355	fea363pos	0	post-noncultural	n	n				557.1422	540.2859	N/A	N/A	N/A	N/A	N/A		14.4202
31MA774	364	1535	553.151	538.4159	108.7608	fea364pos	0	post-noncultural	n	n				553.151	538.4159	N/A	N/A	N/A	N/A	N/A		0.8847
31MA774	365	1536	551.4915	539.7104	108.6945	fea365pos	0	post-noncultural	n	n				551.4915	539.7104	N/A	N/A	N/A	N/A	N/A		9.2271
31MA774	366	1537	549.7925	542.7803	108.5634	fea366pos	0	post-noncultural	n	n	appears to			549.7925	542.7803	N/A	N/A	N/A	N/A	N/A		9.4895
31MA774	367	1538	547.5783	543.0209	108.4396	fea367pos	0	post-noncultural	n	n				547.5783	543.0209	N/A	N/A	N/A	N/A	N/A		0.1255
31MA774	368	1539	547.5411	543.6743	108.4126	fea368pos	0	post-noncultural	n	n	faint in pr			547.5411	543.6743	N/A	N/A	N/A	N/A	N/A		0.7779
31MA774	369	1540	546.8864	544.4874	108.3625	fea369pos	0	post-noncultural	m	n	faint in pr		0.48	546.8864	544.4874	N/A	N/A	N/A	N/A	N/A		21.3671
31MA774	370	1541	547.0078	545.3337	108.3858	fea370pos	0	post-noncultural	n	n	However,			547.0078	545.3337	N/A	N/A	N/A	N/A	N/A		4.461
31MA774	371	1542	547.46	545.6168	108.4169	fea371pos	0	post-noncultural	n	n				547.46	545.6168	N/A	N/A	N/A	N/A	N/A		3.8367
31MA774	373	1544	547.8495	546.6313	108.4469	fea373pos	0	post-noncultural	m	n	Y Hyp ref I		0.31	547.8495	546.6313	N/A	N/A	N/A	N/A	N/A		8.9542
31MA774	374	1545	546.7606	547.2834	108.3308	fea374pos	0	post-noncultural	n	n		on large li		546.7606	547.2834	N/A	N/A	N/A	N/A	N/A		1.5929
31MA774	375	1546	546.1847	547.9264	108.3214	fea375pos	0	post-noncultural	m	n	In pro and		0.31	546.1847	547.9264	N/A	N/A	N/A	N/A	N/A		17.0446
31MA774	376	1547	541.5299	544.9946	107.9555	fea376pos	0	post-noncultural	n	n	however,			541.5299	544.9946	N/A	N/A	N/A	N/A	N/A		7.3908
31MA774	377	1548	540.428	547.263	107.8523	fea377pos	0	post-noncultural	n	n	However,			540.428	547.263	N/A	N/A	N/A	N/A	N/A		22.6327
31MA774	379	1550	540.2589	550.5081	107.776	fea379pos	0	post-noncultural	n	n				540.2589	550.5081	N/A	N/A	N/A	N/A	N/A		18.9083
31MA774	395	1668	534.3966	535.943	107.1625	fea395pos	0	post-noncultural	n	n				534.3966	535.943	N/A	N/A	N/A	N/A	N/A		6.0816
31MA774	396	1669	532.4346	538.7552	107.1533	fea396pos	0	post-noncultural	n	n				532.4346	538.7552	N/A	N/A	N/A	N/A	N/A		20.0707
31MA774	432	1701	536.8535	572.2234	107.4495	fea432pos	0	post-noncultural	n	m				536.8535	572.2234	N/A	N/A	N/A	N/A	N/A		15.3975
31MA774	433	1702	535.8737	572.7767	107.3894	fea433pos	0	post-noncultural	m	n	pro and 3D		0.15	535.8737	572.7767	N/A	N/A	N/A	N/A	N/A		10.1756
31MA774	434	1703	531.2065	573.7244	107.0439	fea434pos	0	post-noncultural	m	n	in pro, fai		0.25	531.2065	573.7244	N/A	N/A	N/A	N/A	N/A		15.4999
31MA774	435	1704	530.5752	573.3858	106.9277	fea435pos	0	post-noncultural	m	n	very faint		0.26	530.5752	573.3858	N/A	N/A	N/A	N/A	N/A		22.7917
31MA774	445	1708	538.0829	536.433	107.5319	fea445pos	0	post-noncultural	n	n	Pro and 3D		0.19	538.0829	536.433	N/A	N/A	N/A	N/A	N/A		10.9043
31MA774	446	1709	541.0512	537.6908	107.8799	fea446pos	0	post-noncultural	n	n				541.0512	537.6908	N/A	N/A	N/A	N/A	N/A		13.7934
31MA774	447	1710	539.748	538.7527	107.7916	fea447pos	0	post-noncultural	m	n	very faint		0.27	539.748	538.7527	N/A	N/A	N/A	N/A	N/A		3.5508
31MA774	448	1711	533.8193	537.7135	107.2421	fea448pos	0	post-noncultural	n	n	coupling e			533.8193	537.7135	N/A	N/A	N/A	N/A	N/A		16.2209
31MA774	449	1712	551.2019	541.3014	108.7166	fea449pos	0	post-noncultural	n	n				551.2019	541.3014	N/A	N/A	N/A	N/A	N/A		21.5683
31MA774	450	1713	537.556	574.6103	107.4981	fea450pos	0	post-noncultural	n	n				537.556	574.6103	N/A	N/A	N/A	N/A	N/A		1.2179
31MA774	451	1714	537.391	578.1147	107.3374	fea451pos	0	post-noncultural	n	n				537.391	578.1147	N/A	N/A	N/A	N/A	N/A		20.4614
31MA774	452	1715	537.2579	578.4014	107.3369	fea452pos	0	post-noncultural	n	n				537.2579	578.4014	N/A	N/A	N/A	N/A	N/A		12.0562
31MA774	453	1716	537.3142	580.1502	107.2392	fea453pos	0	post-noncultural	n	n				537.3142	580.1502	N/A	N/A	N/A	N/A	N/A		8.8029
31MA774	454	1717	537.1562	580.4972	107.2369	fea454pos	0	post-noncultural	m	n	very very		0.19	537.1562	580.4972	N/A	N/A	N/A	N/A	N/A		20.3391
31MA774	455	1718	537.0998	580.6595	107.2174	fea455pos	0	post-noncultural	m	n	faint Pro c		0.14	537.0998	580.6595	N/A	N/A	N/A	N/A	N/A		12.3185
31MA774	456	1719	537.01	581.063	107.1965	fea456pos	0	post-noncultural	n	n				537.01	581.063	N/A	N/A	N/A	N/A	N/A		2.6521
31MA774	457	1720	536.6823	580.943	107.1718	fea457pos	0	post-noncultural	n	n				536.6823	580.943	N/A	N/A	N/A	N/A	N/A		16.7588
31MA774	458	1721	536.5072	581.0773	107.1697	fea458pos	0	post-noncultural	n	n				536.5072	581.0773	N/A	N/A	N/A	N/A	N/A		2.5772
31MA774	459	1722	536.6231	581.1846	107.1694	fea459pos	0	post-noncultural	m	n	very faint		0.15	536.6231	581.1846	N/A	N/A	N/A	N/A	N/A		7.2564
31MA774	460	1723	538.0092	581.4647	107.2211	fea460pos	0	post-noncultural	m	y	pro and 3D		0.27	538.0092	581.4647	N/A	N/A	N/A	N/A	N/A		9.9497
31MA774	476	1736	532.5857	579.6481	107.0048	fea476pos	0	post-noncultural	n	n	however s			532.5857	579.6481	N/A	N/A	N/A	N/A	N/A		18.6374
31MA774	507	1745	532.5283	578.0776	107.1123	fea507pos	0	post-noncultural	m	y	Pro only; t	center of l	0.28	532.5283	578.0776	N/A	N/A	N/A	N/A	N/A	noncultur	0.5882
31MA774	372	1543	547.3826	546.4865	108.3745	fea372pos	1	post-real	n	n				547.3826	546.4865	12	16	N/A	N/A	N/A		19.9563
31MA774	431	1700	537.4149	572.2344	107.536	fea431pos	1	post-real	n	m				537.4149	572.2344	20	32	N/A	N/A	N/A		20.7197
31MA774	444	1707	530.055	577.5162	106.8184	fea444pos	2	post-ambiguous	n	y				530.055	577.5162	11	N/A	N/A	N/A	N/A		13.3921
31MA774	339	1997	545.9486	550.2975	108.1458	fea339cen	3	pit-real	y	y	In Pro and		0.31	545.9486	550.2975	N/A	N/A	120	112	21	Late Quall	4.1339
31MA774	349	1799	543.7754	549.6647	107.8869	fea349cen	3	basin-real	m	n	Pro only; t		0.22	543.7754	549.6647	N/A	N/A	105	95	20	Late Quall	17.7023
31MA774	350	1800	543.7859	548.386	107.8067	fea350cen	3	pit-real	y	y	Pro and 3D		0.19	543.7859	548.386	N/A	N/A	145	145	35	Late Quall	14.4535
31MA774	357	1950	541.0108	548.3582	107.9064	fea357cen	3	smudge pit	n	n				541.0108	548.3582	N/A	N/A	30	25	9	Unknown	0.327
31MA774	393	1987	536.9636	545.8745	107.4597	fea393cen	3	basin-real	n	n	edge of gr	along dipc		536.9636	545.8745	N/A	N/A	80	77	17	Late Quall	12.515
31MA774	508	1809	535.5656	572.4146	107.0835	fea508cen	3	pit-real	m	m	In pro and	within dar	0.35	535.5656	572.4146	N/A	N/A	79	75	27	Late Quall	14.8123
31MA774	510	1972	532.027	577.1105	107.0067	fea510cen	3	pit-real	n	y	strata cha	in center c		532.027	577.1105	N/A	N/A	47	32	9	Late Qual	14.457
31MA774	511	1975	532.087	578.1528	106.9667	fea511cen	3	pit-real	n	y	strata cha	in center c		532.087	578.1528	N/A	N/A	49	30	9	Late Qual	4.6501
31MA774	340	1369	554.9223	541.4502	109.093	fea340gra	4	grave	n	y	noise and			554.9223	541.4502	N/A	N/A	130	70	n/a	Qualla	0.6606